INVESTIGATING THE MECHANISMS OF TELOMERE MAINTENANCE IN ZEBRAFISH TISSUES AND HUMAN BRAIN CANCER CELL LINES

A THESIS SUBMITTED TO

THE GRADUATE SCHOOL OF ENGINEERING AND SCIENCE

OF BILKENT UNIVERSITY

IN PARTIAL FULFILLMENT OF THE REQUIREMENTS FOR

THE DEGREE OF

MASTER OF SCIENCE

IN

NEUROSCIENCE

By

Naz Şerifoğlu

September 2019

INVESTIGATING THE MECHANISMS OF TELOMERE MAINTENANCE IN ZEBRAFISH TISSUES AND HUMAN BRAIN CANCER CELL LINES

By Naz Şerifoğlu

September 2019

We certify that we have read this thesis and that in our opinion it is fully adequate, in scope and in quality, as a thesis for the degree of Master of Science.

Michelle Marie Adams (Advisor)

Ayça Arslan Ergül (Co-Advisor)

Fahriye Duygu Çetinkaya

Urartu Özgür Şafak Şeker

Approved for the Graduate School of Engineering and Science

Ezhan Karaşan

Director of the Graduate School

ABSTRACT

INVESTIGATING THE MECHANISMS OF TELOMERE MAINTENANCE IN ZEBRAFISH TISSUES AND HUMAN BRAIN CANCER CELL LINES

Naz Şerifoğlu

M.Sc. in Neuroscience

Advisor: Michelle Marie Adams

Co-Advisor: Ayça Arslan Ergül

September 2019

Telomeres are nucleoprotein complexes formed at each end of the chromosomes to protect these ends from deterioration. In each round of cellular division, telomeric sequences shorten due to the end replication problem of DNA polymerase. Progressive telomere shortening results in replicative senescence in healthy somatic cells. To evade replicative senescence, cells need to maintain their telomere length either by activating the telomerase enzyme or through the alternative lengthening of telomeres (ALT). Telomerase is a holoenzyme, which is composed of dyskerin, telomerase RNA subunit (TR or TERC), and telomerase catalytic subunit (TERT). Dyskerin and TR are constitutively expressed in all cells but TERT expression is silenced in adult somatic cells. Thus, telomerase activity is dependent on the expression of TERT. Current studies show that TERT re-activation is a common feature of cancer cells and 85-90% of cancers utilize telomerase enzyme in maintaining telomeres to become immortal. Remaining of cancer cells maintain their telomeres by the alternative lengthening of telomeres (ALT), which is a DNA repair pathway dependent mechanism. Current models suggest that ALT is achieved by homology-directed DNA repair, through the interaction of multiple proteins.

DNA methylation is regarded as a key player in epigenetic silencing of transcription. DNA methyltransferase inhibitors are currently being used in cancer treatments. Recent studies show that DNA methyltransferases and their expression levels impact both telomerase- and ALT mediated lengthening of telomeres, and have different outcomes in different tissue types.

In this study, we worked on the zebrafish brain and human brain cancer cell lines. In zebrafish brain, we observed differences in methylated regions at Sp1 binding site between young and old that can be associated with telomere shortening. By silencing DNMT1 and DNMT3B in brain cancer cell lines, we investigated the changes in gene expression levels of telomerase and ALT related genes, telomerase activity, population doubling time and replicative senescence status. To further investigate TERT regulation, we introduced mutations to the Sp1 binding sites in the promoter region and measured the promoter activity with luciferase assay. Our results show that Sp1 methylation sites in the telomerase promoter region are critical in brain aging, dependent on their position. We propose a therapeutical option for brain aging and tumorigenesis.

Keywords: Aging, zebrafish, brain cancers, telomerase, TERT, ALT, Sp1, gene expression, qTRAP, site-directed mutagenesis

ÖZET

ZEBRABALIĞI DOKULARINDA VE İNSAN BEYİN KANSERLERİNDE TELOMERLERİN SÜRDÜRÜLME MEKANİZMALARININ İNCELENMESİ

Naz Şerifoğlu

Nörobilim Lisansüstü Programı, Yüksek Lisans

Tez Danışmanı: Michelle Marie Adams

Tez Eş Danışmanı: Ayça Arslan Ergül

Eylül 2019

Telomerler kromozom sonlarında bulunan nükleoprotein yapılardır ve kromozom uçlarını korurlar. Hücre bölünmesinin her turunda telomerler, DNA polimerazın çalışma mekanizmasına bağlı olarak kısalırlar. Telomer uzunluğu kritik bir uzunluğun altına düştüğünde, sağlıklı somatik hücreler replikatif senesense girerler. Replikatif senesensi atlatmak için hücrelerin telomer uzunluklarını korumaraları gerekmektedir. Bu telomeraz enzimi veya telomerlerin alternatif uzatılması (ALT) ile sağlanabilir. Telomeraz holoenzimi diskerin, telomeraz RNA alt ünitesi (TR veya TERC) ve telomeraz katalitik alt ünitesinden (TERT) oluşur. Diskerin ve TR hücrelerde her daim sentezlenir ancak TERT ifadesi erişkin somatik hücrelerde susturulur. Buna bağlı olarak telomeraz aktivitesi, TERT geninin ifade edilmesine bağlıdır. Güncel yayınlar göstermektedir ki TERT geninin yeniden aktive edilmesi kanser hücrelerinin sık görülen bir özelliğidir. Kanserlerin %85-90'ı telomeraz enzimi ile telomer uzunluklarını sürdürürler ve ölümsüzlüklerini sağlarlar. Geriye kalan kanser hücreleri, telomerlerini ALT ile devam ettirirler. ALT DNA tamir mekanizması temelli bir yolaktır. Güncel modeller ALT mekanizmasını çoklu protein etkileşimiyle sağlanan homolog rekombinasyon tamiri ile açıklar.

DNA metilasyonu, gen ifadesinin susturulmasında önemli bir epigenetik yol olarak kabul edilmektedir. DNA metilasyonunu engelleyen ajanlar günümüzde kanser tedavilerinde kullanılmaktadır. Yakın zamanda yapılan çalışmalar göstermiştir ki DNA metiltransferaz enzimleri ve ifade seviyeleri, hem telomeraz enzimine bağlı hem de ALT mekanizmasına bağlı telomer uzunluğu sürdürülmesini doku tipine bağlı olarak etkilemektedir. Biz bu çalışmada Genç ve yaşlı zebrabalığı beyinlerinde, Sp1 bağlanma bölgesinde metilasyon seviyesinde farkları gözlemledik. Bu metilasyon farklarının telomer uzunluğunu etkilediğini düşünüyoruz. DNMT1 ve DNMT3B ifadesini engellediğimiz insan beyin kanseri hatlarında, telomeraz ve ALT mekanizmasıyla ilgili genlerin ifade seviyesini, telomeraz aktivitesini, popülasyon katlanma zamanını ve replikatif senesens durumunu inceledik. TERT promotor aktivitesini lusiferaz ölçümü ile, Sp1 bağlanma bölgelerinde, bölgeye yönelik mutasyonlar varlığında ve yokluğunda hesap ettik. Bulgularımız TERT promotor bölgesinde Sp1 metilasyon alanlarının, pozisyona bağlı olarak, beyin yaşlanmasında önemli olduğunu göstermektedir. Biz sonuçlarımız doğrultusunda beyin yaşlanması ve tümör oluşumu için bir tedavi seçeneği önermekteyiz.

Anahtar Sözcükler: Yaşlanma, zebrabalığı, beyin kanserleri, telomeraz, TERT, ALT, Sp1, gen ifadesi, qTRAP, bölgeye yönelik mutasyon

Acknowledgment

I want to thank Prof. Michelle M. Adams and Assoc. Prof Ayça Arslan Ergül for their guidance, support and allowing me to work on this project. I am grateful to them for always being open to my ideas and trusting my decisions. I have learned a lot from them, and I am honored to have them as advisors.

I would like to thank Prof. Duygu F. Uçkan Çetinkaya and Assoc. Prof Urartu Özgür Şafak Şeker for their kindness on accepting to take part in my thesis committee. I am thankful to Prof. Duygu F. Uçkan Çetinkaya for also allowing me to conduct experiments at PEDI-STEM, Hacettepe University.

I consider my self very lucky to know and work with my labmates. Narin Ilgım Ardıç and Begün Erbaba never failed to make me smile. Bihter Muratoğlu, Melis Temel, Rumeysa Tuncer, Cansu Üstüner, Melek Umay Tüz, and Elif Tuğçe Karoğlu, I am thankful for their support and their friendship. I would also like to thank my friends at PEDI-STEM, Hacettepe University, for their positive energy and welcoming nature.

I am thankful to Barış Oralalp, Yiğit Yılmaz, Eylül Celtemen, Gülce Kale, and Mustafa Ege Can Şulan for their friendship and support in every aspect of my life.

Finally, I would like to express my profound gratitude to my family, Mefaret and Refik Şerifoğlu, for providing me with unconditional love, support, and encouragement. I could not have written the thesis without their help. Thank you.

Experiments in this thesis were supported partially by The Scientific and Technological Research Council of Turkey 1001 grant (no: 114S548) and two Hacettepe University Scientific BAP grants (no: THD-2017-15492 and no: THD-2018-16904).

TABLE OF CONTENTS

LIST OF TABLES

LIST OF FIGURES

CHAPTER 1

INTRODUCTION

1.1. Telomeres: Structure and Function

Linear eukaryotic chromosome ends are specialized nucleoprotein complexes, known as telomeres. In mammals, telomeric DNA consist of double-stranded tandem repeats of 5'-TTAGGG-3' followed by 3-guanine-rich single-stranded overhangs. Telomeric repeats interact with the Shelterin complex, and this interaction protects chromosome ends from being recognized as DNA damage [1]. Shelterin is a multimeric protein complex and consists of TRF1, TRF2, TIN2, RAP1, POT1, and TPP1 in humans [2]. Association of telomeric repeats with Shelterin complex, result in the formation of a lariat like structure, known as the t-loop.

Several cascades of molecular events lead to t-loop formation. Double-stranded telomeric repeats fold back on itself, and the terminal single-stranded overhang invades into duplex TTAGGG repeats. This invasion displaces double-stranded TTAGGG repeats and forms the displacement loop (d-loop). Displaced telomeric repeats at d-loop are only bound by POT1 and TPP1. Double-stranded TTTAGG repeats are directly bound by TRF1, TRF2, and POT1 [2]. Rest of the Shelterin complex members do not have the capacity to interact with the telomeric repeat sequences. RAP1 interacts with TRF2 to localize on telomeres [3] [4]. TPP1 interacts with POT1 and shown to be enhancing POT1 affinity to TTAGGG repeats [5]. TIN2 is accepted as a central component of the Shelterin complex since it directly interacts with TRF1, TRF2, and TPP1 [6]. Overall, this molecular arrangement maintains and protects telomeres.

The primary function of telomeres is to protect chromosome ends from being recognized as DNA damage. This way, telomeres contribute to genomic stability by preventing chromosome fusions [1]. They also function in nuclear architecture and chromosome positioning by helping the organization of chromosomes [7].

Telomere shortening is known to be accompanying healthy aging and telomeres are accepted as mitotic clocks. In humans, telomeres are 8 to 12 kbp in length at birth, and total loss of 2 to 4 kbp in average telomere length is observed in chromosomes [8]. Pathological telomere dysfunctions, such as short telomeres due to telomerase deficiency in early development and telomere uncapping, are shown to be accelerating aging in mammals. Experimental mouse models with shortened and lengthened telomeres show decreased and increased life span, respectively [9] [10]. Meta-analysis studies in humans also indicate a strong relationship between premature mortality and short telomeres [11].

Telomeres shorten due to the working mechanism of DNA polymerase and thus the end replication problem in cells, in the absence of the telomerase enzyme. Apart from the end replication problem, exonucleolytic activities and oxidative damage are also shown to be contributing to telomere shortening [12] [13]. After a critical point is reached, shortening of telomeres triggers either apoptosis or growth arrest, known as the replicative senescence. Replicative senescence is believed to be the initial barrier against tumor formation and accepted as a hallmark of aging [14].

1.2. Replicative Senescence

Senescent cells can be characterized by the absence of proliferation markers, enlarged cell size, increase in senescence-associated β-galactosidase activity, and increased $p16^{INK4a}$ expression [15]. The onset of replicative senescence is usually determined by the length of the shortest telomere, but the loss of TRF2 or POT1 (telomere uncapping) can also lead to cell cycle arrest [16].

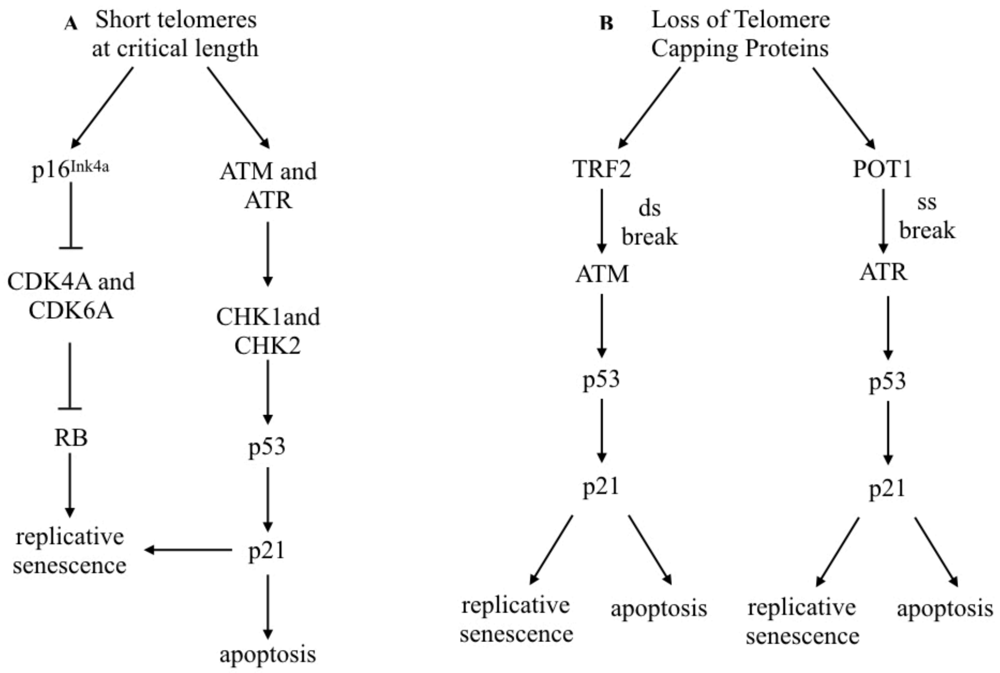

Figure 1.1: Telomere induced DNA damage response pathways. A) Telomere length mediated DNA damage response activates p16, ATM, and ATR mediated pathways. B) Capping protein-mediated DNA damage response activates ATM or ATR mediated pathways depending on the lost telomere capping molecule.

Telomere induced DNA damage response (DDR) is achieved by several different signaling events (Figure 1.1). Shortening of telomeres shown to be inducing $p16^{Ink4a}$-Rb, ATM, and ATR mediated pathways. In the $p16^{Ink4a}$-Rb pathway, p16 inhibits CDK4 and CDK6, which represses Rb. Release of the inhibition of Rb results in replicative senescence [17]. In ATM and ATR signaling, stimulation of CHK1 and CHK2 activates p53. p53 can induce apoptosis or activate p21 to induce senescence. Telomere uncapping induced DNA damage response is mediated by ATM or ATR, depending on the lost capping protein. TRF2 loss and double stand breaks result in ATM-mediated DNA damage response. POT1 loss and single-strand breaks induce ATR mediated DNA damage response [17]. In both pathways, cells either enter replicative senescence, through p21 activity or enter apoptosis, through p53 activity.

By preventing further cellular divisions, replicative senescence protects the genetic information from being lost and contributes to genomic stability. However, growth arrest can be by-passed by the loss of tumor suppressors and other oncogenic changes. When the growth arrest is by-passed, telomeres continue to shorten and eventually, chromosome bridge-fusion-breakage cycles occur. These cycles result in genomic instability and increased risk of cancer [7]. Extensive cell death occurs; however, certain rare cells escape the crisis, start maintaining their telomeres and become malignant. This can be achieved by either re-activating or up-regulating the telomerase reverse transcriptase (TERT) gene, coding for the catalytic subunit of the telomerase holoenzyme, or lengthening their telomeres by the alternative lengthening of telomeres, using DNA recombination pathways [18] [19].

1.3. Telomerase

Telomerase is the enzyme that can elongate telomeres by adding TTAGGG repeats onto chromosome 3'-ends *de novo*. It is a ribonucleoprotein complex, and in humans, it consists of TERT, telomerase RNA component (TERC or TR) and human telomerase-associated protein 1 (TEP1) or dyskerin (DKC1). For telomerase to function, several proteins are required. Regulator of Telomere Elongation Helicase 1 (RTEL1), Telomerase Cajal body protein 1 (TCAB1) and CST complex (Cdc13/Ctc1, Stn1, and Ten1) are some of the identified contributors to telomerase activity in yeast. For telomere replication, T-loop needs to dissociate. RTEL1 helicase is the enzyme responsible for t-loop dissociation. DNA replication yields in a blunt-ended telomere end at the leading-strand synthesis and an RNA primer-ended telomere end in lagging strand synthesis. RNA primer-ended telomere ends are processed by the CST complex and Apollo before telomerase activity. TCAB1 in the Cajal bodies promotes assembly of telomerase and telomerase localizes onto the replicated and processed telomere.

Localization is achieved by interaction with TCAB1 and TPP1 and telomeres add 50 to 100 base pairs of new telomere repeats to the G-overhang. When the telomerase activity is done, CST complex and DNA polymerase-α perform a fill-in reaction and nucleolytic processing. This way, extended telomeres are closed to further telomerase action [20].

Telomerase activity is dependent on TERT expression. TERC and DKC1 are constitutively expressed, but TERT expression is highly regulated [1]. TERT is active during early development in humans, but gets transcriptionally silenced between the 12th and the 18th weeks of gestation [21]. However, in adults, TERT is actively being expressed in stem cell compartments and embryonic stem cells. In somatic cells, TERT expression or telomerase activity are usually undetectable or at low levels [22]. In contrast, in 85-90 % of cancer cells, TERT is up-regulated, which leads to the re-activation of telomerase [23].

1.4. TERT Re-activation and Telomerase Regulation in Cancer

Majority of cancer cells maintain their telomeres through re-activation of the TERT gene, and several cellular events can contribute to this re-activation. Epigenetic modifications are one such example. They play a major role in TERT re-activation, and the most common ones are DNA methylation in CpG islands, histone methylation, and histone acetylation. Methylation is generally associated with gene silencing, and it functions by inhibiting protein binding to the target DNA sequence. However, in the TERT promoter site, the opposite is observed. In healthy adult somatic tissues, CpG islands of the TERT promoter is hypo or non-methylated. On the contrary, cancer cells with TERT expression, have methylated CpG islands at TERT promoter site. CCCTC binding factor (CTCF) inhibitory proteins are one of the reasons behind hypo-methylation of CpG at the TERT promoter sites [24].

The methylation code, produced by DNA methyltransferases, DNA demethylases, and several other interacting proteins, differ in between cell types. In colon cancer cell line HCT116, and lung cancer cell line H209, proximal promoter site up to -150 bp shows no DNA methylation and shows hypermethylation between -150 and -650 bp. In embryonic stem cells, hypomethylation is observed between -650 and -400 bp, and no methylation is observed from -400 bp to transcription start site [25]. Current studies suggest that methylation code at the TERT promoter site can have different outcomes at different severities depending on the cell type.

Promoter mutations can also lead to TERT expression and the telomerase re-activation. Human tumors show variation in terms of frequency of TERT promoter mutations. In colon, pancreatic, breast, prostate, and thyroid cancers, TERT promoter mutations are not observed frequently. On the other hand, in cancers such as primary glioblastoma, oligodendrogliomas, medulloblastoma, and liver cancer TERT promoters are frequent. Other brain cancers such as astrocytoma and neuroblastoma also show mutations at the TERT promoter site but less frequently, where the frequency is around 10% [26]. Mutations at the TERT promoter site can re-activate the expression through several transcription factors. The core promoter, which is upto -2000 bp from the transcription site, has binding sites for transcription factors like Myc/Max and Sp1 [27]. Mutations at SP1 binding site were shown to be affecting transcription factor binding and thus the promoter activity. In the same study, it was also shown that SP1 over-expression increased the telomerase activity in a cell type-dependent manner [27]. Analysis of conserved binding sites at the promoter area up to -4000 bp from the ATG start codon of TERT showed that first 1000 bp is critical and sufficient for regulation of TERT expression [28]. Number of studies report cell type-dependent response to mutations at the TERT promoter site, and a recent model was proposed to explain this difference in cellular response (Figure 1.2).

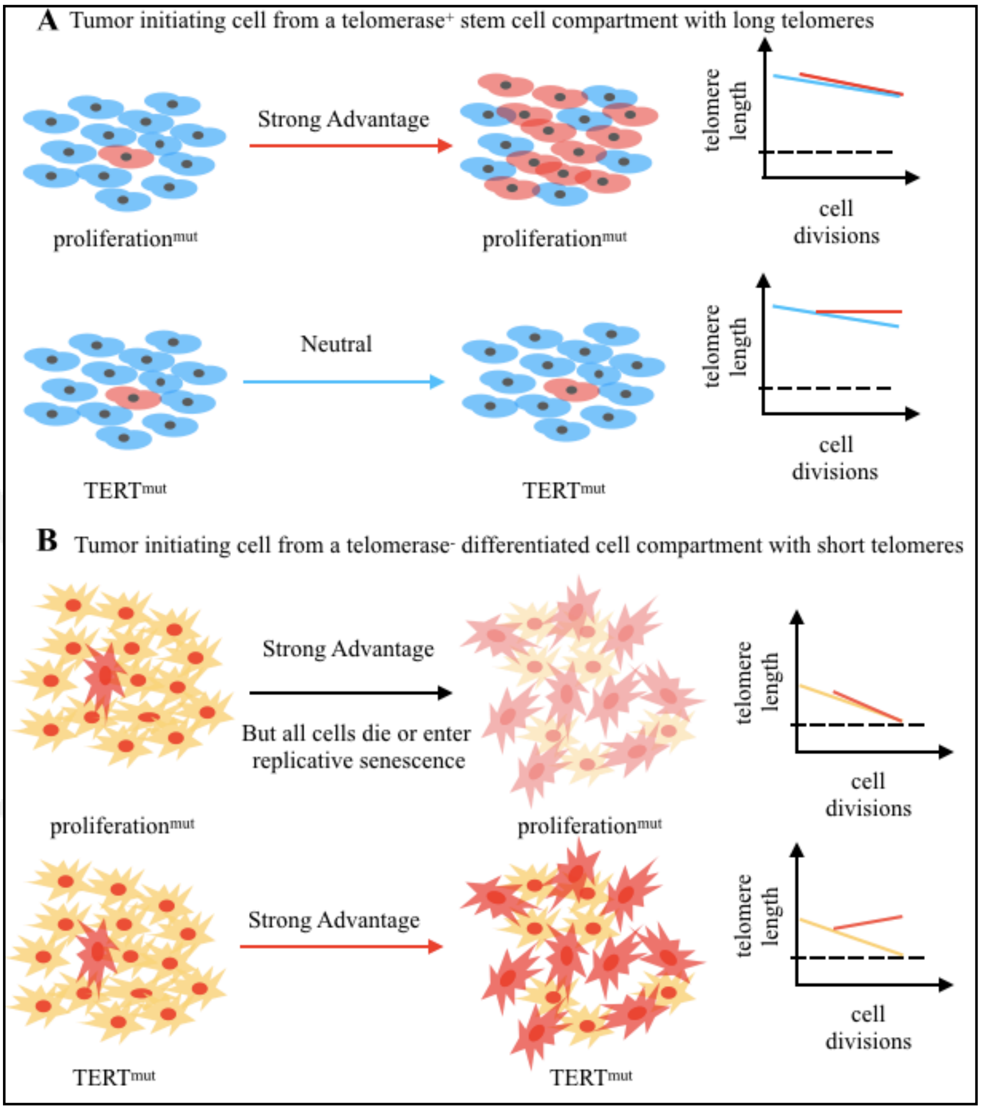

Figure 1.2: Relationship between TERT promoter mutations and proliferative advantage in tumor-initiating cells. A) Proliferative outcomes in tumor-initiating cells from stem cell compartments with long telomeres. B) Proliferative outcomes in tumor-initiating cells from differentiated cell compartments with short telomeres. Adapted from Chiba et al. 2015

In this model, the response firstly relies on the telomerase positivity and telomere length of the tumor-initiating stem cell. If the cell is telomerase positive and has long telomeres in the first place, mutations affecting proliferation would cause a strong advantage towards tumor formation. On the other hand, mutations at the TERT promoter site would be neutral in terms of tumor formation. In other words, mutations of TERT promoter at such cells, will not be a tumor-initiating event since it does not cause a proliferative advantage. If the tumor-initiating cell is from a telomerase negative differentiated cell compartment with short telomeres and has mutations that are increasing cell proliferation, even though the cell has a strong tumor initiating advantage due to cellular senescence or apoptosis, it will not be able to form a tumor. However, if the same cell type has a mutation at the TERT promoter area that is activating telomerase, it will have a strong advantage towards tumor formation since it can avoid cellular senescence [29].

1.5. ALT Mechanisms in Cancer

Apart from the telomerase-dependent lengthening of telomeres, cells can avoid entering into cellular senescence by the alternative lengthening of telomeres (ALT). This phenomenon was first observed in telomerase knock-out model of yeast. Even though the model was telomerase-deficient, it was able to maintain telomere length and continue proliferation. When a double knock-out for RAD52 was performed, these cells failed to survive and proliferate [30]. Since RAD52 is an important protein for double-strand break repair by homologous recombination, these observations were the first to suggest that telomeres could be maintained through DNA recombination-dependent pathways. Other studies, using exogenous DNA integration into telomeres, have shown the presence of ALT and shed light on how it employs homologous recombination [31].

Several models have been proposed to explain the working mechanism of ALT (Figure 1.3). The first model is based on break-induced repair, and the DNA is synthesized away from the break site using an HR donor template, which is the telomeric DNA in this case. This model is divided into three sub-models. In the first two sub-models, there is a loss of genetic material in the recipient telomeres, but the timing of the lagging strand is different. In the third sub-model, unidirectional replication fork requires a Holliday junction at the end of the process. In this model, both the donor and the recipient telomeres are semi-conserved [32] [33]. The second model suggested for ALT is unequal telomeric sister chromatid exchange (T-SCE) due to the observation of increased sister chromatid exchange in ALT positive cells [34]. The last model is based on the presence of extrachromosomal telomeric repeats (ECTRs) in ALT positive cells. In this model, extrachromosomal telomeric repeats are suggested to be templates in telomere elongation through homologous recombination (HR) driven telomere elongation or rolling circle replication [31].

Current studies suggest that 10-15% of cancer cells utilize ALT to maintain telomeres [17]. ALT-positive cells are characterized by the presence of heterogeneity in telomere lengths, high level of telomeric sister chromatid exchange, extrachromosomal telomeric repeats, and the ALT-associated promyelocytic leukemia bodies (APBs), special telomeric nuclear bodies [35] [36]. Although the mechanism and the cause of ALT are still not well characterized, several different proteins and complexes are shown to be contributing to the ALT activation during cell immortalization and cancer progression. Alpha Thalassemia/Mental Retardation Syndrome X-linked (ATRX), Death Domain Associated Protein (DAXX) and transcription activating histone variant H3.3 are amongst the most studied proteins in ALT. ATRX and DAXX form a chromatin remodeling complex that functions in the deposition of H3.3 histone variant into telomeric and pericentromeric chromatin [31]. Identification of ATRX and DAXX inactivating mutations in ALT positive cells suggested that ATRX and DAXX loss is promoting ALT activation. ATRX loss increases susceptibility to DNA damage at heterochromatic regions and replicative stress [37]. Several studies showed that ATRX re-expression suppresses the ALT mechanism [38] [39].

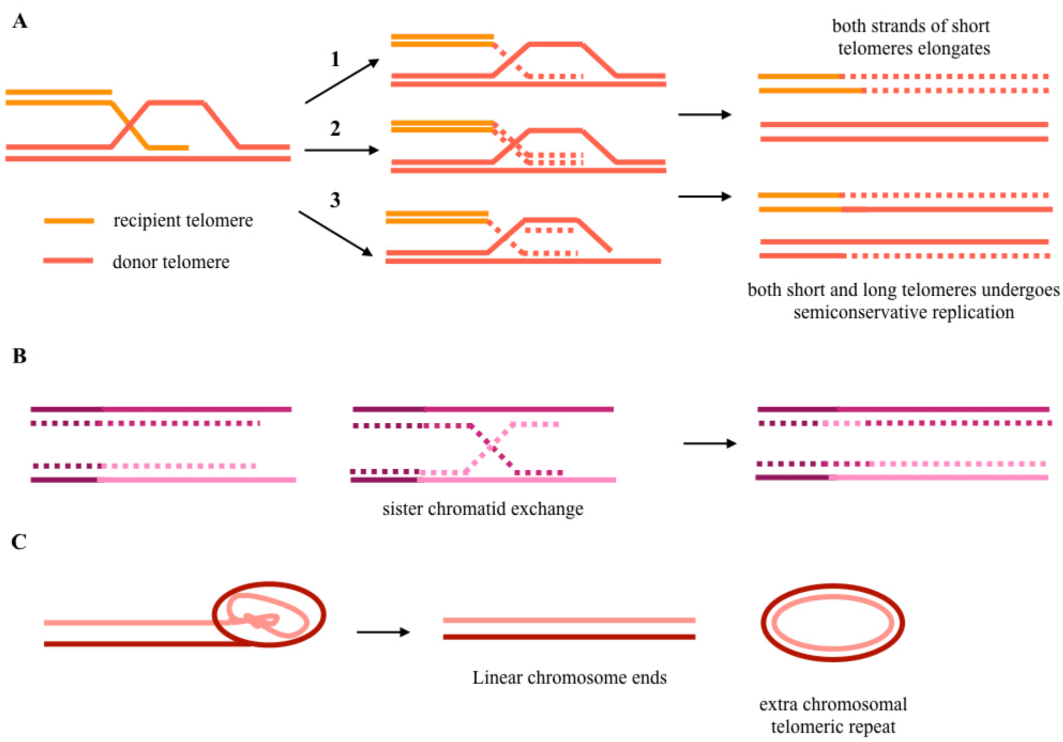

Figure 1.3: Currently proposed ALT mechanisms. A) Break Induced Repair based ALT model. B) Sister Chromatid Exchange based ALT model.C) Homologous Recombination and Rolling Circle based ALT model. Adapted from Amorim et al. 2016.

Other proteins associated with ALT phenotype include but not limited to RAD50 Double-Strand Break Repair Protein (RAD50), RAD51 Recombinase (RAD51), Structural Maintenance of Chromosome 5 and 6 (SMC5/6) complex, WRN RecQ Like helicase (WRN), Telomeric Repeat Binding factor 2 (TRF2), MUS81 Structure-Specific Endonuclease Subunit (MUS81), X-Ray Repair Cross Complementing 6 (Ku70), X-Ray Repair Cross Complementing 5 (Ku80), Flap Structure-Specific Endonuclease (FEN1), Chromobox 3 (CBX3), BLM RecQ Like helicase (BLM), Anti-Silencing Function 1 Histone Chaperone (ASF1), SWI/SNF Related Matrix Associated Actin Dependent Regulator of Chromatin Subfamily A Like 1 (SMARCAL1), and Replication Protein A (RPA) [31]. Early studies in yeast show that ALT mechanism is achieved by homologous recombination through RAD50 and RAD51 [40]. In human WI38-VA13/2RA cell line, depletion of RAD51 results in telomere shortening. Moreover, an increase in apoptosis is observed in these RAD51 depleted cells [41]. SMC5/6 Complex depletion in U-2 OS cell line results in shortening of telomeres, disruption of ALT-associated promyelocytic leukemia bodies formation, and impaired extrachromosomal telomeric repeats formation [42]. WRN helicase deficiency in U-2 OS and VA13 cell lines, result in inhibition of ALT-associated promyelocytic leukemia bodies formation and shortening of telomeres [43]. Depletion of TRF2 and disruption of Shelterin complex in SUSM1 and U-2 OS cell lines decrease telomeric signals and shortens telomeres [44]. Depletion of MUS81 in GM847, U-2 OS, and SAOS-2 cell lines shown to be inhibiting T-SCEs and results in growth arrest. On the other hand, MUS81 depletion does not affect telomere length in these cell lines [45]. Ku70/80 is shown to be promoting proliferation in ALT positive cell line CCL75.1 and depletion results in reduced number of extrachromosomal telomeric repeats. However, telomere length remains unchanged when Ku70/80 is depleted [46]. FEN1 depletion is associated with telomere dysfunction and in U-2 OS cell line inhibition of FEN1 results in increased telomeric DNA response [47]. RNA sequencing experiments revealed an association of CBX3 with ALT pathways [37]. Another study revealed that CBX3 is contributing to the maintenance of sister telomere cohesion and telomere length through interaction with TINF2 [48]. Over-expression of BLM Helicase in WI-38 VA-13/2RA and GM-847 cell lines increases telomeric DNA synthesis [49]. Depletion of ASF1 in IMR90, WI38, and HeLa is shown to be inducing ALT hallmarks. Extrachromosomal telomeric repeats and ALT-associated promyelocytic leukemia bodies forms in the absence of this protein [50]. SMARCAL1 inhibition in HeLa 1.3 and U-2 OS cells results in accumulation of extrachromosomal telomeric repeats and telomere-associated DNA damage response [51]. RPA depletion in GM-847 and U-2 OS cell lines accumulates G-rich telomeric single-stranded DNA and results in proliferation arrest [52].

1.6 DNA Methyltransferases, Cancer, and Stemness

DNA methylation is a key epigenetic modification involved in gene expression regulation and genomic integrity maintenance. It is a heritable and reversible modification that is regulated by DNA Methyltransferases (DNMTs). These proteins transfer methyl groups from S-adenosyl-L-methionine (SAM) to the C-5 position of the cytosines [53]. DNMT1 is accepted as maintenance DNMT since it preferentially methylates hemimethylated DNA. DNMT2 is actually an RNA methyltransferase. It methylates the cytosine-38 in the anticodon loop of aspartic acid tRNA [54]. DNMT3A and DNMT3B, known as the de novo methyltransferases, both have a preference to methylate unmethylated CpG dinucleotides [55]. DNMT3L, last member of DNMTs, lacks enzymatic activity and functions in the binding of de novo methyltransferases to SAM [55].

Typically, tumor cells exhibit aberrant DNA methylation patterns during malignant transformation [56]. Recent findings suggest that the relationship between telomeres, methylome, aging, and cancer is more intricately linked than originally supposed. DNMT1 depletion in healthy cells increases microsatellite instability and chromosomal translocation frequency [57]. DNMT1, DNMT3A, and DNMT3B are shown to be over-expressed in colon, prostate, breast, and liver cancers. Silencing of DNA methyltransferases in an antisense approach inhibits tumorigenesis [58]. Studies on stem cell differentiation revealed a direct link between telomere integrity, de novo DNA methylation, and stem cell pluripotency. Embryonic stem cells (ESCs) and induced pluripotent stem cells (iPSCs) with short telomeres exhibit reduced expression of DNMT3A and DNMT3B [59] [60]. A recent study showed that ESCs with short telomeres cannot differentiate stably, and thus their proliferation capacity is limited. In these cells, Nanog regulation is impaired, and both DNA and Histone 3 Lysine tri-methylation are altered. Enforced DNMT3B expression or telomere elongation, rescue differentiation capacity, and impaired DNA methylation [61].

CHAPTER 2

OBJECTIVES AND RATIONALE:

In this thesis, we aimed to shed light on telomere maintenance during aging of the zebrafish brain, in the brain cancers and the effect of DNA methylation for both conditions we aimed to provide data for future translational studies. We had four objectives and our first objective was to study telomere shortening in a zebrafish model of aging. For this purpose, we have measured the telomere length in the different organs of the aging wild-type zebrafish and investigated the methylation levels of TERT promoter in these samples. Although zebrafish adult tissues produce telomerase at low levels, we expected to observe a decreasing trend through the aging process with different speeds in an organ-specific manner. Observation of long telomeres in some of the old zebrafish tissues lead us to study methylation levels in the TERT promoter since TERT promoter is rich in CpG islands and telomerase activity is generally dependent on TERT transcription.

Our second and third objectives were concerning the telomere maintenance in human brain cancer cell lines and DNA methylation machinery. Our second objective was to focus on the telomerase-dependent telomere maintenance in these cell lines. For this purpose, we have investigated the effect of point mutations affecting Sp1 binding sites at the TERT promoter, the effect of DNA methylation inhibition in the gene expression of telomerase-associated genes, and the telomerase activity. The third objective was focused on the alternative lengthening of telomeres in these cell lines. We investigated the expression of ALT-associated genes for this purpose when the DNA methylation was blocked. For both of these objectives, telomere lengths were also measured in the presence and absence of DNA methylation.

Our last objective was to investigate the relationship between the DNA methylation machinery and the onset of replicative senescence. Our rationale was based on that DNMTs are accepted as stemness markers and over-expressed in most tumor cells. Population doubling assays and Beta-Galactosidase staining experiments were performed for this objective.

CHAPTER 3

MATERIALS AND METHODS

3.1 Materials

3.1.1. Cell Culture Reagents

Table 3.1.1: List of cell culture reagents

DMEM F-12 w/o L-Glutamine w/o Hepes	L0090, BioWest, Nuaillé, France
PBS	L0615-500, BioWest, Nuaillé, France
Trypsin	L0930-100, BioWest, Nuaillé, France
L-glutamine	25030-024, Gibco, Paisley, UK
Non Essential Aminoacids	X0557, BioWest, Nuaillé, France
Penicillin-Streptomycin	15140122, Gibco, Paisley, UK
Fetal Bovine Serum	S181H-500, BioWest, Nuaillé, France
DMSO	1.16743.1000, Merck, Billerica, USA
Vidaza/Azacytidine	8699538774815, Erkim ilaç, Istanbul, Turkey
Adriamycin/Doxorubicin	8699511796056, Saba ilaç, Istanbul, Turkey
Cell Culture grade water	L0970-500, BioWest, Nuaillé, France

3.1.2. General Enzymes

Table 3.1.2: List of general enzymes

Phusion High Fidelity Master Mix with High GC content	F-532, Thermo Scientific, Vilnius, Lithuania
Taq DNA polymerase	A140303, Ampliqon, Odense, Denmark
ZymoTaq PreMix	E2004, Zymo Research, Irvine, USA

Table 3.1.2: Continued

Fast Start SYBR Green Master	04 673 492 001, Roche, Mannheim, Germany
SensiFAST ™ SYBR® No-ROX Kit	BIO-98020, Bioline, Luckenwalde, Germany

3.1.3. General Kits, Reagents and Chemicals

Table 3.1.3: List of general kits, reagents and chemicals

QIAamp DNA Mini Kit	51304, Qiagen, Hilden, Germany
DNeasy Blood&Tissue Kit	69506, Qiagen, Hilden, Germany
Epitect Fast DNA Bisulfite Kit	59824, Qiagen, Hilden, Germany
EZ Methylation Lightning Kit	D5030, Zymo Research, Irvine, USA
PureLink Quick PCR Purification Kit	K310001, Thermo Fisher Scientific, Vilnius, Lithuania
DNA Clean & Concentrator ™-25	D4034, Zymo Research, Irvine, USA
Zyppy Miniprep Kit	D4019, Zymo Research, Irvine, USA
ZymoPURE Plasmid Maxiprep Kit	D4202, Zymo Research, Irvine, USA
RNeasy Mini Kit	74104, Qiagen, Hilden, Germany
RNase free DNase set	79254, Qiagen, Hilden, Germany
Transcriptor High Fidelity cDNA Synthesis Kit	05081963001, Roche Diagnostics, Mannheim, Germany
Senescence *β-gal* staining kit	9860, Cell Signalling Technologies, Frankfurt am Main, Germany
Luciferase Assay	E1500, Promega, Madison, USA
Transfex	ACS-4005, ATCC, Virginia, USA
Nuclease Free Water	AM9937, Ambion, Austin, USA
PBS Tablets	P4417-100TAB, Sigma, St. Louis, USA
Trizma® Base	T1503-1KG, Sigma, St. Louis, USA

Table 3.1.3: Continued

Boric Acid	1.00165.1000, Merck, Darmstadt, Germany
EDTA	E5134-500G, Merck, St. Louis, USA
Agarose Tablets	BIO-41027, Bioline, Luckenwalde, Germany
Ethidium Bromide	A1152,0025, AppliChem, Darmstadt, Germany
DNA ladder	BIO-33053, Bioline, Luckenwalde, Germany
Loading dye	B7024S, New England Biolabs, Ipswich, USA

3.1.4. Cloning Enzymes and Buffers

Table 3.1.4: List of cloning reagents

pGL3-Basic Luciferase Reporter Vector	E1751, Promega, Madison, USA
T4 DNA ligase	M0202S, New England Biolabs, Ipswich, USA
Ligation Buffer	B0202S, New England Biolabs, Ipswich, USA
KpnI-HF	R3142S, New England Biolabs, Ipswich, USA
SacI-HF	R3156S, New England Biolabs, Ipswich, USA
DpnI-HF	R0176S, New England Biolabs, Ipswich, USA
CutSmart Buffer	B7204S, New England Biolabs, Ipswich, USA

3.1.5. Microbiology Reagents and Solution Recipes

Table 3.1.5: List of microbiology reagents and solution recipes

Agar	1802.00, Conda, Madrid, Spain
NaCl	1.06404.1000, Merck, Darmstadt, Germany
Tryptone	LP0042, OXOID, Hampshire, England
Yeast Extract	1.03753.05000, Merck, Darmstadt, Germany
Ampicillin	8699828270126, Koçak Farma, Istanbul, Turkey
LB Agar	20 g Agar, 20 g NaCl, 10 g Tryptone, 5 g Yeast Extract per liter. Autoclave. 1000x Ampicillin is added around 56 ºC, in the final concentration of 1x
LB Broth	10 g NaCl, 10 g Tryptone, 5 g Yeast Extract per liter. Autoclave. 1000x Ampicillin is added after cooling, in the final concentration of 1x

3.1.6. siRNAs and Reagents

Table 3.1. 6: List of siRNA and Reagents

DNMT1 ON-TARGETplus siRNA	L-004605-00-0005, Dharmacon, Lafayette, USA
DNMT3B ON-TARGETplus siRNA	L-006395-00-0005, Dharmacon, Lafayette, USA
GAPDH ON-TARGETplus siRNA	D-001830-10-05, Dharmacon, Lafayette, USA
Non-Targeting ON-TARGETplus siRNA	D-001810-10-05, Dharmacon, Lafayette, USA
RNAse free 5x siRNAbuffer	B-0020000-UB-100, Dharmacon, Lafayette, USA

Table 3.1. 6: Continued

DharmaFECT Reagent 1	T-2001-03, Dharmacon, Lafayette, USA

3.1.7 qTRAP Buffers and Reagents

Table 3.1.7: List of qTRAP Buffers and Reagents

Hepes-KOH	sc- 286007A, ChemCruz, Dallas, USA
$MgCl_2$	MA00350500, Scharlau, Barcelona, Spain
KCl	P9541-500G, Sigma, St. Louis, USA
EGTA	E3889-100G, Sigma, St. Louis, USA
PMSF	830000-5G-F, Sigma, St. Louis, USA
Chaps	C3023-1G, Sigma Aldrich, St. Louis, USA
Beta-Mercaptoethanol	8.05740.0250, Merck, Darmstadt, Germany
Glycerol	K49564692 742, Merck, Darmstadt, Germany
Tween	8.22184.0500, Merck, Lyon, France
BSA	P6155-100GR, BioWest, Nuaillé, France
CHAPS Lysis Buffer	1 mM $MgCl_2$, 1 mM EGTA, 0.1 mM PMSF, 0.5% Chaps, 10% glycerol, 5 mM Beta-Mercaptoethanol, 10 mM Tris-HCl, complete to 10 ml with cell culture grade water. Store at +4°C
10 x QTRAP Buffer	200 mM Tris-HCl, 15 mM $MgCl_2$, 630 mM KCl, 0.5% Tween, 10 mM EGTA, 1mg/ml BSA, complete to 10 ml with cell culture grade water. Store at -20°C

3.1.8 Equipments Used

Table 3.1.8: List of Equipments Used

Thermal Cycler	T100, Biorad
Centrifuge	5810 R, Eppendorf
Centrifuge	Microfuge 16, Beckman Coulter
qPCR	Mic qPCR, Bio Molecular Systems
Incubator	Galaxy 170 R, New Brunswick
Laminar Flow	Class II Safety Cabinet, Metisafe
Microscope	DP71 CKX41, Olympus
pH meter	SevenEasy, Mettler Toledo
Spectrophotometer	ND-1000, Nanodrop
Power Supply	PS 1006 P, Apelex
Gel Tank	MSCHOICE7, Cleaver Scientific
Imaging Cabinet	Fluorchem FC3, Protein Simple
Luminometer	Lucetta, LONZA
Orbital Shaker	613.11.001, Isolab

3.2 Methods

3.2.1. Zebrafish Maintenance:

Wild-type zebrafish (AB) is used for tissue collection. All fish were kept in Techniplast aquarium system, with a 14:10 hour light: dark cycle. All fish are fed *ad-libitum*, twice with dry flakes and once with Artemia, on a daily basis.

3.2.2. Tissue Collection :

Fish used in tissue collection is given in Table 3.1.1 Age groups are determined as 8-, 13-, 19- and 25-month old. Fish are euthanized in ice-water for 10 minutes until the gills stop moving and decapitated with a scalpel in ice-cold 1 x PBS. Organs were dissected, snap frozen in liquid nitrogen and stored in - 80°C until DNA isolation. Gender determination is performed by direct gonadal examination. Samples with no visible gonad remained as undetermined and labeled as no gonad (NG). Experiments are approved by Bilkent University Animal Ethics Committee with approval number of 2014/18.

Table 3.2.1: List of zebrafish used in tissue collection.

Fish ID	**Sex**	**Length**	**Weight**	**Date of Birth**	**Date of Death**	**Age (Months)**
N1	F	4.3	0.79	06/05/2014	04/06/2015	13
N2	F	3.2	0.41	06/05/2014	04/06/2015	13
N3	NG	3.1	0.29	06/05/2014	04/06/2015	13
N4	F	3.4	0.36	24/10/2013	04/06/2015	19
N5	NG	4.5	0.94	24/10/2013	09/07/2015	25
N6	NG	4.0	0.54	24/10/2013	09/07/2015	25
N7	NG	3.5	0.54	24/10/2013	09/07/2015	25
N8	NG	4.0	0.51	24/10/2013	09/07/2015	25
N9	NG	4.0	0.57	24/10/2013	09/07/2015	25
N10	NG	4.2	0.87	24/10/2013	09/07/2015	25
N11	F	3.0	0.30	16/10/2014	09/07/2015	8
N12	F	3.2	0.31	16/10/2014	09/07/2015	8
N13	M	3.1	0.30	16/10/2014	09/07/2015	8
N14	F	3.1	0.32	16/10/2014	09/07/2015	8
N15	M	3.2	0.31	16/10/2014	09/07/2015	8
N16	M	3.2	0.27	16/10/2014	09/07/2015	8
N17	M	3.1	0.31	16/10/2014	09/02/2016	8

Table 3.2.1: Continued

Fish ID	Sex	Length	Weight	Date of Birth	Date of Death	Age (Months)
N18	F	4.5	1.25	17/12/2014	09/02/2016	13
N19	F	4.0	1.17	17/12/2014	09/02/2016	13
N20	F	4.3	1.22	17/12/2014	11/02/2016	13
N21	F	4.5	1.06	17/12/2014	11/02/2016	13
N22	M	3.7	0.51	09/07/2014	16/02/2016	19
N23	F	4.3	0.90	09/07/2014	22/02/2016	19
N24	F	4.5	0.78	09/07/2014	22/02/2016	19

3.2.3. Cell Culture:

Cell lines are cultured according to suggestions from ATCC's website and kept in 37°C with 5% CO2. A172, Daoy, SW1088, and WI-38 VA-13 subline 2RA are bought from ATCC and HEK293T cell line is provided by Aerts Kaya lab from Hacettepe University, PEDI-STEM. All cell lines are cultured in DMEM medium (BioWest) with 1% Penicillin-Streptomycin (Gibco), 1% L-glutamine (Gibco), 1% Non-Essential Amino Acids (BioWest) and 10% FBS (BioWest). Complete medium is renewed twice a week, and cells are passaged once in every week. A172, Daoy, and HEK293T are passaged in 1:10 ratio. SW1088 and WI-38 VA-13 subline 2RA are passaged in 1:5 ratio. Cells were routinely checked for mycoplasma contamination using BioWest's MycoKit.

3.2.4. DNA Isolation:

For genomic DNA isolation from zebrafish tissues, Qiagen's QIAamp DNA Mini kit is used according to the manufacturer's instructions. 180 µl Buffer ATL is added to tissues in 1.5 ml eppendorf tubes and 20 µl proteinase K added on top of the mixture. Tissues are disrupted with a sterile syringe, the mixture is vortexed and incubated overnight at 56°C. Completely lysed samples are briefly centrifuged and 200 µl Buffer AL is added. Samples are then incubated at 70°C for 10 minutes, briefly centrifuged and 200 µl 96-100% ethanol is added. Samples are mixed by vortexing for 15 seconds and briefly centrifuged. Mixture, including the precipitate, is transferred to QIAamp mini spin columns and centrifuged at 6000 x g for 1 minute. QIAamp mini spin column is transferred into a clean 2 ml collection tube and 500 µl Buffer AW1 is added onto the column matrix. Samples are centrifuged at 6000 x g for 1 minute and the QIAamp mini spin column is transferred into a new collection tube. 500 µl AW2 is added and centrifuged at 20,000 x g for 3 minutes. QIAamp mini spin columns are transferred into a 1.5 ml collection tube, 200 µl Buffer AE is added, incubated at room temperature for 1 minute and centrifuged at 6000 x g for 1 minute. Previous step is repeated by transferring the elute to the spin column. Eluted DNA concentration and elution quality is checked with Nanodrop ND-1000. Isolated zebrafish DNA samples are used in telomere length measurements, bisulfite conversion, and sequencing experiments.

For genomic DNA isolation from brain cancer cell lines, Qiagen's DNeasy Blood & Tissue kit is used according to manufacturer's instructions. Cells are collected, and centrifuged at 1500 x rpm for 5 minutes. Culture medium is removed, and the cell pellets are resuspended in 200 µl 1 x PBS. Following 20 µl proteinase K addition, 200 µl buffer AL is added to each tube, and mixed thoroughly by vortexing for 15 seconds. Tubes are incubated for 10 minutes at 56°C, and 200 µl 96-100% EtOH is added after the tubes are cooled down. Tubes are mixed thoroughly by vortexing, and the mixture is pipetted into a DNeasy Mini Spin Column. Columns are centrifuged at ≥ 6000 x g for 1 minute, and the flow-through is discarded. Spin column is placed into a new collection tube, and 500 µl buffer AW1 is added. Tubes are centrifuged at ≥ 6000 x g for 1 minute. After discarding the flow through, and collection tubes, and the spin column is placed into a new collection tube. 500 µl Buffer AW2 is added, and the tubes are centrifuged at maximum speed for 3 minutes. Column is transferred into a clean 1.5 ml eppendorf, and 50 µl Buffer AE is added directly onto the column matrix. After a 1-minute incubation at room temperature, samples are centrifuged at ≥ 6000 x g for 1 minute. For increased DNA yield, last step is repeated after reloading Buffer AE to the column matrix. Following DNA isolation, each samples concentration and quality is checked with Nanodrop ND-1000. Isolated DNA samples are used for TERT promoter amplification, and telomere length measurement experiments.

3.2.5. Bisulfite Conversion:

EpiTect Fast DNA Bisulfite kit (Qiagen), and EZ DNA methylation kit (Zymo Research) is used according to manufacturer's instructions. For EpiTect Fast DNA Bisulfite, these steps are followed. 25 µl (250 ng) DNA, 15 µl RNase-free water, 85 µl Bisulfite solution, and 15 µl DNA protect buffer is mixed in 0.2 ml PCR tube. Mixture is incubated at 95°C for 5 minutes, 60°C for 20 minutes, 95°C for 5 minutes, and 60°C for 20minutes in a thermal cycle. Upon completion of bisulfite conversion, PCR tubes are briefly centrifuged, and transferred into a clean 1.5 ml eppendorf tubes. 310 µl freshly prepared Buffer BL with 1% carrier RNA is added to each sample, vortexed, and briefly centrifuged. 250 µl 96-100% ethanol is added on top, vortexed for 15 seconds, and briefly centrifuged. Mixture is transferred into MinElute DNA spin columns, and centrifuged for 1 minute at 10,000 x g. Flow-through is discarded, and 500 µl Buffer BW is added to each spin column. Samples are centrifuged for 1 minute at 10,000 x g, flow through is discarded, and 500 µl Buffer BD is added to each spin column. Columns are incubated at room temperature for 15 minutes, and centrifuged for 1 minute at 10,000 x g. Flow-through is discarded, 500 µl Buffer BW is added, and samples are centrifuged at 10,000 x g for 1 minute. Last step is repeated once, and 250 µl 96-100% ethanol is added to each spin column. Samples are centrifuged for 1 minute at 10,000 x g, columns are transferred into new 2 ml collection tubes, and centrifuged for 1 minute at 10,000 x g. Columns are transferred into 1.5 ml eppendorf tubes, 15 µl Buffer EB is directly added onto the center of the spin column, and incubated 1 minute at room temperature. Following incubation, samples are eluted by centrifuging at 10,000 x g for 1 minute. Purified samples are stored at -20°C for long term storage.

For EZ DNA Methylation Lightning kit following procedure is performed. 130 µl Lightning Conversion Reagent is added to 20 µl DNA sample in 0.2 ml PCR tube, mixed, and briefly centrifuged. Mixture is incubated at 98°C for 8 minutes, and 54°C for 1 hour. 600 µl M Binding Buffer is loaded into Zymo spin IC column- collection tube assembly. Sample is loaded into the spin column with the M Binding Buffer, and mixed by inverting the tubes several times. Columns are centrifuged at full speed for 30 seconds, and the flow through is discarded. 100 µl M Wash Buffer is added into the column, centrifuged at full speed for 30 seconds, and the flow-through is discarded. 200 µl L-desulphonation Buffer is added, and the columns are incubated for 20 minutes in room temperature. Following incubation, samples are centrifuged at full speed for 30 seconds. Columns are washed twice by adding 200 µl M Wash Buffer to the column, and centrifuging at full speed for 30 seconds. Columns are then placed into 1.5 ml eppendorf tubes, and 10 µl M Elution Buffer is directly added to the column matrix. Samples are centrifuged at full speed, and eluted samples are stored at -20°C for short term, and -80°C for long term storage.

Bisulfite treated DNA is quantified with Nanodrop ND-1000 with RNA quantification settings, where 40 ug/ml for Ab260 is equal to 1.

3.2.6. PCR for TERT Promoter Sites:

PCRs are performed for amplifying core, and distal TERT promoter area from different cell lines while adding restriction enzyme recognition site at each end of the product. Primer pair for core promoter is TERT 4F: 5'- GGT ACC TCG CCG CAC GCA CCT GTT -3', and TERT 2R: 5'-GAG CTC CAC GAA CGT GGC CAG CGC-3'. For distal promoter area TERT 5F: 5'-GGT ACC ACC AGT GGC CGT GTG GCT T-3' with TERT 2R. Thermo Scientific's Phusion High Fidelity Master Mix with High GC content is used for reactions. 50 ng of genomic DNA is used as a template. Each reaction contains 10 µl 2x Phusion Master Mix, 0.5 µl of each primer, and 0.4 µl DMSO for distal promoter amplification or 0.8 µl DMSO for core promoter amplification. Volume is completed to 20 µl with PCR grade water. Annealing temperature is decreased to 68.5°C from 69.4 for distal promoter, and decreased to 71.1°C from 72.9°C for core promoter by adding DMSO. Cycling conditions are 98°C for 90 seconds (initial denaturation), 98°C for 10 seconds, 68.5-71.1°C for 20 seconds, 72°C for 30 seconds (total of 30 cycles), and 72°C for 5 minutes (final extension). Expected PCR product is 1144 bp for the distal, and 574 for the core promoter site.

To increase restriction enzyme digestion efficiency, six random nucleotides are added before the restriction enzyme recognition site by PCR. Both for core, and distal promoter new TERT reverse: 5'- ATG TAG GAG CTC CAC GAA CGT GGC -3' is used. For core promoter area new TERT 4F: 5'- GTA ATA GGT ACC TCG CCG CAC GCA -3' is used, and for the distal promoter area new TERT 5F: 5'- GTA TGA GGT ACC ACC AGT GGC CGT G -3' is used as forward primer. 15 ng PCR product is used as template DNA in a 50 µl reaction. 4%, and 2% DMSO is used for core, and distal promoter amplification, respectively. Final primer concentration was 0.1 uM for each reaction. Cycle conditions are 98°C for 1 minute 30 seconds (initial denaturation), 98°C for 10 seconds, 69.4°C for 20 seconds, 72°C for 30 seconds (total of 30 cycles), and 72°C for 5 minutes (final extension). Expected PCR product size is 1156 for the distal, and 582 for the core promoter site. All PCR products are run on 1% agarose gel for 1 hour, and cleaned up with PureLink PCR purification kit before restriction enzyme digestion.

3.2.7. PCR for Bisulfite Sequencing:

Zebrafish TERT promoter sites are amplified following bisulfite treatment for sequencing. ZymoTaq Premix (Zymo Research) is used for PCRs. Tert-CpG F: 5'-ATA GTA GGA TAG GGT TTT GGT TTT G-3', and Tert-CpG R: 5'-CCT TCA ATT CTT CAA AAA ATT AAC TC-3' are used for promoter amplifications. Each 50 µl reaction is consisted of 25 µl ZymoTaq Premix, 2 µl forward primer, 2 µl reverse primer, 4 µl bisulfite converted DNA, and 17 µl PCR grade water. Cycling conditions are 95°C for 7 minutes (initial denaturation), 95°C for 1 minute, 54°C for 2 minutes, 72°C for 2 minutes (total of 40 cycles), and 72°C for 10 minutes (final extension). Expected product size is 232 bp. All PCR products are run on 1.5% agarose gel for 1 hour. Amplified reactions are sent for Sanger sequencing. Sequence alignments are done on ApE-A Plasmid Editor v2.0 (by Wayne Davis) to reference sequence obtained from ZFIN Data on GRCz10 for TERT gene.

3.2.8. PCR Clean Up:

PureLink PCR purification kit (Invitrogen) is used for PCR products. 4 volumes of Binding Buffer HC (B3) with isopropanol is added to 1 volume of PCR sample, and mixed thoroughly by pipetting. Sample is loaded into a PureLink Spin Column in a collection tube, and centrifuged at >10,000 x g for 1 minute. Flow through is discarded, and 650 μl Wash Buffer W1 with ethanol is added onto the column matrix. Samples are centrifuged at >10,000 x g for 1 minute, and the flow through is discarded. After returning the spin column back to the same collection tube, tubes are centrifuged at maximum speed for 3 minutes. Columns are then transferred into a new 1.5 ml eppendorf, and 50 μl elution buffer is added to the center of the column. Following 1 minute incubation at room temperature, samples are centrifuged at maximum speed for 3 minutes. Purified PCR products' concentration and quality is checked with Nanodrop ND-1000, and stored at 4°C.

3.2.9. Restriction Enzyme Digestion:

KpnI-HF, SacI-HF, and DpnI-HF restriction enzymes are bought from NEB, and stored at -20°C upon arrival. KpnI-HF, and SacI-HF are used for pGL3-Basic (Promega), and TERT promoter digestion. DpnI-HF is used for digestion of template DNA from site-directed mutagenesis PCRs. For each digestion reaction, 1 microgram of DNA is used. For double digestion, DNA sample volume is completed to 43 μl with Nuclease free water. For DpnI digestion, the volume is completed to 44 μl with Nuclease Free water. 5 μl 10x SmartCut Buffer is then added to PCR tubes containing DNA, and water. 1 μl of KpnI-HF, and 1 μl of SacI-HF are used in pGL3, and TERTp digestion reactions, and 1 μl of DpnI-HF is used for site directed mutagenesis samples. All reactions are set up on ice, and incubated at 37°C for 15 minutes. For inactivation of double digestion, tubes are incubated at 65°C for 20 minutes. For DpnI digestion inactivation, tubes are incubated at 80°C for 20 minutes.

3.2.10. DNA Clean Up:

Zymo DNA clean and concentrator kit is used according to manufacturer's protocol with minor modifications to clean up restriction enzyme digested pGL3-Basic, and TERTp samples prior to ligation reaction. Five volumes of DNA binding buffer is added to each volume of PCR product. The mixture is loaded into the Zymo Spin Column, and centrifuged at 11,000 x g for 1 minute. 200 µl DNA Wash Buffer is added directly to the column, and centrifuged at 11,000 x g for 1 minute. Wash step is repeated, and the column is transferred into a clean 1.5 ml eppendorf. 25 µl DNA elution buffer is added directly to the center of the column, and centrifuged at 11,000 x g for 1 minute. Eluted PCR samples are quantified using Nanodrop ND-1000.

3.2.11. DNA Ligation:

1:3 molar ratio of plasmid: insert is used in core promoter ligation reactions, and 1:5 molar ratio is used for distal core ligation reactions. All calculations are made using NEBioCalculator (New England Biolabs). Length of pGL3-Basic is 4818 bp. Insert length is 538 for new TERT 2R-4F reaction (core promoter), and 1150 for new TERT 2R-5F reaction (distal promoter). 28,6 ng pGL3-Basic is used for both ligation reactions. For core promoter ligation, 15.99 ng DNA is used, and for distal promoter ligation 34 ng DNA is used. 2 µl 10 x T4 DNA ligase buffer is added to tube containing vector, insert, and water. 1 µl T4 ligase is then added on ice, and reaction is incubated at room temperature for 10 minutes. Ligation product is directly used for transformation without further steps.

3.2.12. Transformation:

Ligation and DpnI-HF digestion products are directly used for transformation without further isolation steps. Chemically competent Jm109 strain of E. coli is used for transformation. For ligation reactions, 5 µl is mixed with 50 µl bacteria on ice. For digestion reactions, 2 µl is mixed with 50 µl bacteria on ice. After incubation at 4°C for 5 minutes, 200 µl LB without antibiotics is added on tubes containing bacteria, and plasmid DNA. Bacteria is incubated for 1 hour at room temperature, and then spread on LB plates with Ampicillin. Plates are incubated at 37°C overnight, and colony PCR is performed to check formed colonies.

3.2.13. Colony PCR:

Colonies are numbered on the plate, and touched with the pipette tip without contacting the agar. Tips are then submerged into 20 µl PCR grade water, and then put into 15 ml falcons containing 1 ml LB with Ampicillin. Tubes containing PCR grade water: bacteria suspension are incubated at 95°C for 15 minutes following 12°C for 15 minutes. After cooling down, samples are spun down briefly, and kept on ice. For PCRs Taq DNA Polymerase 2x master mix (Ampliqon) is used. RVprimer3: 5'- CTA GCA AAA TAG GCT GTC CC- 3', and GLprimer2: 5'- CTT TAT GTT TTT GGC GTC TTC CA -3' are used as primers. 10 µl reaction contains 5 µl enzyme premix, 0.2 µl of each primer, 4.1 µl PCR grade water, and 0.5 µl bacteria sample. Cycle conditions are 95°C for 2 minutes (initial denaturation), 95°C for 20 seconds, 50.1°C for 20 seconds, 72°C for 1 minute (30 cycles), 72°C for 5 minutes (final extension). Expected band size is 1220 bp for vector construct containing the distal promoter site, and 675 bp for vector construct containing the core promoter site. All PCR products are run on 1% agarose gel for 1 hour.

3.2.14. Plasmid Isolation:

Zyppy Plasmid Miniprep (Zymo), and ZymoPure Plasmid Maxiprep (Zymo) kit are used for plasmid isolation following the manufacturer's instructions. Mini prep products are used for sequencing, and maxi prep products are used for transfection experiments. For mini prep, 600 µl of bacterial culture grown in LB is transferred into a clean 1.5 ml eppendorf, and 100 µl 7x Lysis Buffer is added. Tube is mixed by inverting 4 to 6 times, and incubated for 2 minutes. After complete lysis, 350 µl ice cold Neutralization buffer is added, and mixed thoroughly. Sample turns yellow, and precipitate is formed when the neutralization is completed. Then the sample is centrifuged at > 11,000 x g for 4 minutes. Transfer the supernatant without disturbing the pellet into a Zymo-Spin IIN column in a collection tube. Centrifuge the samples for 15 seconds at > 11,000 x g, and discard the flow-through. Return the Zymo-Spin IIN column to the collection tube, and 200 µl Endo-Wash buffer. Centrifuge the samples for 30 seconds at > 11,000 x g, and discard the flow-through. 400 µl Wash buffer is then added to the column, and the samples are centrifuged for 1 minute at > 11,000 x g. The column is transferred into a clean 1.5 ml eppendorf, and 30 µl Elution buffer is directly added to the column matrix. Following 1 minute of incubation, samples are centrifuged at > 11,000 x g for 1 minute to elute the plasmids.

For maxi prep, 150 ml bacterial culture grown in LB is centrifuged at ≥ 3,220 x g for 10 minutes to pellet the cells. Bacterial cell pellet is resuspended completely with 14 ml ZymoPure P1, and then 14 ml ZymoPure P2 is added. Following addition, immediately mix gently by inverting the tube 6 times, and incubate at room temperature for 3 minutes. When the cells are completely lysed, it turns into clear purple, and the solution appears viscous. 14 ml ZymoPure P3 is added, and mixed thoroughly but gently by inverting the tubes. Solution turns into yellow, and a yellow precipitate is formed when the neutralization is completed. ZymoPure syringe filter is placed upright in a tube rack, the lysate is loaded into it, and incubated 8 minutes at room temperature. When the precipitate is floated to the top, luer lock plug is removed from the bottom of the syringe, and placed into a clean 50 ml falcon tube. Plunger is placed in the syringe, and the solution is pushed through the filter until 35 ml of cleared lysate is recovered. 14 ml ZymoPure Binding buffer is added to cleared lysate, and mixed thoroughly by inverting the tube 10 times. 50 ml reservoir is removed from the top of the ZymoSpin V-P Column Assembly and placed into a 50 ml falcon tube. It is important to make sure that the connection between the 15 ml conical reservoir, and V-P column is finger tight. 14 ml of the mixture is added to 15 ml conical reservoir & V-P column assembly, and centrifuged at 500 x g for 2 minutes. This step is repeated until the entire sample is passed through the column, and the 50 ml falcon is emptied in between the centrifuge steps. 5 ml ZymoPure Wash 1 buffer is added to the column, and centrifuged at 500 x g for 2 minutes. After the 50 ml falcon is emptied, and the column is placed back into it, 5 ml ZymoPure Wash 2 buffer is added to the column, and centrifuged 2 minutes at 500 x g. This step is performed twice. The V-P column is removed from the 15 ml conical reservoir, and placed in a collection tube. V-P column in collection tube is centrifuged at ≥ 10,000 x g for 1 minute to remove buffer residues, and transferred into a clean 1.5 ml eppendorf. 400 µl ZymoPure Elution Buffer is added directly to the column matrix, incubated at room temperature for 10 minutes, and centrifuged at ≥ 10,000 x g for 1 minute in a micro centrifuge. Following plasmid isolation all samples are quantified with Nanodrop ND-1000.

3.2.15. Site Directed Mutagenesis of TERT Promoter:

Isolated plasmid containing A172 TERTp distal is serially diluted so that final concentration was 1,3 ng/µl. Used primers, and final concentration used in PCRs are shown in Table 3.2.2. 2x Phusion Mater Mix with High GC (Thermo Scientific) is used for mutagenesis PCRs. For primer pairs with annealing temperatures higher than 72°C DMSO is added to reactions. Final DMSO percentages are listed in Table 3.2.3. Each reaction contains 10 µl 2x Phusion premix, 1 µl plasmid, 2 µl forward, and reverse primer mix, and completed to 20 µl with PCR grade water or PCR grade water: DMSO mixture. For SDM PCRs cycle conditions are 98°C for 1 minute (initial denaturation), 98°C for 10 seconds, 72°C for 2 minutes 15 seconds (30 cycles), and 72°C for 5 minutes (final extension) except primer pair 11. Cycle conditions for this construct is 98°C for 1 minute (initial denaturation), 98°C for 10 seconds, 70.8°C for 15 seconds, 72°C for 1 minute (30 cycles), and 72°C for 5 minutes (final extension). All SDM PCR products are run on 1% agarose gel for 1.5 hour.

Table 3.2.2: Primer pairs used in site directed mutagenesis experiments, and final concentrations in the reaction.

Primer Pair	**Forward Primer (5' to 3')**	**Reverse Primer (5' to 3')**	**Final Primer Mix Concentration**
SDM 1	GCGCACGTAATAGCC CTGGCCCCGGC	CAGGGCAATTACGT GCGCAGCAGGAC	0.5 uM
SDM 2	GCGAGTTTCCGGCAG CGCTGCGTCCTG	AGCGCTGCCGGAAA CTCGCGCCGCGAG	0.5 uM
SDM 3	CCGCGGCCATACCCT CTCCTCGCGGCG	GGAGAGGGTATGG CCGCGGAAAGGAA G	0.1 uM
SDM 4	CCTTTCCAAGGCCCC GCCCTCTCC	CGGGGCCTTGGAAA GGAAGGGGAG	0.5 uM
SDM 5	GCCCTCCCATACCCTC CCCTTCCTTTC	GGGGAGGGTATGG GAGGGCCCGGAGG G	0.1 uM
SDM 6	CAGCCCCTTCCGGGC CCTCCCAG	GCCCGGAAGGGGCT GGGCCGGGG	0.1 uM
SDM 7	GGTCCCCGAACCAGC CCCCTCCGGGC	GGGGCTGGTTCGGG GACCCGGGAGGG	0.1 uM
SDM 8	GACCCCTCCCGGGTC CCCGGCCC	GACCCGGGAGGGG TCGGGACGGG	0.5 uM
SDM 9	GGACCCCGAACCGTC CCGACCCCTCC	CGGGACGGTTCGGG GTCCGCGCGGAG	0.05 uM
SDM 10	GCCTCCTCCAAGCGG ACCCCGCCCCGTC	GGGGTCCGCTTGGA GGAGGCGGAGCTG G	0.1 uM

Table 3.2.2: Continued

Primer Pair	Forward Primer (5' to 3')	Reverse Primer (5' to 3')	Final Primer Mix Concentration
SDM 11	CCTTCCATATCCGCCT CCTCCGCG	AGGCGGATATGGA AGGTGAAGGGG	0.5 uM
SDM 12	CCCGGGTCCAACCGG AGCAGCTGCGCTG	CTGCTCCGGTTGGA CCCGGGGGTCTGGG	0.1 uM
SDM 13	GAAGCGCGAACCAGA CCCCCGGGTCC	GGGTCTGGTTCGCG CTTCCCCGCCCG	0.1 uM
SDM 15	CTGGAGGCAAACCTG GGTCTCCGGATC	GACCCAGGTTTGCC TCCAGGTCCGGAC	0.1 uM
SDM 16	CGCCCCGTATCCGGA CCTGGAGGC	GTCCGGATACGGGG CGTCGGGCTC	0.5 uM
SDM 17	CGTCCCCATTCGCGTC TACGCGCCTC	TAGACGCGAATGGG GACGAACCCGAG	0.25 uM
SDM 18	CCCTCGCCTTCTGAG AACCTGCAAAG	GTTCTCAGAAGGCG AGGGGTCCCCAC	0.5 uM
SDM 19	GACGGGACCTATCCG GTGGGTGATTAAC	CCCACCGGATAGGT CCCGTCGAGAAAAG	0.5 uM
SDM 20	GTGCCGGGTTCCAGG GTCAAGGCCG	ACCCTGGAACCCGG CACTCTGTCTG	0.1 uM

Table 3.2.3: Final DMSO concentration in the site directed mutagenesis reactions

Primer Concentration	Final DNMSO Concentration	Primer Concentration	Final DNMSO Concentration
SDM 1	%10	**SDM 11**	%0
SDM 2	%10	**SDM12**	%10
SDM 3	%10	**SDM 13**	%10
SDM 4	%0	**SDM 15**	%10
SDM 5	%10	**SDM 16**	%0

Table 3.2.3: Continued

Primer Concentration	**Final DNMSO Concentration**	**Primer Concentration**	**Final DNMSO Concentration**
SDM 6	%10	**SDM 17**	%0
SDM 7	%10	**SDM 18**	%0
SDM 8	%10	**SDM 19**	%0
SDM 9	%10	**SDM 20**	%8
SDM 10	%10		

3.2.16. Transfection:

All cell lines are plated 24 hours before transfection to 6 well plates with 25 to 50% confluency depending on their doubling time. Per each well of a 6 well plate, 200 µl of serum free DMEM F12 is mixed with 2 ug plasmid DNA, and 4 µl transfex transfection reagent (ATCC) under the laminar flow. Mixture is vortexed, centrifuged briefly, and incubated 15 minutes at room temperature. Medium is meanwhile replaced with 2 ml complete DMEM F12 without P/S. After the incubation is done, 200 µl of transfex: plasmid complex is added to the different areas of the wells in a drop wise manner, and incubated 24 hours at 37°C with 5% CO2. For 24 well plates, components of the mixture are scaled down by 4.

3.2.17. Luciferase Assay:

Four volumes of cell culture grade water is mixed with 5 x cell culture lysis reagent (Promega), and equilibrated to room temperature prior starting the protocol. At the 24th hour of transfection, growth medium is removed, and cells are rinsed with 1 x PBS. For 6 well plates, 128 µl lysis buffer is added, culture plates are rocked several times, and then the cells are scraped. Scraped cells are transferred into 1.5 ml eppendorf tubes, and put on ice. Each sample is vortexed 15 seconds, and centrifuged at 12,000 x g for 15 seconds at room temperature. Supernatant is transferred into a new 1.5 ml eppendorf. 20 µl of the cell lysate is set aside for luciferase assay, and the rest is stored at -70°C. Luciferase assay reagent is thawed at room temperature, and equilibrated to room temperature with the samples. 100 µl of the luciferase assay reagent is dispensed to luminometer tubes for each sample. Luminometer (Lucetta Single Tube Luminometer, LONZA) is programmed to perform 2 seconds measurement delay following a 10 seconds measurement read. 20 µl cell lysate is added to luminometer tube, and mixed by pipetting up, and down for 3 times. The tube is placed in the luminometer, read is initiated and recorded.

3.2.18. siRNA Transfection:

DNMT1, DNMT3B, GAPDH, and Non Targeting ON-TARGETplus siRNAs are purchased from Dharmacon, GE Healthcare. 5 nmol siRNA pellet is resuspended in 100 µl RNase free 1x siRNA buffer by pipetting up, and down 3-5 times. Tubes are securely sealed, and placed on orbital mixer for 30 minutes at room temperature. Tubes are briefly centrifuged, and quantified with Nanodrop ND-1000. For siRNA 13.3 ng/µl is equal to 1uM. 20 uM siRNA stocks are aliquoted, and stored at -20°C.

A172, Daoy, SW1088, and WI-38 VA-13 subline 2RA are plated one-day prior transfection to 6, 24 or 96 well plates. 5 uM siRNA solution is prepared with 1x siRNA buffer from 20 uM stock solution. In separate tubes siRNA, and DharmaFECT transfect reagent 1 is diluted with serum free antibiotic free DMEM-F12. For each well of 6 well plates, 10 µl of 5 uM siRNA is mixed with 190 µl medium (tube 1), and 2 µl DharmaFECT reagent is mixed with 198 µl medium (tube 2). Contents of the tubes are gently mixed by pipetting, and incubated for 5 minutes at room temperature. Tube 1 and Tube 2 is mixed by pipetting, and incubated for 20 minutes at room temperature.

1600 µl complete medium without antibiotic is added to achieve transfection medium with 25 nM final siRNA concentration. Culture medium is aspirated from wells, 2 ml transfection medium is added to each well, and cells are incubated at 37°C with 5% CO_2. At 24 hours post transfection, medium is changed with complete culture medium to reduce cytotoxicity. Cells are incubated 48 hours post transfection for gene expression analysis, and 96 hours post transfection for protein analysis.

3.2.19. Azacytidine and Adriamycin Treatment of Cell Lines:

20 uM Azacytidine (Er-kim), 10 nM Azacytidine (Er-kim), and 10 nM Adriamycin (Saba İlaç) treatments are used as positive controls for Beta Galactosidase staining experiments. 20 uM Azacytidine is used for positive controls for qPCR experiments. A172, Daoy, SW1088, and WI-38 VA-13 subline 2RA seeded onto 6 (for qPCR) or 96 well plates (for Beta Galactosidase staining) one-day prior treatment. Stocks are diluted in complete medium, and added to the cell culture plates. Mediums with anticancer drug are replaced with complete medium at the 24th hour, and cultured until 96 hours post treatment.

3.2.20. RNA Isolation:

At 48-hour post siRNA transfection, growth medium is removed, and cells are rinsed with 1x PBS twice. Cell are trypsinized, collected, and centrifuged at 500 x g for 5 minutes. Pellets are washed with 1 x PBS once, centrifuged at 500 x g for 5 minutes, and placed on ice after the supernatant is discarded. RNeasy Mini Kit (Qiagen) is used for RNA isolation from cell lines, and all steps are performed at room temperature. 20 µl 2M DTT is added per 1 ml of buffer RLT prior starting the RNA isolation. 350 µl RLT buffer with DTT is added to the cell pellet, and the pellet is resuspended. Following resuspension 350 µl freshly prepared 70% ethanol is added to each sample, and the mixture is transferred to the column. Columns are centrifuged at

≥ 8,000 x g for 15 seconds, and the flow through is discarded. 350 µl buffer RW1 is added, and the samples are centrifuged at ≥ 8,000 x g for 15 seconds. To eliminate DNA carryover, RNase-free DNase Set (Qiagen) is used. 10 µl of DNase I stock is mixed with 70 µl buffer RDD, mixed by inverting the tube, and quick spun. 80 µl DNase I working solution is added directly to the column matrix, and incubated at room temperature for 15 minutes. 350 µl buffer RW1 is added on top following the incubation, and samples are centrifuged at ≥ 8,000 x g for 15 seconds. Flow through is discarded, placed back to the collection tube. 700 µl buffer RW1 is added, and centrifuged at ≥ 8,000 x g for 15 seconds. Flow through is discarded, 500 µl RPE is added, and centrifuged at ≥ 8,000 x g for 15 seconds. 500 µl RPE buffer is added again, and centrifuged at ≥ 8,000 x g for 2 minutes. Columns are transferred into a new collection tube, and centrifuged at maximum speed for 1 minute to eliminate RPE buffer remains. Columns are transferred into 1.5 ml eppendorf tubes, and 30 µl RNase free water is added directly to the column matrix. After centrifugation at ≥ 8,000 x g for 1 minute. Concentration, and quality of RNA samples are measured with Nanodrop ND-1000. Samples are stored at -20°C for short term, and at -80°C for long term storage.

3.2.21. cDNA Synthesis:

Transcriptor HighFidelty cDNA synthesis kit (Roche) is used for cDNA synthesis. Kit reagents are thawed on ice prior to use. For Daoy, A172, and WI-38 VA-13 subline 2RA 3 ug RNA is used for cDNA synthesis. For SW1088 1 ug RNA is used for cDNA synthesis. 1 µl anchored oligo(dt) primer is added to RNA samples in PCR tubes. Volume of the tube is completed to 11,4 µl with nuclease free water. Reagents are mixed, centrifuged briefly, and incubated at 65°C for 10 minutes. After the incubation is done, tubes are immediately placed on ice. 4 µl 5x reaction buffer, 0.5 µl RNase inhibitor, 2 µl dNTP mix, 1 µl DTT, and 1,1 µl reverse transcriptase are added to each RNA: primer: water mix on ice. Tubes are mixed carefully, briefly centrifuged and placed into a thermal cycler with a heated lid. Samples are incubated at 50°C for 30 minutes, and 85°C for 5 minutes. After the incubation is done, samples are diluted with nuclease free water, and stored at -20°C until further use.

3.2.22. qPCR:

Sensifast SYBR No ROX 2x master mix (Bioline) is used for qPCR experiments. Primers are listed in Table 3.2.4. For 20 µl reaction, each tube contains 10 µl 2x master mix, 2 µl primer mix or 1 µl of each primer, 6 µl PCR grade water, and 2 µl cDNA. Reactions are carried out in Mic qPCR (Bio Molecular Systems). Cycle conditions are 95°C for 2 minutes (initial denaturation), 95°C for 5 seconds, 60°C for 10 seconds, and 72°C for 20 seconds, total of 45 cycles. Gene expression is calculated by normalizing to RPL13A (neuro-housekeeping gene), and delta delta Ct method.

Table 3.2.4: List of qPCR primers.

Primer pair	**Forward (5’ to 3’)**	**Reverse (5’ to 3’)**
ATRX	CGCTGAGCCCATGAGATAAA	AGTGCAGCTCACAATCCCAT
CBX3	TGTACAGGAGAGTTCGCTGC	GAGCTATTACGTTCGCGGC
DAXX	CGAGAGACGGTTTCTGAGCAGG	GCTGTTAGCGGTGGCCATA
DNMT1	TGGAAAGAGACAGCTTAACAGAA	CGTAATTTGGTTTCCAAGTCACATA
DNMT3A	ACCGGCCATACGGTGGA	GTGTTGAGCCCTCTGGTGAA
DNMT3B	TCGTGCAGGCAGTAGGAAAT	GCCATTTGTTCTCGGCTCTG

Table 3.2.4: Continued

Primer pair	Forward (5’ to 3’)	Reverse (5’ to 3’)
FEN1	CCGCTAAGCTGAGAAGGGAG	GGAGGGATGACTGGCCTTTG
RPL13A	AGCCTACAAGAAAGTTTGCC TAT	TCTTCTTCCGGTAGTGGATC TTGGC
TERT	TGTCAAGGTGGATGTGACGG	GAGGAGCTCTGCTCGATGAC
TR	CCCTAACTGAGAAGGGCGTA	AGAATGAACGGTGGAAGGC G
TRF2	AGCCCTACCTCCTCACGATG	AGGATTCCGTAGCTGCCTTG
WRN	GAAAGAAAGGCATGTGTTCG GA	TGGGGAAAAACTGACATGG AAGA

3.3.23. Population Doubling Assay:

Cells are counted with Bürker counting chamber prior seeding to 24 well plates, and incubated at 37°C with 5% CO2 for 96 hours, post siRNA or cytotoxic drug treatment. Cells are washed with 1x PBS twice, trypsinized, and counted. Formulas for population doubling assays are given below.

Cells underwent n population doublings = 3.32 x (log (Number of cells harvested)-log(Number of cells inoculated))

Multiplication rate (r) = 3.32 x (log (Number of cells harvested)-log (Number of cells inoculated))/(t2-t1)

Population doubling time (PDT) = 1/r

3.3.24. Beta Galactosidase Staining:

To measure replicative senescence, SA *β-gal* staining kit (9860S, Cell Signaling Technologies) is used according to manufacturer’s suggestions. Fixative solution is diluted to 1x with dH2O prior starting to staining protocol. Culture medium is aspirated, and each well is washed with 500 µl 1 x PBS for 24 well plates. PBS is removed, 250 µl 1x fixative solution is added, and cells are incubated for 15 minutes at room temperature. Staining solution is prepared by re-dissolving 10x staining solution at 37°C while shaking, and diluting to 1x. For each well, Beta Galactosidase staining solution is prepared by mixing 232.5 µl staining solution, 2.5 µl staining solution supplement A, 2.5 µl staining solution supplement B, and 12.5 µl 20 mg/ml X-gal in DMF. pH should be between 5.9 and 6.1 for successful staining. After staining, fixative solution is aspirated, and wells are washed twice with 500 µl 1x PBS. 250 µl Beta Galactosidase staining solution is added, and cells are incubated at 37°C over-night in a dry incubator. Cells are checked for blue color development, beta gal staining solution is removed, 70% glycerol is added, and wells are imaged using Olympus DP71 CKX41. Plates are stored at 4°C after imaging. Image quantification is done using Fiji (ImageJ) software. Unbiased and blind measurements were followed in counting.

3.3.25. Telomere Length Measurement:

Fast Start SYBR Green Master (Roche) is used for telomere length measurements in zebrafish tissues. DNA samples are diluted to 10 ng/µl, and measured with Nanodrop ND-1000 prior setting up the reaction. Primer pairs are listed below in the Table 3.2.5. 20 µl reaction contains 10 µl 2x Fast Start SYBR Green Master, 2 µl DNA,2 µl primer mix, and 6 µl PCR grade water. Reactions are performed in a LightCycler® 480 (Roche). Cycle conditions are 95°C for 10 min (initial denaturation), 95**°C** for 15 seconds, and 60°C for 1 minute (total of 40 cycles). Relative telomere length is calculated by the formula 2^-(Cttelo- Ctp3dio).

Sensifast SYBR No ROX 2x master mix (Bioline) is used for telomere length measurements in cell lines. DNA samples are diluted to 10 ng/µl, and measured with

Nanodrop ND-1000 prior starting the protocol. Primer pairs are listed below in the Table 3.2.5. 20 µl reaction contains 10 µl 2x master mix, 2 µl DNA, 2 µl primer mix, and 6 µl PCR grade water. Reactions are carried out in Mic qPCR (Bio Molecular Systems). Cycle conditions are 95°C for 3 minutes (initial denaturation), 95°C for 5 seconds, 60°C for 15 seconds, and 72°C for 20 seconds, total of 40 cycles. Relative telomere length is calculated by the formula 2^-(Cttelo- Ct36b4).

Table 3.2.5: List of telomere length measurement primers.

Primer pair	**Forward (5' to 3')**	**Reverse (5' to 3')**
zebrafish-Telo	ATAGTAGGATAGGGTTTGGTTTTG	CCTTCAATTCTTCAAAAATTAACTC
zebrafish-P3dio	GGGGACGGCAGAAGAAATGA	AGGTCCACACTAAGCAAGCC
human-Telo	CGGTTTGTTTGGGTTTGGGTTTGGGTTTGGG TTTGGGTT	GGCTTGCCTTACCCTTACCCTTACCCTTACCCTTACCCT
human-36B4	CAGCAAGTGGGAAGGTGTAATCC	CCCATTCTATCATCAACGGGTACAA

3.3.26. qTRAP:

Culture medium is removed, washed twice with 1x room temperature PBS, and trypsinized. Cells are counted with a Bürker counting chamber. 300.000 cells are centrifuged at 500 x g for 5 minutes, and resuspended in 1 ml 1x room temperature PBS. Cells are centrifuged at 650 x g for 5 minutes at 4°C. PBS is removed, and 75 µl freshly prepared 1x Chaps Lysis is added. Samples are incubated for 30 minutes on ice, and then centrifuged at 14.000 rpm for 20 minutes at 4°C. Cell lysate is transferred into a new tube, aliquoted, and stored at -80°C until use. ACX: 5'- GCG CGG CTT ACC CTT ACC CTT ACC CTA ACC-3' and TS: 5'- AAT CCG TCG AGC AGA GTT-3' used as primers. Components, and cell lysates are thawed on ice prior to use.

5 µl cell lysate (4000 cells/µl) is mixed with 0.9 µl 10x TRAP buffer, 0.4 µl 10 mM dNTP, 1ul 14.49 uM primer TS, 1 µl 1 mg/ml BSA, and 0.6 µl PCR grade water. Samples in 0.2 ml PCR tubes are incubated at 30°C for 30 minutes, and at 95°C for 5 minutes. Tubes are immediately put on ice. Mixture of 10 µl 2x Sensifast SYBR master mix, 1 µl 4.44 uM primer ACX, and 0.1 µl 10x TRAP buffer is added. Reactions are transferred into mic qPCR tubes, and placed inside the instrument. Cycle conditions are 95°C for 2 minutes (initial denaturation), 95°C for 5 seconds, 50°C for 6 seconds, and 72°C for 10 seconds (total of 45 cycles), followed by a melt curve. Calculations are made by plotting a standard curve using positive control dilution series vs. log10 of number of cells. Unknown test sample data is converted to relative telomerase activity by using the linear equation.

3.3.27. Statistical Analysis:

The GraphPad Prism 8 (GraphPad Software, Inc.) was used for statistical analysis. For zebrafish experiments homogeneity of variance is tested with Kolmogorov-Smirnov and Sharpio-Wilk tests. For cases with equal variance univariate analysis of ANOVA is used, followed by Tukey's test. For cases with unequal variance, non-parametric Kruskal-Wallis test is used, followed by Dunn's test. For human cell line experiments, homogeneity of variance is tested with Sharpio-Wilk tests. In Luciferase assay experiments, RM One-Way ANOVA with Geisser-Greenhouse correction and Sidak's multiple comparison is used for data analysis. In population doubling time experiments and Beta-Galactosidase staining experiments, Ordinary One-Way ANOVA with Dunnet's multiple comparisons is used for data analysis. In qTRAP experiments, Ordinary One-Way ANOVA with Geisser-Greenhouse correction and Sidak's multiple comparisons is used for data analysis. In gene expression analysis experiments, Ordinary One-Way ANOVA with Dunnet's multiple comparisons is used in the analysis. In all experiments, a cut off of $p<0.05$ is used for statistical significance determination.

CHAPTER 4

RESULTS

4.1. Telomere Lengths Change Throughout Aging in All Organs

Comparison of telomere length during aging in different zebrafish organs are shown in Figure 4.1 and 4.2. In heart samples, telomere length increases after the 8th month and stay relatively high until the 19th month. Kruskal-Wallis test for multiple comparison showed significant effect of age on telomere lengths in heart samples (KW=10.34, p=0.0159). The Dunn's test revealed a significant change in telomere length at 19th and 25th months of age in heart. In brain samples, telomere length seems to fluctuate between ages. Telomeres lengthen between the 13th and the 19th months, reaching the lowest levels at 25 months of age. Kruskal-Wallis test shows a significant effect of age on telomere lengths in brain samples (KW=8.958, p=0.029). With uncorrected Dunn's test, we found significant change in telomere length between 8- and 25-month (p=0.0113) and 19- and 25-month (p=0.0241) For heart and brain samples, transition between 19th and 25th months of age seems critical for telomere erosion. Overall telomere length average, for all ages is 36.25 (SE: 7.675, n=21) for the heart, and 17.8 (SE: 4.365, n= 22) for the brain.

For the rest of the organs, no significant change in telomere length was found in the aging process. Intestine, spleen, and gills have the highest numerical differences at 19 months of age. Muscle and skin showed varied telomere lengths through aging. Spleen, skin, and caudal fin have overall higher telomere lengths, in accordance with their regenerative capacities. The high variation within a group indicates that there are individual differences. Although we group fish according their age, and assume normal distribution in the group, fish of the same age exhibit different cellular characteristics. These results show that telomere length depend on the organ type and is variable throughout the lifespan.

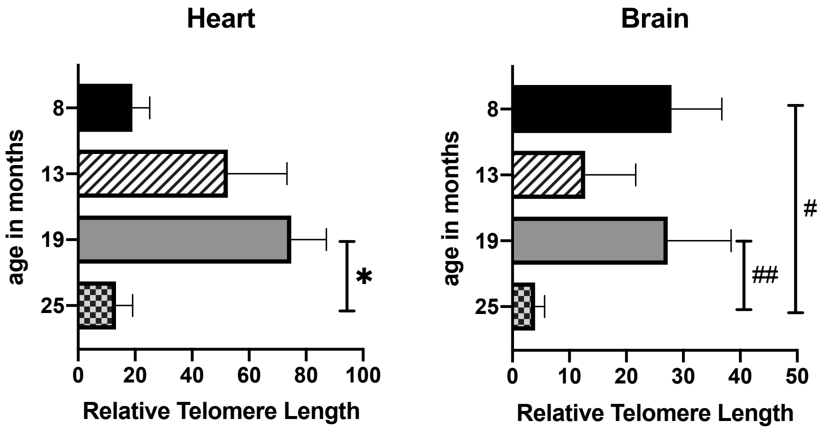

Figure 4.1: Relative telomere length in aging zebrafish heart and brain. Y-axis shows the age in months and X-axis shows the relative telomere length. Graphs are drawn using GraphPad Prism. Error bars represent the +SEM. *: p = 0.03, #: p = 0.0113, ##: p = 0.0241.

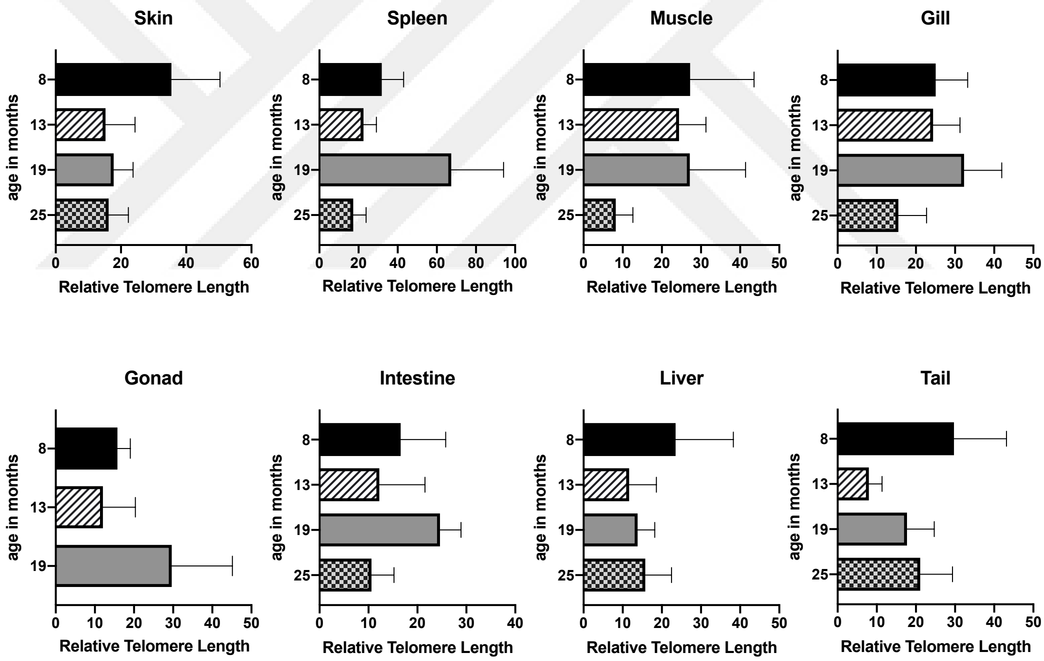

Figure 4.2: Relative telomere length in aging zebrafish organs. Y-axis shows the age in months and X-axis shows the relative telomere length. Graphs are drawn using GraphPad Prism. Error bars represent the +SEM.

4.2. Brain Samples Show Variation in Distal Upstream Zebrafish TERT Gene Methylation

Due to high sample variation in telomere length, distal TERT promoter region in individual tissues is analyzed with bisulfite sequencing for brain, skin, spleen, and muscle samples. These tissues were selected because they showed different critical periods for telomere shortening. Brain and spleen showed a similar pattern, with an increase between 13th and 19th month and a decrease between 19th and 25th month. Muscle had stable telomere length until throughout aging process. Skin samples showed a reversed pattern, with long telomeres only at 8 months.

Figure 4.3, 4.4, 4.5 and 4.6 shows sequence alignment of the bisulfite converted distal TERT promoter. Figure 4.3 and Figure 4.7 shows the hypo-methylated site at chromosome 19 position 627,118 (-972) in brain samples N9 and N10 in detail. These are shown with an arrow. For skin (Figure 4.4), spleen (Figure 4.5), and muscle (Figure 4.6) this region is conserved. These samples did not show methylation changes in transcription binding sites at the distal TERT promoter.

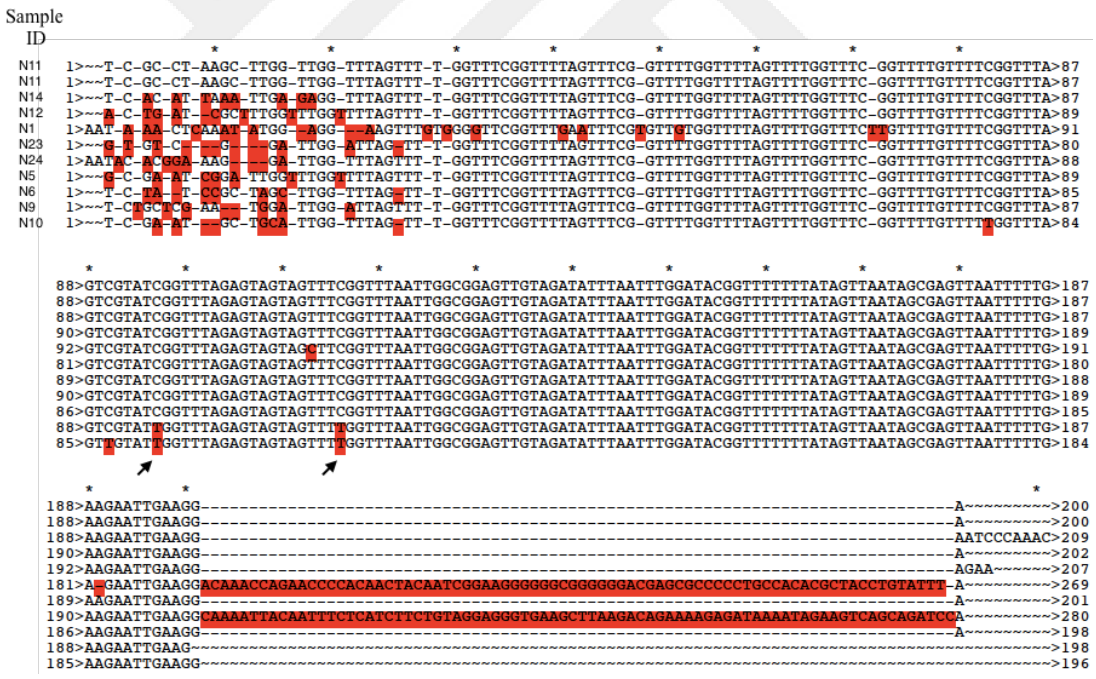

Figure 4.3: Sequence alignment of distal TERT promoter site in brain samples. Aligned sequences are from N11, N14, N12, N1, N23, N24, N5, N6, N9, and N10 respectively. Disrupted Sp1 binding sites are shown with an arrow. Alignments are made to sample N11 with Ape-A plasmid editor v2.0.Mismatches are highlighted with red and gaps are shown with hyphen.

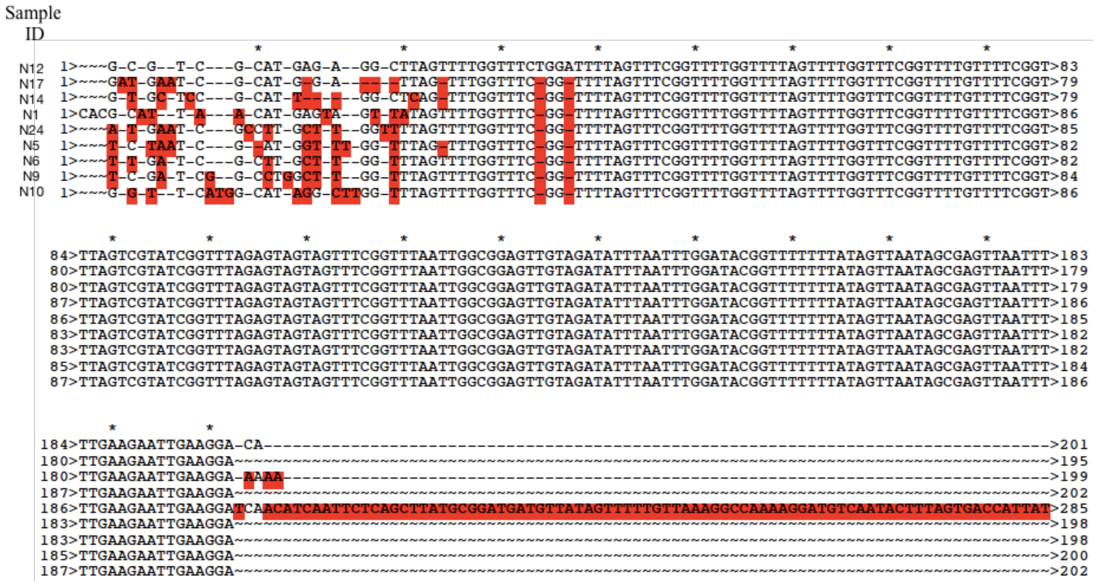

Figure 4.4: Sequence alignments of distal TERT promoter site in skin samples. Aligned sequences are from N12, N17, N14, N1, N24, N5, N6, N9 and N10 respectively. Alignments are made with Ape-A plasmid editor v2.0. Mismatches are highlighted with red and gaps are shown with hyphen.

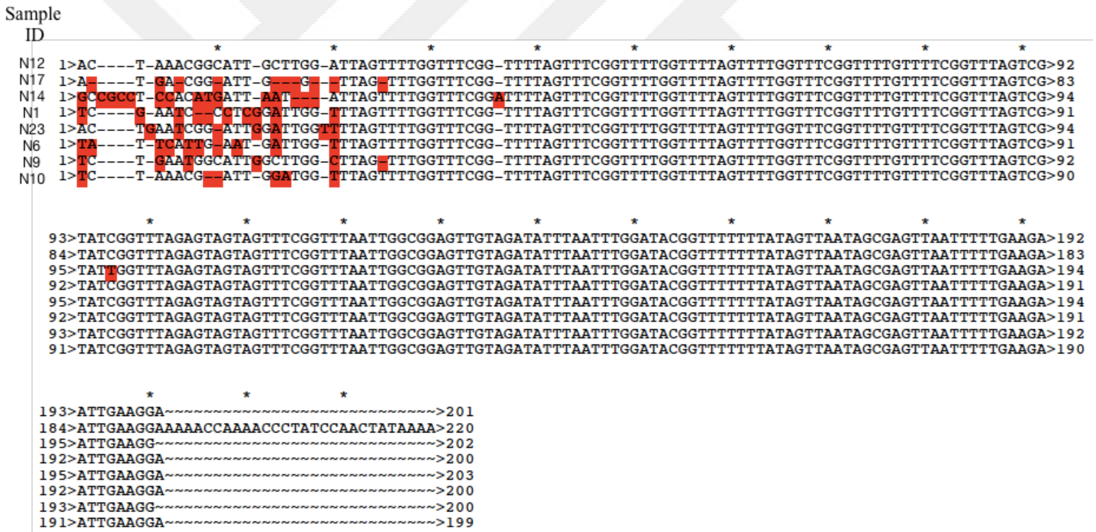

Figure 4.5: Sequence alignments of distal TERT promoter site in spleeen samples. Aligned sequences are from N12, N17, N14, N1, N23, N6, N9 and N10 respectively Alignments are made with Ape-A plasmid editor v2.0. Mismatches are highlighted with red and gaps are shown with hyphen.

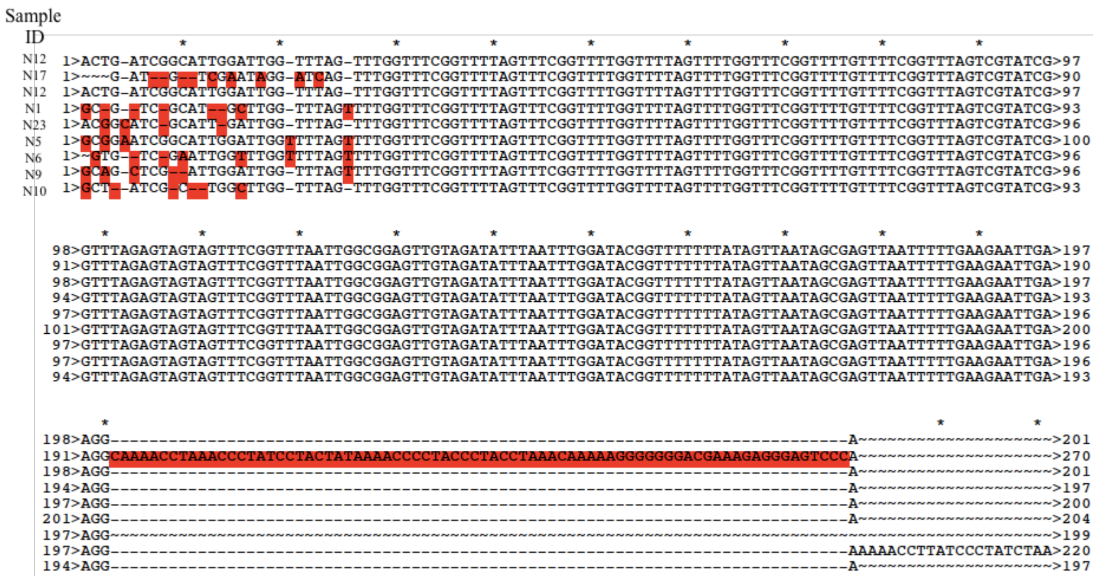

Figure 4.6: Sequence alignments of distal TERT promoter site in muscle samples. Aligned sequences are from N17, N12, N1, N23, N5, N6, N9 and N10 respectively. Alignments are made to sample N12 with Ape-A plasmid editor v2.0. Mismatches are highlighted with red and gaps are shown with hyphen.

Brain samples of N9 and N10 had extremely short telomeres that can be explained by a change in binding capacity of SP1 transcription factor at the 972nd position from tert transcription start site. Figure 4.7 shows brain samples in detail with an alignment to the reference sequence of interest (labeled as ORI, obtained from NCBI). Sp1 binding site is indicated with an underlie, and the change in the nucleotide is indicated with bold letters.

Fish ID	Methylation	Sequence
Ori	-	CCGCACCGGCCCAGAGCAGCAGCTTCGGTTCA
N24	Yes	TCGTATCGGTTTAGAGTAGTAGTTTCGGTTTA
N23	Yes	TCGTATCGGTTTAGAGTAGTAGTTTCGGTTTA
N14	Yes	TCGTATCGGTTTAGAGTAGTAGTTTCGGTTTA
N12	Yes	TCGTATCGGTTTAGAGTAGTAGTTTCGGTTTA
N1	Yes	TCGTATCGGTTTAGAGTAGTAGCTTCGGTTTA
N5	Yes	TCGTATCGGTTTAGAGTAGTAGTTTCGGTTTA
N6	Yes	TCGTATCGGTTTAGAGTAGTAGTTTCGGTTTA
N9	No	TCGTATTGGTTTAGAGTAGTAGTTTTGGTTTA
N10	No	TTGTATTGGTTTAGAGTAGTAGTTTTGGTTTA

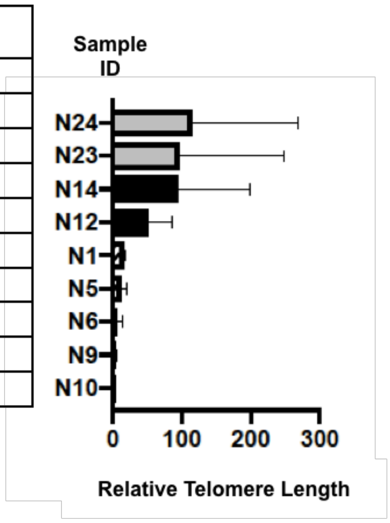

Figure 4.7: Relative telomere length in individuals and methylation status between 627,112 and 627,137 of chromosome 19. Table shows fish ID, methylation status and alignment to reference sequence. Graph is drawn using GraphPad Prism. Error bars represent the +SEM.

4. 3. Hypomethylation at ch19: 627,118 (-972 from tert transcription start site) is Related with Aging in Zebrafish Brains

To further analyze hypomethylation at ch19: 627,118 (-972) position of TERT promoter, zebrafish brain samples from a previous study [62] are used for bisulfite sequencing experiments (Figure 4.8). In the old animals (26 to 32.5 months old), four out of five samples had the same hypomethylation mark at the -972nd position whereas none of the young animals (8 to 8.5 months old) show hypomethylation at the -972nd position.

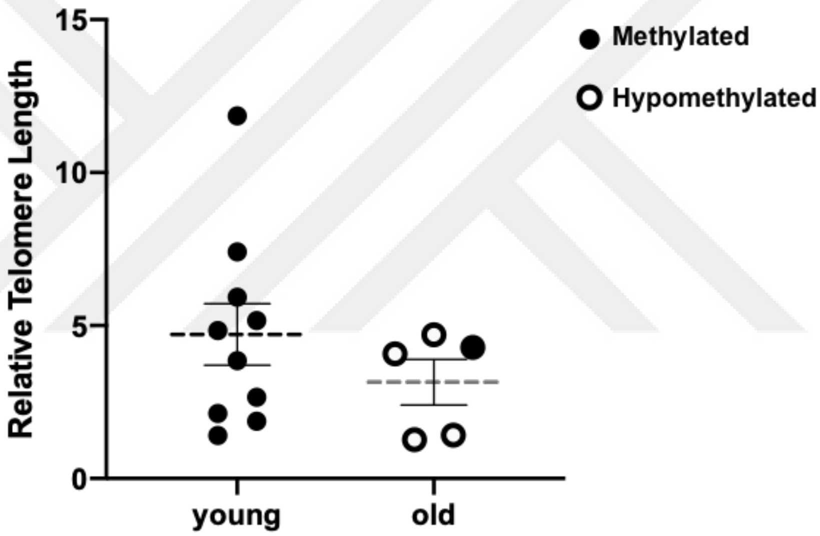

Figure 4.8: Relative telomere length and methylation status in -972th position of TERT promoter in young and old zebrafish brains. Y axis shows the relative telomere length and X axis shows the age groups. Individual data points are color coded according to their methylation status, where methylation is shown with black and hypo-methylation is shown with white. Graph is drawn with GraphPad Prism. Error bars represent the +SEM.

4. 4. Mutations at SP1 Binding Sites Abrogate Promoter Activity in Brain Cancer Cell Lines

To further analyze SP1 binding to TERT promoter and its regulatory role, A172, Daoy, and SW1088 cell lines are transfected with mutant and wild type TERT promoters in pGl3 plasmid vector. Transfected cells are subjected to luciferase assay 24 hours post transfection. Normalized promoter activities are shown in Figure 4.9 and 4.10, and normalized to TERT distal promoter without mutation (no mutation).

Repeated measures One-Way ANOVA with Geisser-Greenhouse correction and with Sidak's multiple comparison is applied to data.

Table 4.1: Effect of SP1 binding site mutations on TERT promoter activity

Plasmid ID	A172	Daoy	SW1088
Sdm 1	6.6 fold reduction	20 fold reduction	5 fold reduction
Sdm 2	No activity	No activity	No activity
Sdm 3	10 fold reduction	No activity	50 fold reduction
Sdm 4	40 fold reduction	No activity	No activity
Sdm 9	No activity	No activity	No activity
Sdm 13	No activity	No activity	No activity
Sdm 16	No activity	No activity	No activity
Sdm 17	10 fold reduction	12.5 fold reduction	5 fold reduction
Sdm 18	10 fold reduction	8.3 fold reduction	2 fold reduction
Sdm 19	No activity	No activity	No activity

SDM 2 (A172 $p=0.0012$, $F=1.808$, Daoy $p=0.0007$, $F= 1.808$, SW1088 $p=0.0006$, $F=0.2324$), SDM 9 (A172 $p=0.0014$, Daoy $p=0.0007$, SW1088 $p=0.0005$), SDM 13 ($p=0.0014$, Daoy $p=0.0007$, SW1088 $p=0.0005$), SDM 16 (A172 $p=0.0014$, Daoy $p=0.0007$, SW1088 $p=0.0005$) and SDM 19 (A172 $p=0.0014$, Daoy $p=0.0007$, SW1088 $p=0.0005$) abrogated promoter activity completely in all cell lines. SDM 4 showed very low activity only in A172 ($p=0.0013$) and completely abrogated the promoter activity in Daoy ($p=0.0007$) and SW1088 ($p=0.0006$) cell lines. Other mutant promoters showed varied promoter activity depending on cell type. SDM1 reduced promoter activity 6.6 fold in A172 ($p=0.0011$), 20 fold in Daoy ($p=0.0007$), and five-fold in SW10888 ($p=0.0012$). SDM3 reduced ten-fold in A172 ($p=0.0013$) and SW1088 ($p=0.0008$), 50 fold in Daoy ($p=0.0002$). SDM4 completely abrogated promoter activity in Daoy ($p=0.0002$) and SW1088 ($p=0.0006$) whereas reduced 40 fold in A172 ($p=0.0013$). SDM 17 reduced promoter activity ten-fold in A172 ($p=0.0005$), 12.5 fold in Daoy ($p=0.0002$) and five-fold in SW1088 ($p=0.0015$). SDM

18 resulted in ten-fold reduction in A172 (p=0.0005), 8.3 fold in Daoy (p=0.0002) and 2 fold in SW1088 (p=0.0032).

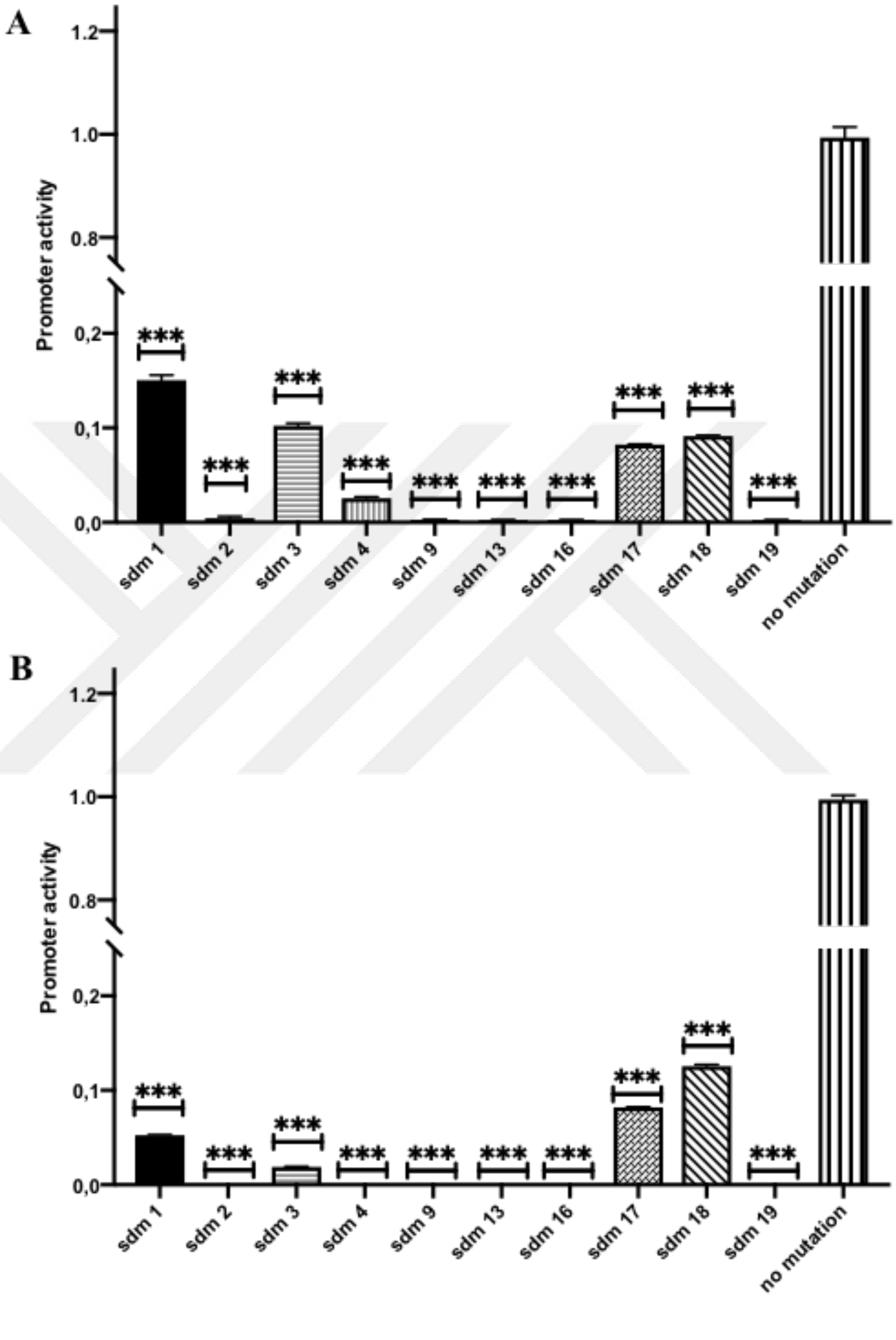

Figure 4.9: Normalized promoter activity in A172 and Daoy cell lines. Y axis shows the relative promoter activity and X axis lists the mutant and wild type TERT distal promoter. A) A172. B) Daoy. No mutation value is set to 1. Graphs are drawn using GraphPad Prism. Error bars represent the +SEM. ***: p<0.001

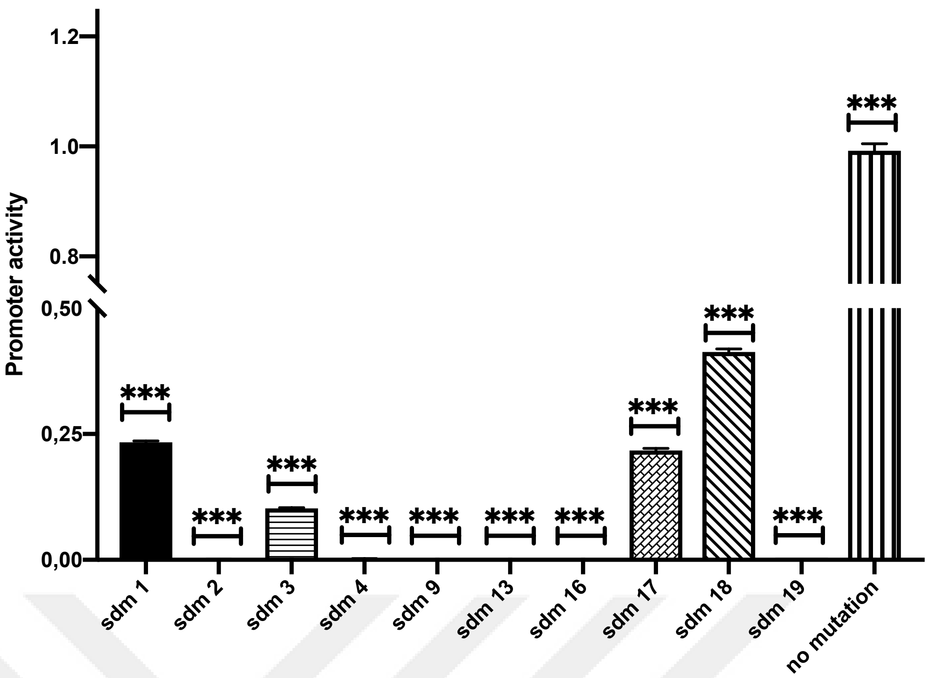

Figure 4.10: Normalized promoter activity in SW1088 cell line. Y axis shows the relative promoter activity and X axis lists the mutant and wild type TERT distal promoter. No mutation value is set to 1. Graphs are drawn using GraphPad Prism. Error bars represent the +SEM. ***: p<0.001

4.5. DNA Methylation Inhibition Through RNAi Does Not Change Population Doubling Time in Brain Cancer Cell Lines

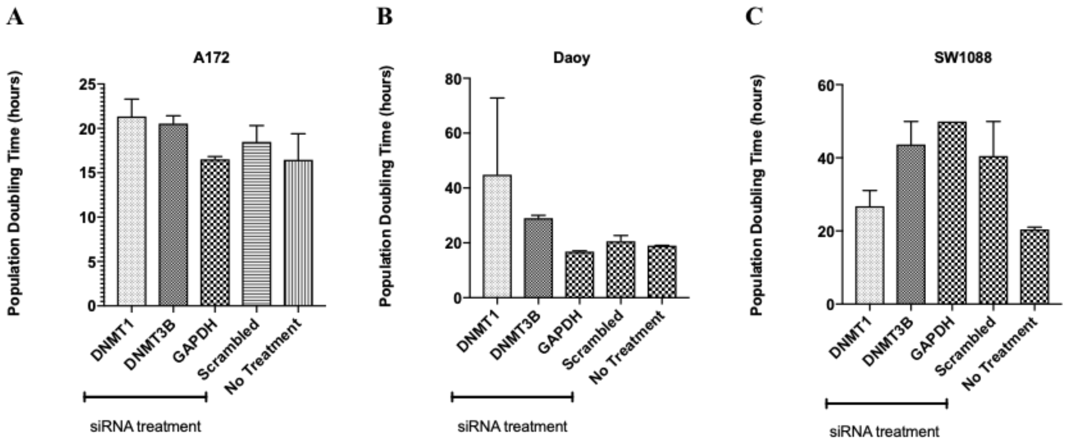

Figure 4.11: Population doubling time in brain cancer cell lines. Y axis shows the population doubling time in hours and X axis lists the treatment type. Population doubling time in A) A172, B) Daoy, C) SW1088. Final concentration of 25 nM siRNA is used for transfection. Scrambled is non-targeting siRNA. Graphs are drawn using GraphPad Prism. Error bars represent the +SEM.

siRNA treated cells are tested for population doubling time to investigate the effect of DNA methylation machinery on proliferative capacity. Population doubling times are given at Figure 10 and scrambled siRNA is non-targeting siRNA. Ordinary

One-Way ANOVA with Dunnet's multiple comparisons is applied to data. No treatment group is the control group. None of the cell lines showed a significant change in population doubling time with siRNA treatment (A172 p=0.323, F=0.8330, Daoy p=0.5579, F=1.526, SW1088 p=0.1326, F=3.379).

4.6. Inhibition of DNA Methylation Have Different Outcomes on Cellular Senescence Induction Depending on Cell Type

To investigate the relationship between DNA methylation and proliferative capacity, siRNA and cytotoxic drug treated cells are stained for Beta-Galactosidase and shown in Figure 4.11. Ordinary One-Way ANOVA with Dunnet's multiple comparisons is applied to the samples, no treatment group is the control group.

In A172 cell line Adriamycin, a chemotherapeutic agent that blocks topoisomerase 2, increased the number of senescent cell significantly (p=0.0026, F=6.375). DNMT1 and DNMT3B siRNA treatment, 10 uM Azacytidine, and 20 uM Azacytidine treatment also numerically increased the number of senescent cells, even though there is no statistical significance (Figure 4.12A).

In Daoy cell line, none of the treatments resulted in a statistically significant increase in the number of beta Galactosidase positive cells (p=0.4644, F=1.013) (Figure 4.12B). In SW1088 cell line, number of beta Galactosidase positive cells significantly increased with DNMT1 siRNA (p=0.0201, F=35.11) and DNMT3B siRNA (p<0.0001) treatment. 10 nM Azacytidine, a chemical agent that blocks DNA Methyltransferases, also increased the number of senescent cells (p<0.0001) (Figure 4.12C). DNMT1 siRNA treatment increased the number of senescent cells by 10-fold (p=0.0201), DNMT3B siRNA treatment increased the number of senescent cells by 25-fold (p<0.0001), and 10 nM Azacytidine treatment increased the number of senescent cells by 35-fold (p<0.001).

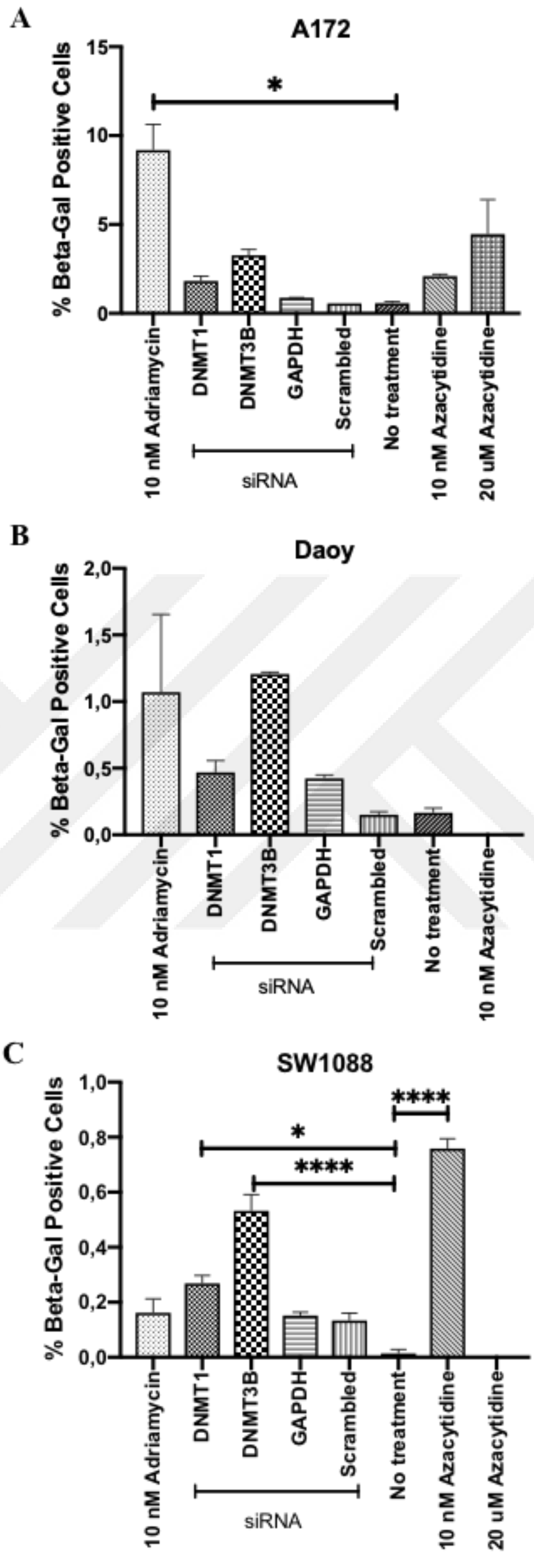

Figure 4.12: Beta-Galactosidase staining in brain cancer cell lines. Y axis shows the percentage of Beta-Galactosidase positive cells and X axis shows the treatment. Final concentration of 25 nM siRNA is used for transfection. A) A172, B) Daoy, C) SW1088. Scrambled is non-targeting siRNA. Graphs are drawn using GraphPad Prism. Error bars represent the +SEM. *: $p<0.05$, ***: $p<0.001$, ****: $p<0.0001$.

4.7. Inhibition of De Novo DNA Methylation Machinery Affects Telomerase Activity in Brain Cancers

To investigate the relationship between DNA methylation machinery and telomere maintenance, siRNA treated cell lines are subjected to quantitative telomeric repeat amplification protocol (qTRAP) 96 hours post transfection (Figure 4.13). Ordinary One-Way ANOVA with Sidak's multiple comparisons test is used for data analysis. No treatment group is used as the control group.

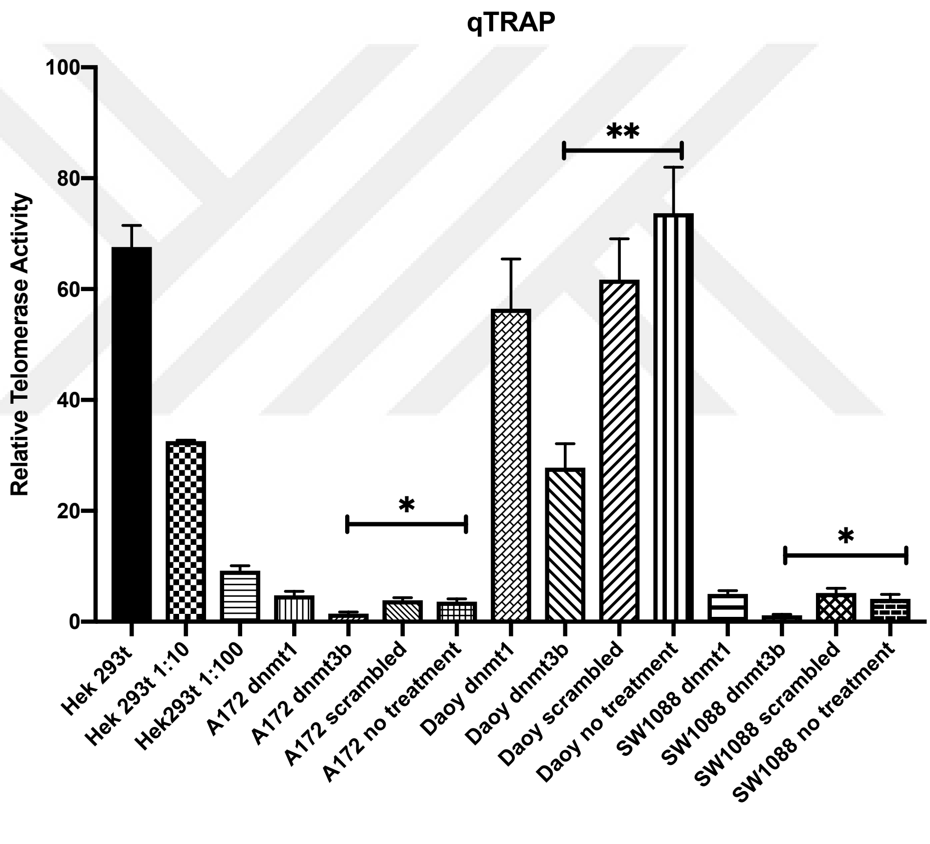

Figure 4.13: Effect of RNAi treatment on telomerase activity. Y axis show the relative telomerase activity and X axis shows the cell type and treatment. Hek293t is used for positive control. Serial dilution of Hek293t is required for standard curve generation, where linear equation is used for relative telomerase activity measurement. Scrambled is non-targeting siRNA. Graph is drawn using GraphPad Prism. Error bars represent the +SEM. *: $p<0.05$, **: $p<0.01$.

Amongst the brain cancer cell lines, Daoy had the highest telomerase activity. Silencing of DNMT3B reduced telomerase activity in all brain cancer cell lines whereas silencing of DNMT1 had no visible effect on telomerase activity. In A172 cell line, telomerase activity is reduced by two-fold with DNMT3B siRNA transfection (p=0.0120, F=7.111) and remained unchanged with DNMT1 siRNA transfection. In Daoy, DNMT3B silencing reduced telomerase activity by 2.5-fold (p=0.0073, F=6.823). In SW1088, short term silencing of DNMT3B reduced telomerase activity by three-fold (p=0.0320, F=7.908). In both cell lines, DNMT1 inhibition did not change the telomerase activity.

4.8. Inhibition of DNA Methyltransferases Does Not Change TERT Expression however, Changes hTR Expression in Brain Cancer Cell Lines

To better understand the relationship between telomerase activity and DNA methylation machinery, brain cancer cell lines and WI-38 VA-13 Subline 2RA are transfected with siRNA or treated with 20 uM Azacytidine, and analyzed for gene expression 48 hours post treatment. In siRNA treated cells DNA Methyltransferase silencing is controlled with qPCR using primers against DNMT1, DNMT3A and DNMT3B. Ordinary One-Way ANOVA with Dunnet's multiple comparisons test is used for analysis. Outliers are identified with Grubbs test, with alpha set to 0.05 and removed from the data. Non Targeting siRNA (Scrambled) is used as the control group. In A172 cell line DNMT1 siRNA treatment numerically decreased DNMT1 expression 48 hours post transfection (Figure 4.14A). DNMT3A expression remained unchanged in DNMT1, DNMT3B, and scrambled siRNA treatments as expected (Figure 4.14B). DNMT3B siRNA treatment did not result in a decrease in DNMT3B expression levels (Figure 4.14C). In Daoy cell line, DNMT1 siRNA treatment numerically reduced the DNMT1 expression (Figure 4.15A). DNMT3A expression remained the same in all treatments (Figure 4.15B). DNMT3B expression was significantly reduced in DNMT3B siRNA treated Daoy cells (Figure 4.15C).

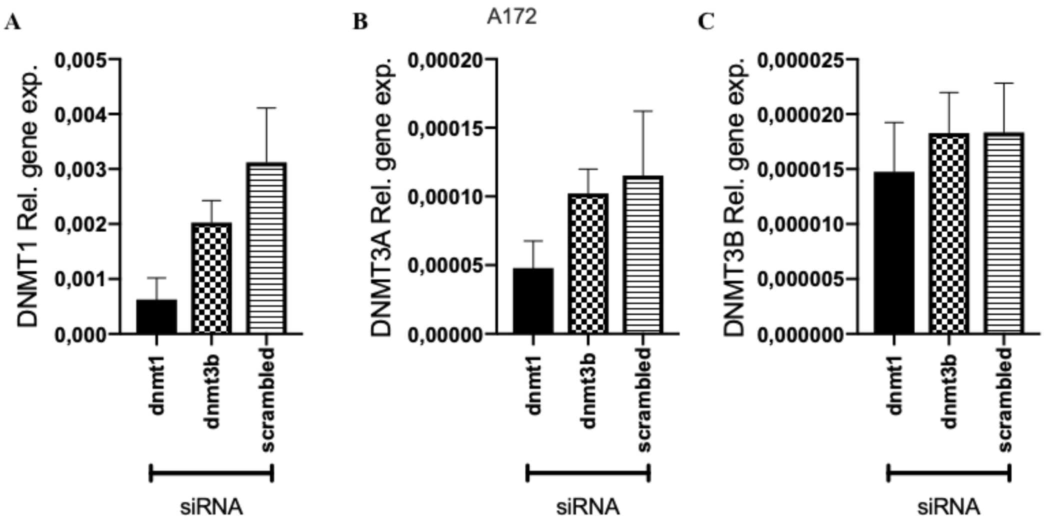

Figure 4.14: Expression of DNA Methyltransferase in A172 cell line 48 hour post treatment. Y axis shows the normalized relative gene expression and X axis shows the treatment type. Final concentration of 25 nM siRNA is used for transfection. A) DNMT1 expression levels, B) DNMT3A expression levels, C) DNMT3B expression levels. Scrambled is non-targeting siRNA. Graphs are drawn using GraphPad Prism. Error bars represent the +SEM.

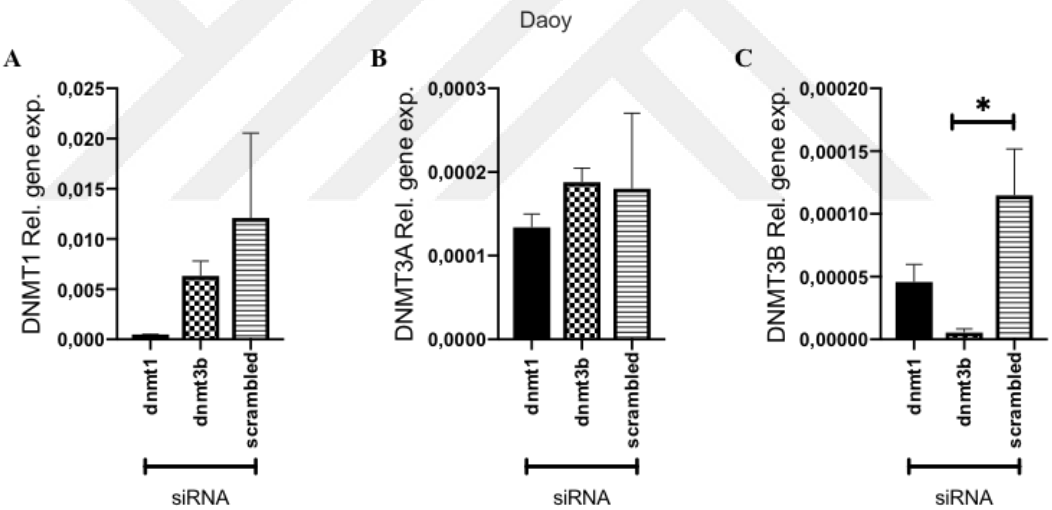

Figure 4.15: Expression of DNA Methyltransferase in Daoy cell line 48 hour post treatment. Y axis shows the normalized relative gene expression and X axis shows the treatment type. Final concentration of 25 nM siRNA is used for transfection. A) DNMT1 expression levels, B) DNMT3A expression levels, C) DNMT3B expression levels. Scrambled is non-targeting siRNA. Graphs are drawn using GraphPad Prism. Error bars represent the +SEM. *: $p<0.05$

In SW1088, treatment with siRNA against DNMT1 reduced the expression levels numerically. Interestingly, in this cell line DNMT3B siRNA treatment numerically increased the DNMT1 expression levels (Figure 4.16A). Numerical changes in DNMT3A expression levels was observed in all groups (Figure 4.16B). DNMT3B siRNA treatment numerically reduced the DNMT3B and DNMT1 levels

(Figure 4.16C). In VA-13, DNMT1 was numerically reduced with siRNA treatment against DNMT1 (Figure 4.17A). DNMT3A expression levels remained the same in all groups (Figure 4.17B) and DNMT3B siRNA treatment was not effective (Figure 4.17C).

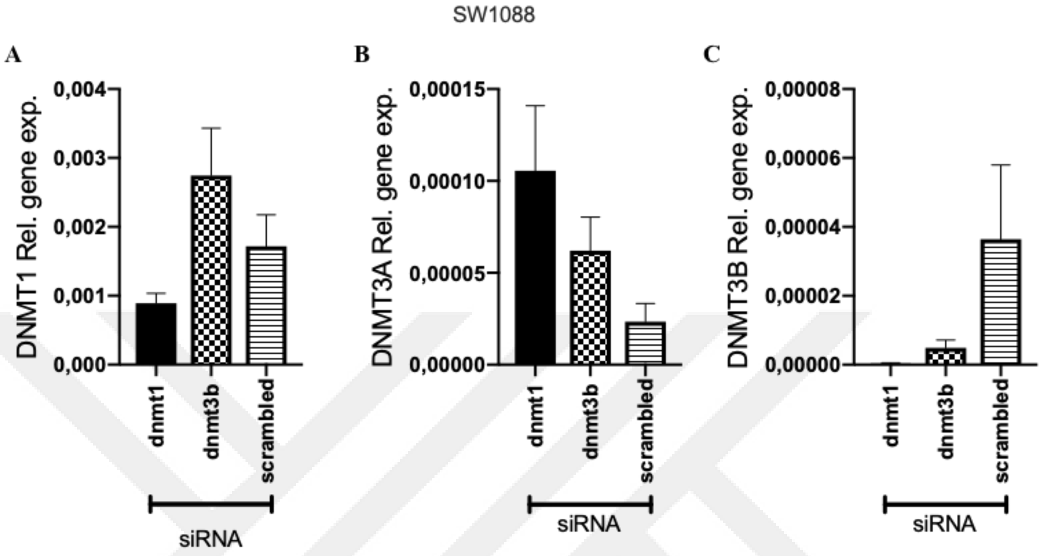

Figure 4.16: Expression of DNA Methyltransferase in SW1088 cell line 48 hour post treatment. Y axis shows the normalized relative gene expression and X axis shows the treatment type. Final concentration of 25 nM siRNA is used for transfection. A) DNMT1 expression levels, B) DNMT3A expression levels, C) DNMT3B expression levels. Scrambled is non-targeting siRNA.Graphs are drawn using GraphPad Prism. Error bars represent the +SEM.

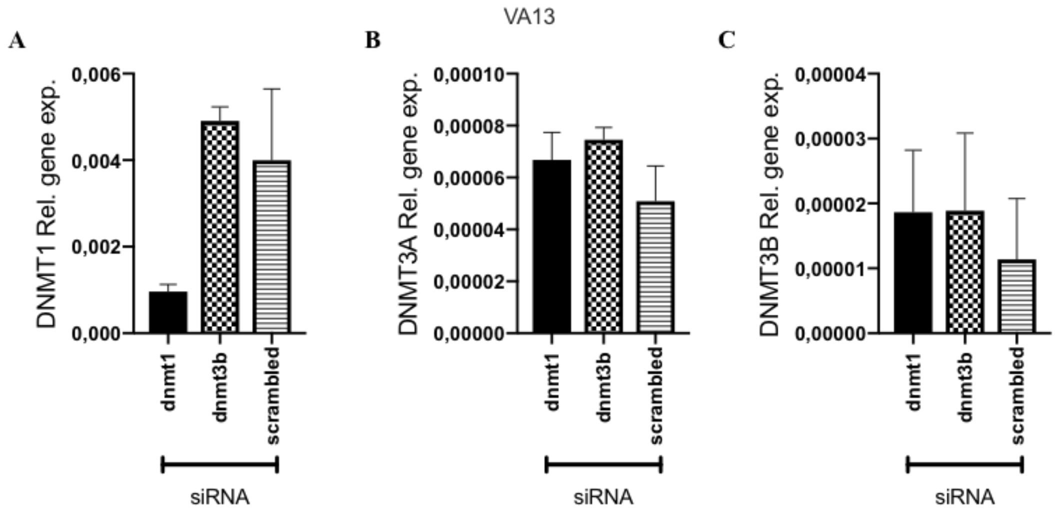

Figure 4.17: Expression of DNA Methyltransferase in VA-13 cell line 48 hour post treatment. Y axis shows the normalized relative gene expression and X axis shows the treatment type. Final concentration of 25 nM siRNA is used for transfection. A) DNMT1 expression levels, B) DNMT3A expression levels, C) DNMT3B expression levels. Scrambled is non-targeting siRNA.Graphs are drawn using GraphPad Prism. Error bars represent the +SEM.

TERT expression was highest in Daoy amongst the cell lines (Figure 4.18A). DNMT1, DNMT3B and 20 uM Azacytidine treatments showed no statistically significant effect on TERT expression levels in brain cancer cell lines (A172 p=0.2431, F=1.665, Daoy p=0.4226, F= 0.9897, SW1088 p=0.5500, F=0.7486) (Figure 4.18 B-D).

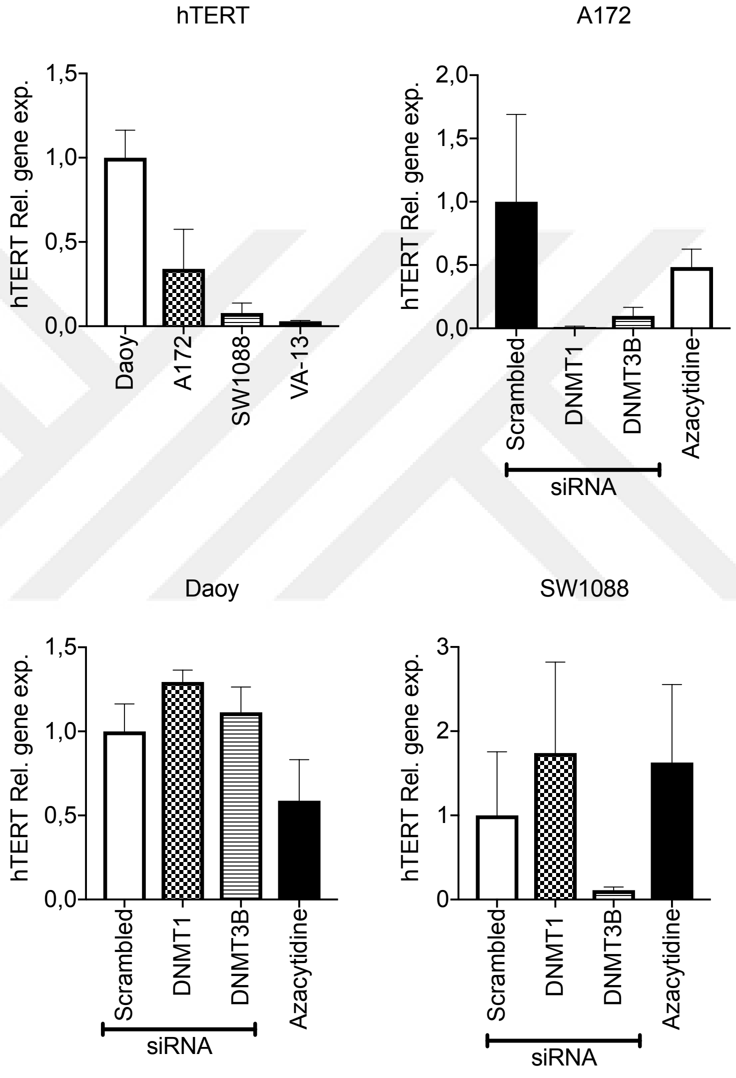

Figure 4.18: Expression of hTERT in brain cancer and control cell lines. Y axis shows the normalized relative gene expression and X axis shows the treatment type. Final concentration oft he treatments are 25 nM for siRNAs and 20 uM for Azacytidine. A) All cell lines without treatment, B) Treated A172 cells, C) Treated Daoy cells, D) Treated SW1088 cells. Scrambled is set to 1. Graphs are drawn using GraphPad Prism. Error bars represent the +SEM.

On the other hand, constitutively expressed hTR showed statistically significant changes in expression levels in all cell lines. 20 uM Azacytidine treatment significantly decreased expression of hTR in A172 (p=0.0301, F=1.026) (Figure 4.19A) and WI-38 VA-13 Subline 2RA (p=0.0467, F=3.133) (Figure 4.19D), whereas increased expression in Daoy (p=0.0002, F=0.7305) (Figure 4.19B). 20 uM Azacytidine treatment did not result in a significant change in SW1088 cell line, even though the expression was decreased. On the other hand, DNMT1 silencing in SW1088 increased the expression of hTR significantly (p=0050, F=2.239) (Figure 4.19C).

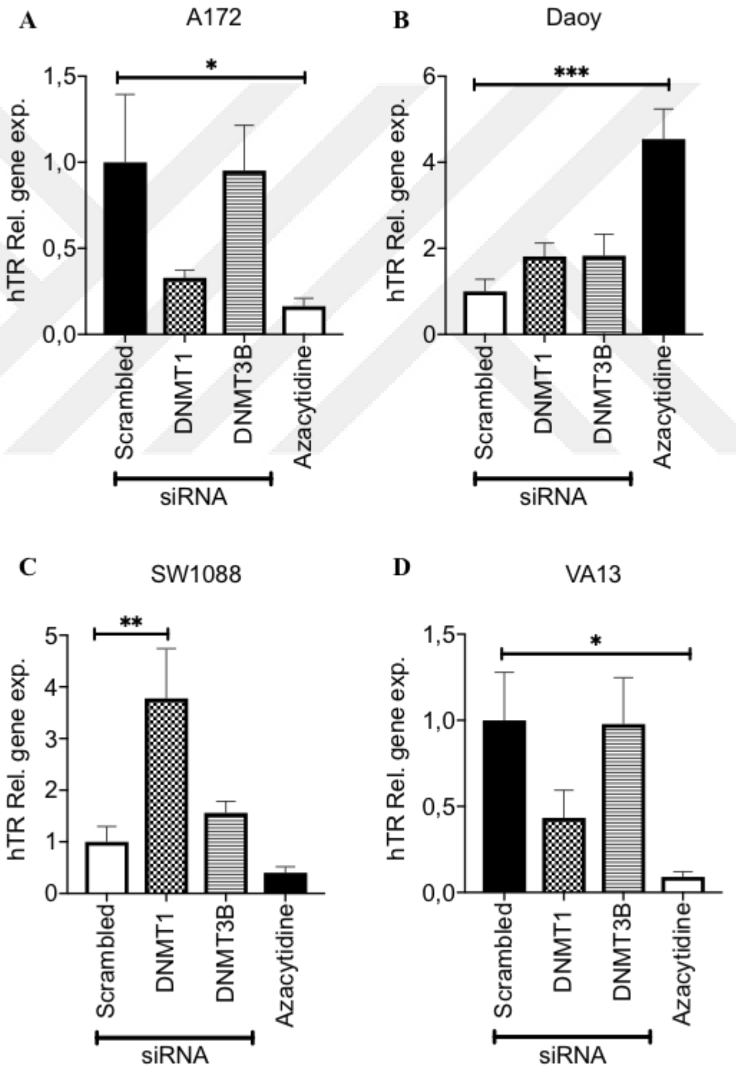

Figure 4.19: Expression of hTR in brain cancer and control cell lines. Y axis shows the normalized relative gene expression and X axis shows the treatment type. Final concentration oft he treatments are 25 nM for siRNAs and 20 uM for Azacytidine. A) A172, B) Daoy, C) SW1088, D) VA-13. Scrambled is set to 1. Graph is drawn using GraphPad Prism. Error bars represent the +SEM. *: p<0.05, **: p<0.01, ***: p<0.001

4.9. Inhibition of DNA Methyltransferases Show Cell Specific Effects on ALT Associated Genes in Brain Cancer Cell Lines

To decipher the relationship with ALT associated genes and telomere maintenance in brain cancer cell lines, qPCR experiments for ATRX, DAXX, TRF2, FEN1, WRN, and CBX3A are performed 48 hours post treatment of 25 nM siRNAs or 20 uM Azacytidine. Ordinary One-Way ANOVA with Dunnet's multiple comparisons test is used for analysis. Outliers are removed with Grubbs test, with alpha set to 0.05. Non Targeting siRNA (Scrambled) is used as the control group.

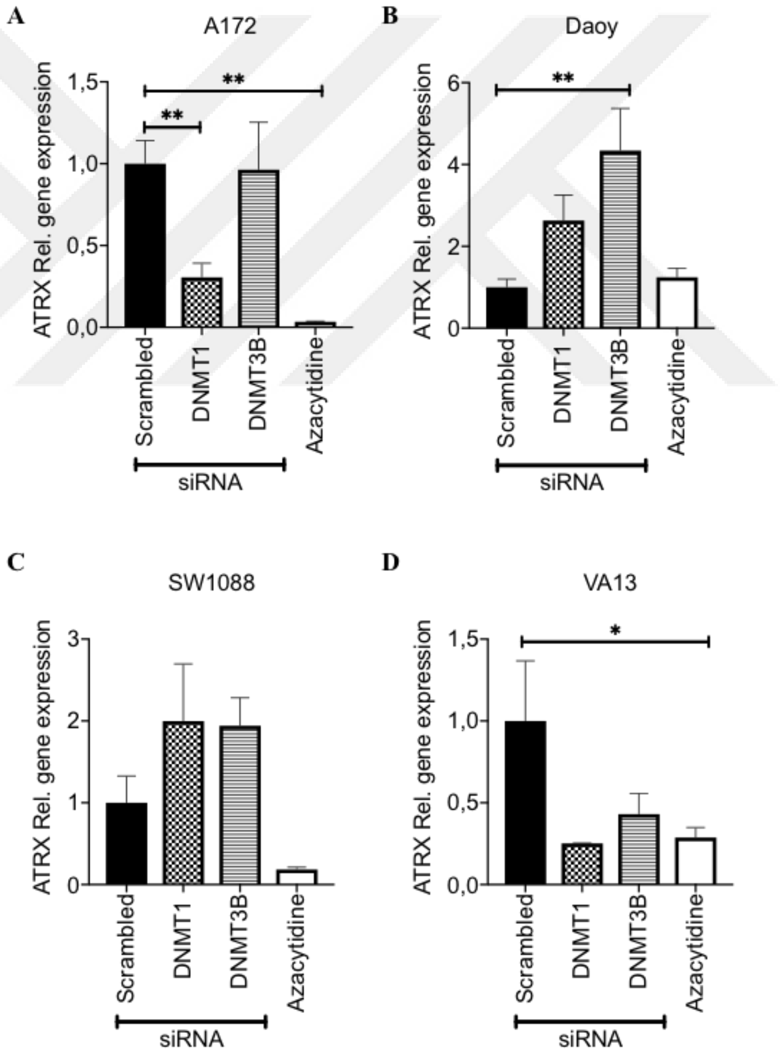

Figure 4.20: Expression of ATRX in brain cancer and control cell lines: Y axis shows the normalized relative gene expression and X axis shows the treatment type. Final concentration oft he treatments are 25 nM for siRNAs and 20 uM for Azacytidine. A) A172, B) Daoy, C) SW1088, D) VA-13. Scrambled is set to 1. Graph is drawn using GraphPad Prism. Error bars represent the +SEM. *: $p<0.05$, **: $p<0.01$

ATRX expression significantly decreased with DNMT1 siRNA (p= 0.0206, F=1.831) and Azacytidine (p=0.0012) treatment in A172 cell line (Figure 4.20A). In Daoy, silencing of DNMT3B increased the expression of ATRX (p=0.0046, F= 18.44) (Figure 4.20B). In SW1088, changes in ATRX expression levels was not statistically significant (Figure 4.20C). In WI-38 VA-13 Subline 2RA, Azacytidine treatment decreased ATRX expression significantly (p=0.0319, F=1.151) (Figure 4.20D).

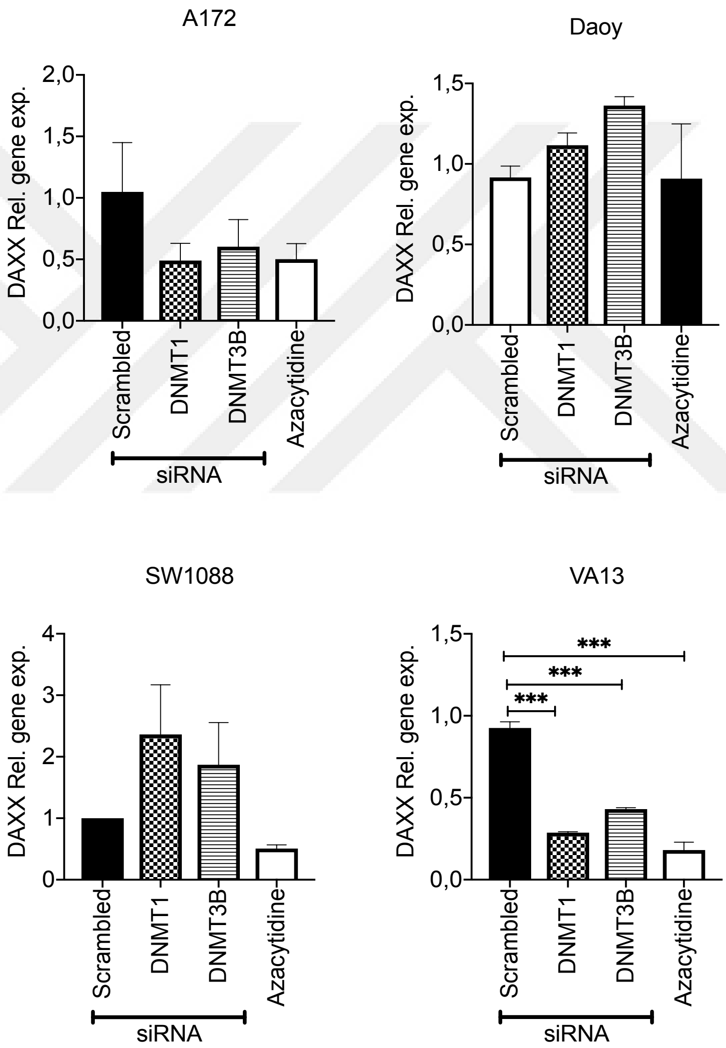

Figure 4.21: Expression of DAXX in brain cancer and control cell lines: Y axis shows the normalized relative gene expression and X axis shows the treatment type. Final concentration oft he treatments are 25 nM for siRNAs and 20 uM for Azacytidine. A) A172, B) Daoy, C) SW1088, D) VA-13. Scrambled is set to 1. Graph is drawn using GraphPad Prism. Error bars represent the +SEM. ***: p<0.001

For brain cancer cell lines, interference of DNA methylation through RNAi or Azacytidine treatment did not significantly changed the DAXX expression levels (Figure 4.21A-C). In WI-38 VA-13 Subline 2RA DAXX expression significantly (F=65.75) with DNMT1 siRNA treatment (p<0.001), DNMT3B siRNA treatment (p<0.001) and Azacytidine treatment (p<0.001) (Figure 4.21D).

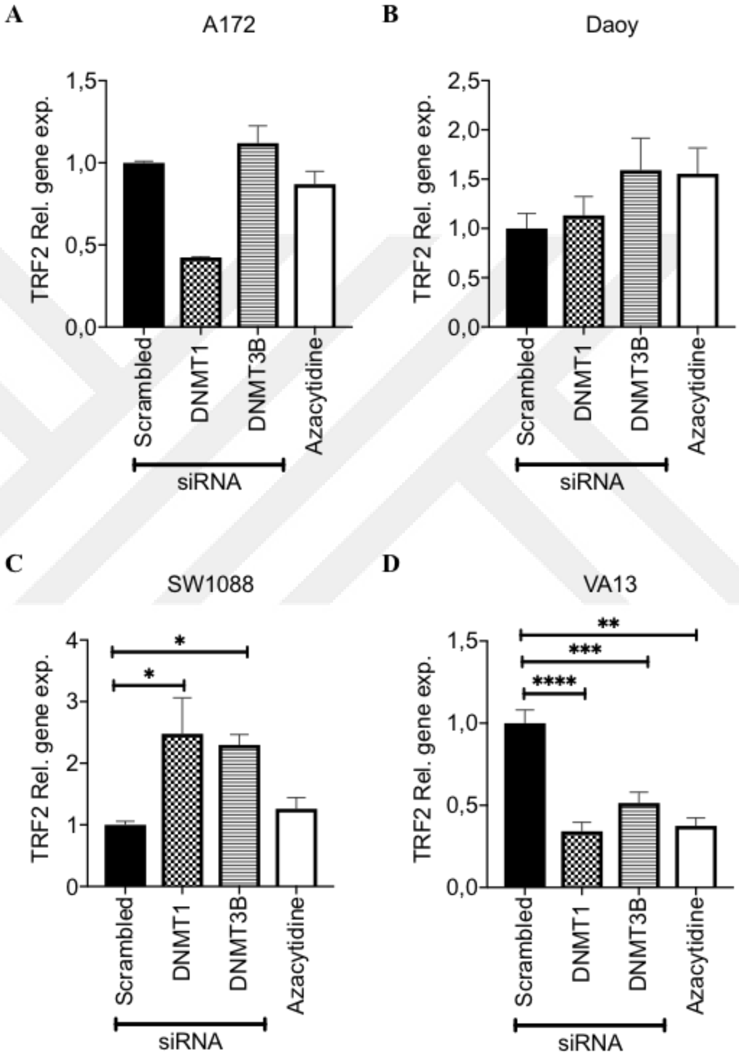

Figure 4.22: Expression of TRF2 in brain cancer and control cell lines: Y axis shows the normalized relative gene expression and X axis shows the treatment type. Final concentration oft he treatments are 25 nM for siRNAs and 20 uM for Azacytidine. A) A172, B) Daoy, C) SW1088, D) VA-13. Scrambled is set to 1. Graph is drawn using GraphPad Prism. Error bars represent the +SEM. *: p<0.05, **: p<0.01, ***: p <0.001, ****: p< 0.0001

In A172 and Daoy cell lines, DNA methylation inhibition through RNAi or Azacytidine did not changed TRF2 expression levels (Figure 4.22A-B). In SW1088, TRF2 expression increased with DNMT1 (p=0.0179, F=2.086) and DNMT3B (p=0.0353) silencing (Figure 4.22C). In WI-38 VA-13 Subline 2RA TRF2 expression decreased with silencing of DNMT1 (p<0.0001, F=0.03138) and DNMT3B (p= 0.0010) siRNA treatment. Azacytidine treatment also decreased the expression levels of TRF2 (p<0.0001) in WI-38 VA-13 Subline 2RA (Figure 4.22D).

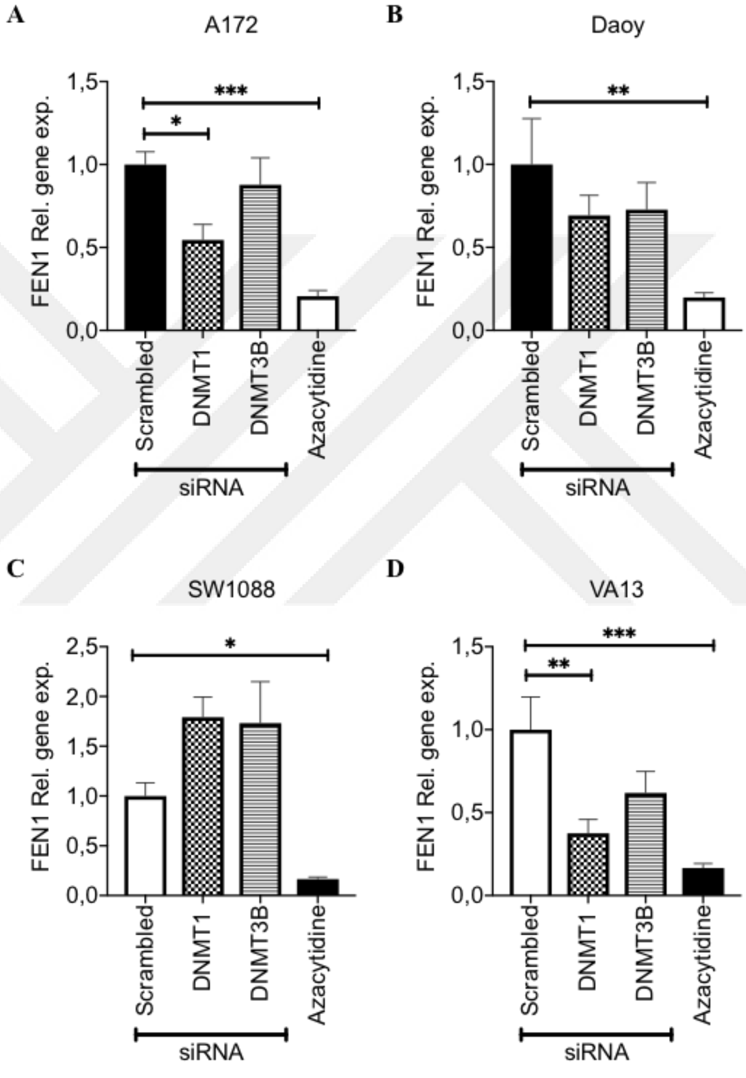

Figure 4.23: Expression of FEN1 in brain cancer and control cell lines: Y axis shows the normalized relative gene expression and X axis shows the treatment type. Final concentration oft he treatments are 25 nM for siRNAs and 20 uM for Azacytidine. A) A172, B) Daoy, C) SW1088, D) VA-13. Scrambled is set to 1. Graph is drawn using GraphPad Prism. Error bars represent the +SEM. *: p<0.05, **: p<0.01, ***: p <0.001, ****: p< 0.0001

In A172 cell line FEN1 expression decreased with DNMT1 silencing (p=0.0176, F=0.5955) and Azacytidine treatment (p=0.0002) (Figure 4.23A). In Daoy, Azacytidine treatment significantly decreased FEN1 expression (p=0.0084, F=2.179)

(Figure 4.23B). Azacytidine treatment decreased (p=0.0299, F=2.633) the expression of FEN1 in SW1088 also (Figure 4.23C). In WI-38 VA-13 Subline 2RA, DNMT1 inhibition (p=0.0078, F=1.497) and Azacytidine treatment (p=0.0005) decreased expression levels of FEN1 (Figure 4.23D).

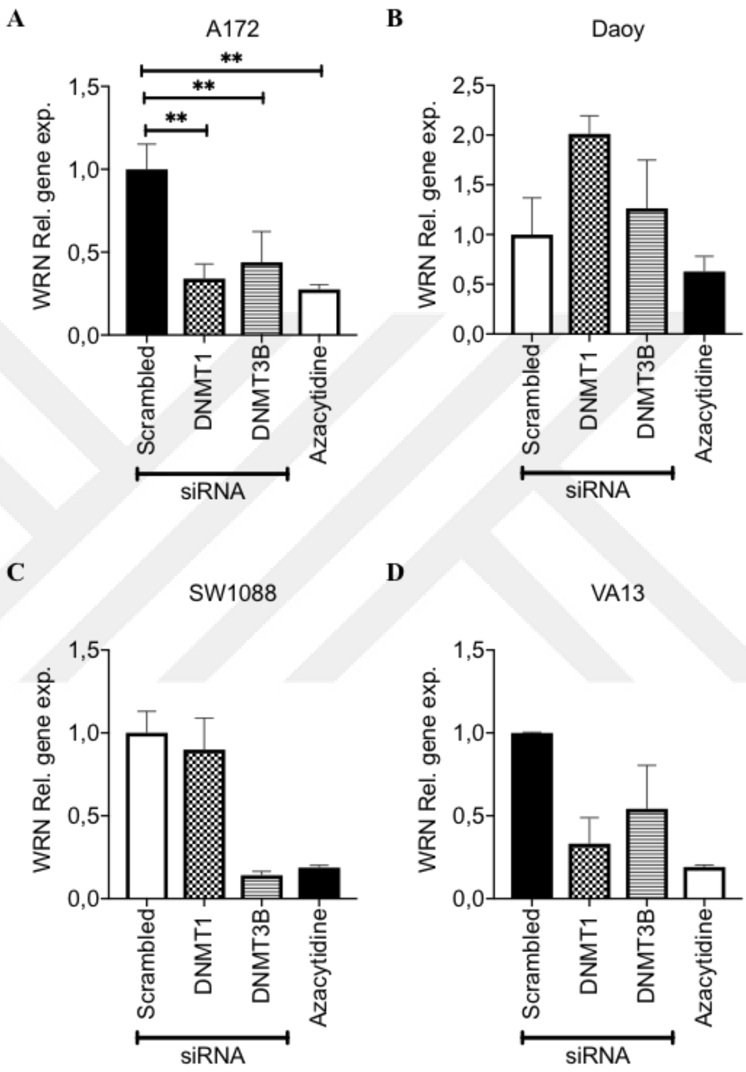

Figure 4.24: Expression of WRN in brain cancer and control cell lines: Y axis shows the normalized relative gene expression and X axis shows the treatment type. Final concentration oft he treatments are 25 nM for siRNAs and 20 uM for Azacytidine. A) A172, B) Daoy, C) SW1088, D) VA-13. Scrambled is set to 1. Graph is drawn using GraphPad Prism. Error bars represent the +SEM. *: p<0.05, **: p<0.01

In A172 cell line, WRN expression significantly decreased with DNMT1siRNA (p=0.0065, F= 1.325), DNMT3B siRNA (p=0.0170) and Azacytidine treatment (p=0.0016) (Figure 4.24A). Daoy, SW1088 and WI-38 VA-13 Subline 2RA showed no significant change in WRN expression profile induced by siRNA or

Azacytidine treatment (Figure 4.24B-D). In SW1088, DNMT3B silencing increased the expression levels of CBX3 (p=0.0063, F=0.4791) (Figure 4.25D). A172, Daoy and WI-38 VA-13 Subline 2RA did not show any significant change with RNAi or Azacytidine treatment (Figure 425A, C, D).

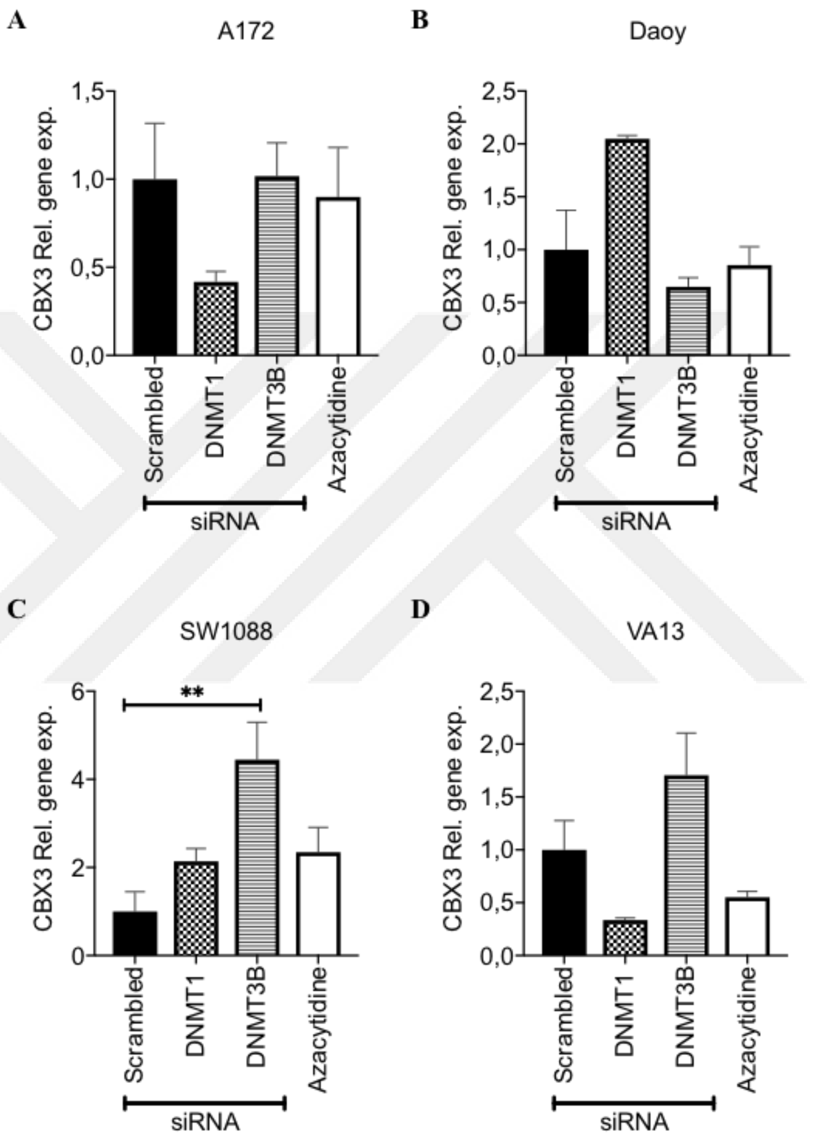

Figure 4.25: Expression of CBX3 in brain cancer and control cell lines: Y axis shows the normalized relative gene expression and X axis shows the treatment type. Final concentration oft he treatments are 25 nM for siRNAs and 20 uM for Azacytidine. A) A172, B) Daoy, C) SW1088, D) VA-13. Scrambled is set to 1. Graph is drawn using GraphPad Prism. Error bars represent the +SEM. *: p<0.05, **: p<0.01

4.10. Short Term Inhibition of DNA Methyltransferases Do Not Change Telomere Length Significantly

To see the effect of short term silencing of DNA Methylation machinery, siRNA treated cells are subjected to qPCR based telomere length assay 96 hours post transfection. Data is subjected to Ordinary One-Way ANOVA with Sidak's multiple comparison. In all cell lines, treatments are normalized to no treatment group.

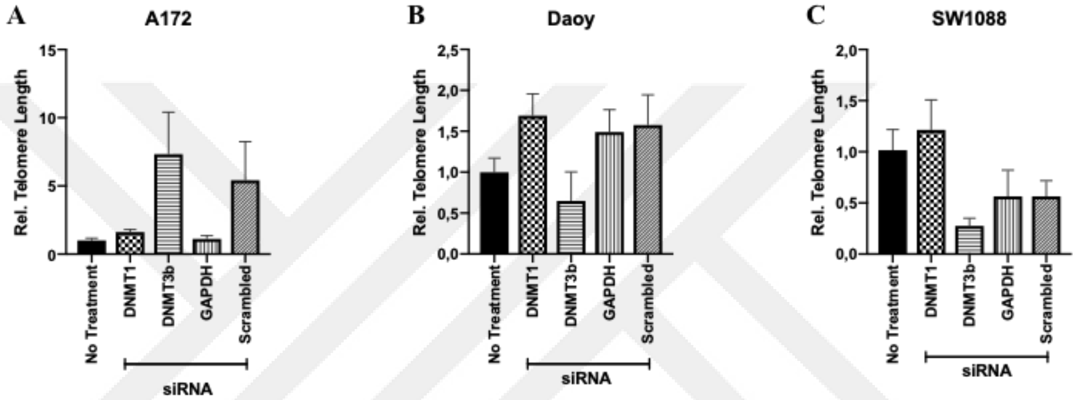

Figure 4.26: Relative Telomere length. Y axis shows the relative telomere length and X shows the treatment. Y axis shows the relative telomere length and X axis show the treatment type. Figure A) Relative telomere length in 25 nM siRNA treated A172 cells. Figure B) Relative telomere length in 25 nM siRNA treated Daoy cells. Figure C) Relative telomere length in 25 nM siRNA treated SW1088 cells. Graphs are drawn using GraphPad Prism. Error bars represent the +SEM.

None of the treatments changed telomere length significantly in brain cancer cell lines. In A172, telomere length seems to be increased with DNMT3B and scrambled siRNA treatment (Figure 4.26A). In Daoy, telomere length seems to increase with DNMT1, GAPDH and Scrambled siRNA treatment. DNMT3B siRNA treatment decreased the telomere length (Figure 4.26B). In SW1088, telomere length was unchanged with DNMT1 siRNA treatment, and decreased with DNMT3B, GAPDH and Scrambled siRNA treatment (Figure 4.26C).

CHAPTER 5

DISCUSSION

5.1. Variation in Telomere Length is Related to the Regenerative Capacity of the Organs

Telomere length is varied amongst organs and changes during the aging process. Regenerative capacities can be the underlying reason for the variation in telomere lengths. A study on aging zebrafish revealed that gonads and gills have the highest levels of tert expression, whereas heart and brain have the lowest levels [63]. In the same study, they have shown that telomeres elongate during adulthood but shorten dramatically with old age. These findings support the variance observed in telomere lengths and suggest that 19 months of age is the critical time point for rapid shortening of the telomeres. Yet again, since qPCR based telomere length assay measures the average telomere in the cells and is not chromosome specific, these findings can be confirmed with more specific techniques like Q-FISH (Quantitative fluorescence in situ hybridization) and STELA (single telomere length analysis) [64]. Both of these techniques are higher in resolution, compared to the qPCR based system, and provide chromosome specific telomere length.

5.2. Methylation Variation at TERT Promoter Can Affect Sp1 Binding to Target Sites and Hypomethylation at -972th position is only seen in old zebrafish brains

In brain samples, variation in methylation levels at -972nd position of the tert promoter is observed. Analysis with ConTra v2.0, transcription factor analysis program, revealed that -972nd position was part of Sp1 binding site. In the TATA-less promoters, Sp1binding site clustering is a common feature, and zebrafish tert promoter has 16 Sp1 binding sites [63]. Sp1 is shown to be required for telomerase catalytic subunit expression and activates the tert promoter with c-myc and NF-κB, synergistically. Even though methylation is generally associated with transcriptional silencing, the opposite is observed in TERT promoter. Highly methylated CpG islands in tert promoter area are observed in telomerase positive ZF4 cell lines and zebrafish embryos [65]. In this study two animals with extremely short telomeres showed hypomethylation at the -972nd site. Bisulfite conversion and sequencing of an independent cohort revealed the same hypomethylation mark in four out of five old brain samples. None of the young animals had hypomethylation at this site. This strongly suggests that hypomethylation at the -the 972nd site is associated with the aging brain. Our data and methylation status of the tert promoter in telomerase positive cells increases the likeliness of a change in binding capacity of Sp1 transcription factor to its target site that is, in turn, affecting the telomere length. To further test this observation, chromatin immunoprecipitation experiments for Sp1 can be performed, followed by qPCR for quantification, and the sample size can be increased.

5.3. SP1 Binding to Target Sequences is Required for TERT Promoter Activity in Brain Cancer Cell Lines

To further decipher the inhibition of SP1 binding to TERT promoter, brain cancer cell lines are transfected transiently with plasmid constructs with or without mutations at the predicted SP1 binding sites. Promoter activity is measured with luciferase assay 24 hours post-transfection. All of the constructs abrogated the promoter activity in varying severity. In a similar study using HeLa cell line reported a decreased TERT promoter activity in the presence of SP1 binding site mutations [66]. Yet, our findings suggest a tighter regulation of TERT expression by SP1 transcription factor in brain cancer cell lines, when compared to HeLa cells. To further investigate this phenomenon observed in brain cancer cell lines, a reporter assay with an internal control can be used.

5.4. Short Term Silencing of DNA Methyltransferases Do Not Change Population Doubling Times however Changes the Induction of Cellular Senescence between Cell Types

Brain cancer cell lines were not affected by short term silencing of DNMT1 and DNMT3B in terms of population doubling time even though both of these enzymes are accepted as stemness markers. Yet, some samples showed within-sample, and this situation sheds questions in terms of data trustability. This problem can be achieved by using an automated cell counting system, and cell viability test, for the seeding and the collecting steps of the cells. On the other hand, reduction in the activity of DNA Methylation machinery had an effect on induction of replicative senescence. Inhibition of DNA methylation through chemotherapeutic agent, Azacytidine or silencing of DNMT1 and DNMT3B, caused an increase in the percentage of Beta-Galactosidase positive cells in the SW1088 cell line. A172 and Daoy cell lines did not show a statistically significant change in the entrance to replicative senescence pathway. A172 only showed an increase in the number of replicative senescent cells with 10 nM Adriamycin (Doxorubicin) treatment. This data shows that brain cancer cell lines used in this study have different severity in terms of immortality, and different agents in varying concentrations have different cellular outcomes. This can be explained by the differences in accumulated mutations between cells. Apart from Beta-Galactosidase staining, amount of p16 and p21 can be measured with Western Blot to investigate the cells at an earlier stage of the cellular senescence pathway.

5.5. Inhibiting the De Novo DNA Methylation, Not the Maintenance DNA Methylation, Reduces Telomerase Activity

To evaluate telomerase activity and decipher the relationship with the DNA Methyltransferases, highly sensitive quantitative telomeric repeat amplification protocol (qTRAP) is performed. Amongst the brain cancer cell lines, Daoy had the highest telomerase activity. Transcriptional silencing of DNMT3B reduced the telomerase activity significantly in all cell lines, whereas DNMT1 silencing did not have a significant effect on the activity of the telomerase enzyme. In A172 and SW1088, silencing of DNMT3B almost completely abrogated the enzymatic activity. In the Daoy cell line, the telomerase activity was significantly reduced with DNMT3B silencing, yet again, this cell line showed high telomerase activity. This can explain the immortal capacity and resistance to replicative senescence observed in population doubling and Beta-Galactosidase staining experiments in this cell line. DNMT3B is known to be required for the subtelomere methylation, and thus telomere maintenance and chromosome stability [67]. Our findings suggests that DNMT3B is also required for the telomerase activity and thus the maintenance of the telomeres in these brain cancer cell lines. To further study the relationship between telomerase activity and DNMT3B, stable knock out experiments can be performed.

5.6. Expression of the Catalytic Subunit of Telomerase Holoenzyme Does Not Change Significantly with RNAi but Telomerase RNA Component Expression Depends on DNA Methylation

Silencing of DNA Methyltransferases or inhibition of DNA Methylation machinery through chemotherapeutic agents did not change the expression of the tert catalytic subunit (TERT) in brain cancer cell lines significantly. On the other hand, these treatments changed the expression levels of the RNA subunit of the telomerase enzyme. In A172 and WI-38 VA-13 Subline 2RA, Azacytidine treatment decreased the expression of TR, whereas it increased the expression in the Daoy cell line. In SW1088, DNMT1 silencing but not Azacytidine treatment increased the TR expression significantly. This is interesting because a recent study using breast cancer cell lines showed that TR promoter is heavily methylated, expressed in low levels and contributing to tumorigenesis [68].

Our findings suggest that DNA Methylation is required for the TR but not for TERT expression. Yet, qPCR experiments for TERT expression had high variance, and this could mask the significant changes in the expression pattern. This problem can be achieved by using probe-based qPCR since the technique provides higher sensitivity. Increasing the technical replicate number can also provide more meaningful data. These findings are interesting because they show cell type dependent effects of the treatments. Further experiments can be performed in stable knock out models and multiple silencing of DNA Methyltransferase family members.

5.7. ALT Associated Genes Show Variable Response to the Inhibition of DNA Methylation Depending on the Cell Type

It is well known that telomerase-dependent and ALT mediated telomere maintenance can co-occur inside a cell. To test some of the characterized ALT-associated, DNA methylation machinery is interfered in brain cancer cell lines. For the ATRX gene, inhibition of DNA methylation decreased expression levels in A172, and WI-38 VA-13 Subline 2RA increased in Daoy. Generally, ATRX is lost in ALT positive cells [69], and a decrease in expression can induce or contribute to ALT phenotype. DAXX, the molecular partner of ATRX, did not significantly changed in brain cancer cell lines used with the treatments. On the other hand, in ALT positive control cell line WI-38 VA-13 Subline 2RA DAXX expression decreased with DNA methylation inhibitory treatments. Inhibition of DNA methylation can contribute to cellular immortality by inducing ALT phenotype, through loss of ATRX in A172 and WI-38 VA-13 Subline 2RA, and loss of DAXX in WI-38 VA-13 Subline 2RA. In SW1088 cell line, TRF2 expression increased with RNA interference.

Table 5.1: List of ALT associated genes that are significantly affected by DNA methylation inhibition

Gene	Cell line	Treatment	Effect
ATRX	A172	DNMt1 siRNA, Azacytidine	Decrease
	Daoy	DNMT3B siRNA	Increase
	VA13	Azacytidine	Decrease
DAXX	VA13	DNMT1 siRNA, DNMT3B siRNA, Azacytidine	Decrease
TRF2	SW1088	DNMT1 siRNA, DNMT3B siRNA	Increase
	VA13	DNMT1 siRNA, DNMT3B siRNA, Azacytidine	Decrease
FEN1	A172	DNMT1 siRNA, Azacytidine	Decrease
	Daoy	Azacytidine	Decrease
	SW1088	Azacytidine	Decrease
	VA13	DNMT1 siRNA, Azacytidine	Decrease
WRN	A172	DNMT1 siRNA, DNMT3B siRNA, Azacytidine	Decrease
CBX3	SW1088	DNMT3B siRNA	Increase

In WI-38 VA-13 Subline 2RA, all treatments decreased the TRF2 expression levels. Molecular outcomes of the changes in TRF2 expression can be seen as a double-edged sword since an increase can contribute to cellular immortality, and a decrease or loss can lead to chromosome fusion-breakage cycles. FEN1 expression patterns were decreased in all cell lines with Azacytidine treatments. DNMT1 silencing decreased the FEN1 expression in A172 and WI-38 VA-13 Subline 2RA. Decrease in FEN1 is favored in cancer cell lines since the DNA damage response would increase, and immortality can be ceased. Yet again, this requires a functioning tumor suppressor genes. Evaluation of gene expression levels of tumor suppressors will be beneficial in these cell lines. WRN expression changed significantly only in the A172 cell line with treatments. A decrease or deficiency in WRN is also favored since it inhibits the formation of ALT-associated promyelocytic leukemia bodies and shortens telomeres. CBX3 expression only changed significantly in an SW1088 cell line with DNMT3B silencing. Increase in CBX3 in cancer cells can promote tumorigenesis further. Overall, this data shows that DNA methylation has different outcomes depending on the cell type and previously accumulated mutations. Further experiments can be performed in stable knock out models and synergistic silencing of DNA Methyltransferase family to validate these findings. Furthermore, these cell lines can be tested for the presence of ALT-associated promyelocytic leukemia bodies and extrachromosomal telomeric repeats with PNA-FISH.

5.8. Short Term Silencing of DNA Methyltransferases Do Not Change the Telomere Lengths

Telomere lengths do not seem to get affected by short term silencing of DNMT1 and DNMT3B. Due to variation, to better evaluate the relationship, these experiments need to be repeated. Yet again, this technique is known to be limited by the variations between and within batches, resolution and it provides the mean length measure. Higher throughput techniques like Q-FISH and STELA can be used instead of the qPCR based method. Duration of silencing protocol is another limiting factor. Long term inhibition of DNA methylation machinery or silencing of DNA Methyltransferases can be beneficial for further experiments.

CHAPTER 6

CONCLUSIONS AND FUTURE PROSPECTS

In this thesis, telomere maintenance in aging zebrafish and human brain cancers is studied. In zebrafish, telomere lengths change throughout aging in all organs. Telomere length also varies between samples of the same age. Bisulfite sequencing of distal tert promoter revealed hypomethylation at the 627,118 (-972) site. With the inclusion of an independent cohort, bisulfite sequencing experiments showed hypomethylation at -972 of the tert transcription start site is related to aging. This finding was interesting because -972nd site was a part of the Sp1 binding site and hypomethylation at this site can change the binding dynamics. Sp1 is a transcription factor and regulate tert expression both directly and through interactions with c-myc and NF-κB. Mutant promoter constructs are transfected to brain cancer cell lines for measuring the regulatory role of SP1 in TERT expression. These constructs showed lower promoter activity compared to the wild type. The population doubling time of brain cancer cell lines did not change with interfered DNA methylation machinery. Cell line-specific induction of replicative senescence is observed in chemotherapeutic agents or siRNA treatments. Silencing of DNA Methyltransferases decreased the telomerase activity, but this short term treatment did not change the average telomere lengths significantly. Expression of TERT did not change with Azacytidine or siRNA treatment. TR and ALT-associated genes showed varying response to inhibition of DNA methylation.

This project provides a preliminary understanding of telomere maintenance in brain cancers and suggests therapeutic possibilities. Scope of this work can be increased by additional experiments. Mutations in patients treated with Azacytidine can be investigated since previously accumulated mutations are affecting the cellular outcomes of methylation inhibition. Moreover, identified mutations can be used as a diagnostic panel to select the treatment type in patients. To further decipher the relationship between SP1 binding to TERT promoter, both in zebrafish and human brain cancer cell lines, ChIP experiments can be performed. Luciferase assay for TERT promoter can be performed in cell lines after inhibition of DNA methylation. Stable knock outs for DNA Methyltransferases can also be used to investigate the long term cellular outcomes. Since transient silencing of DNMT1 and DNMT3B result in different cellular dynamics, DNMT3A and DNMT3L can be included in the project in the future. Combinatorial knock out of DNA Methyltransferases can be investigated to see the synergistic effect on telomere maintenance and tumorigenesis. Brain cancer cell lines used in this study can be tested for ALT-associated promyelocytic leukemia bodies and extrachromosomal telomeric repeats with PNA-FISH to study the ALT pathway further. Other ALT or telomerase associated genes can be included in the project.

REFERENCES

[1] de Lange, T. “Shelterin: the protein complex that shapes and safeguards human telomeres” *Genes Dev.*, vol. 19, pp. 2100-2110, 2005

[2] Maciejowski, J. and de Lange T. “Telomeres in cancer: tumor suppression and genome instability” *Nat Rev Mol Cell Biol*, vol. 18, pp. 175-186, 2017

[3] Palm, W. and de Lange, T. “How Shelterin protects mammalian telomeres” *Annu Rev Genet.*, vol. 42, pp. 301-334, 2008

[4] Li, B., Oestreich, S. and de Lange, T. “Identification of human Rap1: implications for telomere evolution” *Cell*, vol.101, pp. 471-483, 2000

[5] Wang, F., Podell, E.R., Zaug, A.J., Yang, Y., Baciu, P., Cech, T.R. and Lei, M. “The POT1-TPP1 telomere complex is a telomerase processivity factor. ” *Nature*, vol. 445, pp. 506-510, 2007

[6] Xin, H., Liu, D. and Songyang, Z. “The telosome/shelterin complex and its functions” *Genome Biol.* 2, vol. 9: 232, 2008

[7] Shay, J.W, “Telomeres and Aging” *Curr Opin Cell Biol*, vol. 5, pp. 1-7, 2018

[8] Blasco, M.A. “Stem Cells and Aging” *Nat Chem Biol.,* vol. 10, pp. 640-649 , 2007

[9] Armanios, M., Adler, J.K, Parry, E.M. Karim, B., Strong, M.A. and Greider, C.W. “Short telomeres are sufficient to cause the degenerative effects associated with aging” *Am J Hum Genet.,* vol 3, pp. 823-832, 2009

[10] Tomás-Loba, A., Flores, I., Fernández-Marcos, P.J., Cayuela, M.L, Maraver, A., Tejera, A., Borrás, C., Matheu, A., Klatt, P. Flores, J.M., Viña, J., Serrano, M. and Blasco, M.A. “Telomerase reverse transcriptase delays aging in cancer-resistant mice.” *Cell*, vol. 4, pp. 609-622, 2008

[11] Boonekamp, J.J., Simons, M.J., Hemerik, L. and Verhulst, S. "Telomere length behaves as biomarker of somatic redundancy rather than biological age." *Aging Cell*, vol 12, pp. 330-332, 2013

[12] Reichert, S. and Stier, A. "Does oxidative stress shorten telomeres *in vivo*? A review" *Biol. Lett.,* vol. 13, pp. 1-7, 2017

[13] Pfeiffer, V. and Lingner, J. "TERRA promotes telomere shortening through exonuclease 1-mediated resection of chromosome ends" *PLoS Genet.*, vol. 8, no: 6, e1002747, 2012

[14] Shay, J.W. "Role of telomeres and telomerase in aging and cancer" *Cancer Discov.*, vol.6, pp. 584-593, 2016

[15] Campisi, J. "Aging, Cellular Senescence, and Cancer" *Annu Rev Physiol.*, vol. 75, pp. 685-705, 2013

[16] Zou, Y., Sfeir, A. Gryaznov, S. M., Shay, J.W. and Wright, W.E. "Does a sentinel or a subset of short telomeres determine replicative senescence?" *Mol. Biol. Cell*, vol. 15, pp. 3709-3718, 2004

[17] Deng, Y., Chan, S. and Chang, S. "Telomere dysfunction and Tumor Suppression - the Senescence connection" *Nat Rev Cancer*, vol. 6, pp. 450-458, 2008

[18] Ozturk, M., Arslan-Ergul, A., Bagislar. S, Senturk, S. and Yuzugullu, H. "Senescence and immortality in hepatocellular carcinoma" *Cancer Lett.*, vol. 286, no. 1, pp. 103-113, 2008

[19] Sharpless, N.E. and DePinho, R.A. "Telomeres, stem cells, senescence, and cancer" *Clin Invest.*, vol. 11, no. 2, pp. 160-168, 2004

[20] Holohan, B., Woodring, E. and Shay, J.W. "Telomeropathies: An emerging spectrum disorder" *j. Cell Biol.*, vol. 205, no. 3, pp. 289-299, 2014

[21] Wright, W.E., Piatyszek, M.A., Rainey, W.E., Byrd, W. and Shay, J.W. "Telomerase activity in human germline and embryonic tissues and cells" *Dev. Genet.*, vol18, pp. 173-179, 1996

[22] Blasco, M.A. "Telomeres and human disease: ageing, cancer and beyond" *Nat Rev Genet,*, vol. 6, pp. 611-622, 2005

[23] Kim, N.W., Piatyszek, M.A., Prowse, K.R., Harley, C.B., West, M.D., Ho, P.L., Coviello, G.M., Wright, W.E., Weinrich, W.E. and Shay, J.W. " Specific association of human telomerase activity with immortal cells and cancer" *Science*, vol. 266, pp. 2011-2016, 1994

[24] Lewis, K.A. and Tollefsbol, T.O. "Regulation of the telomerase reverse transcriptase subunit through epigenetic mechanisms" *Front Genet.*, vol. 7 no: 83, 2016

[25] Zinn, R.L., Pruitt, K., Eguchi, S., Baylin, S.B. and Herman, J.G. "hTERT is expressed in cancer cell lines despite promoter DNA methylation by preservation of unmethylated DNA and active chromatin around the transcription start site" *Cancer Res.*, vol. 67, no. 1, pp. 194-201, 2007

[26] Killela, P.J., Reitman, Z.J., Jiao, Y., Bettegowda, C., Agrawal, N., Diaz, L.A. Jr., Friedman, A.H., Friedman, H., Gallia, G.L., Giovanella, B.C., Grollman, A.P., He, T.C., He, Y., Hruban, R.H., Jallo, G.I., Mandahl, N., Meeker, A.K., Mertens, F., Netto, G.J., Rasheed, B.A., Riggins, G.J., Rosenquist , T.A., Schiffman, M., Shih, IeM., Theodorescu, D., Torbenson, M.S., Velculescu, V.E., Wang, T.L., Wentzensen, N., Wood, L.D., Zhang, M., McLendon, R.E., Bigner, D.D., Kinzler, K.W., Vogelstein, B., Papadopoulos, N. and Yan, H. "TERT promoter mutations occur frequently in gliomas and a subset of

tumours derived from low rates of self-renewal" *Proc Natl Acad Sci U S A*, vol. 110, no. 15, pp. 6021-6026, 2013

[27] Kyo, S., Takakura, M., Kanaya, T., Itoh, H., Yutsudo, M., Ariga, H. and Inoue, M. "Sp1 cooperates with c-Myc to activate transcription of the human telomerase reverse transcriptase gene (hTERT)" *Nucleic Acids Res.*, vol. 28, no. 3, pp. 669-677, 2000

[28] Pericuesta, E., Ramirez, M.A., Villa-Diaz, A., Relaño-Gines, A., Torres, J.M., Nieto, M., Pintado, B. and Gutiérrez-Adán, A. "The proximal promoter region of mTERT is sufficient to regulate telomerase activity in ES cells and transgenic animals" *Reprod Biol Endocrinol.*, vol. 3, pp. 4:5, 2006

[29] Chiba, K., Johnsoni J.Z., Vogan, J.M., Wagner, T., Boyle, J.M. and Hockemeyer, D. "Cancer-associated TERT promoter mutations abrogate telomerase silencing" *Elife*, vol. 4, 2015

[30] Lundblad, V. and Blackburn, E.H "An alternative pathway for yeast telomere maintenance rescues EST1-senescence" *Cell*, vol. 73, pp. 347-360, 1993

[31] Amorim, J.P., Santos, G., Vinagre, J. and Saores, P. "The role of ATRX in the alternative lengthening of telomeres (ALT) phenotype" *Genes* , vol. 7 no. 66, 2016

[32] Durant, S.T "Telomerase-independent paths to immortality in predictable cancer subtypes" *j. Cancer*, vol. 3, pp. 67-82, 2012

[33] Royle, N.J., Foxon, J., Jeyapalan, J.N., Mendez-Bermudez, A., Novo, C.L., Williams, J. and Cotton V.E "Telomere length maintenance- an alternative mechanism" *Cytogenet. Genome Res*, vol.1 22, pp. 281-291, 2008

[34] Blagoev, K.B, Edwin, H.G.and Bailey, S.M. "Telomere sister chromatid exchange and the process of aging" *Aging*, vol. 10, pp. 727-730, 2010

[35] Lallemand-Breitenbach, V. “Pml nuclear bodies” *Cold Spring Harb. Perspect. Bio*l., vol. 2, 2010

[36] Cesare, A.J. and Griffith, J.D. “Telomeric DNA in ALT cells is characterized by free telomeric circles and heterogeneous t-loops” *Mol. Cell. Biol.*, vol. 24, pp. 9948-9957, 2004

[37] Lovejoy, C.A., Li, W., Reisenweber, S.,Thongthip, S., Bronu, J., de Lange, T., De, S., Petrini, H.J., Sung, P.A., Jasin, M. “ Loss of ATRX, genome instability, and an altered DNA damage response are hallmarks of the alternative lengthening of telomeres pathway” *PLoS Genetics,* vol. 8 no. 7, pp. 12-15, 2012

[38] Clynes, D., Jelinska, C., Xella, B., Ayyub, H., Scott, C., Mitson, M., Taylor, S., Higgs, D.R. and Gibbons, R.J. “Suppression of alternative lengthening of of telomere pathway by the chromatin remodelling factor ATRX” *Nat. Commun.*, vol. 6, no. 7538, 2015

[39] Napier, C.E., Huschtscha, L.I., Harvey, A., Bower, K., Noble, J.R., Hendrickson, E.A. and Reddel R.R “ATRX represses alternative lengthening of telomeres” *Oncotarget*, vol. 6, pp. 16543-16558, 2015

[40] Qijun, C., Ijpma, A. and Greider, C.W. “Two survivor pathways that allow growth in the absence of telomerase are generated by distinct telomere recombination events” *Mol Cell Biol*, vol. 5, pp.1819-1827, 2001

[41] Tarsounas, M., Munoz, P., Claas, A., Smiraldo, P.G., Pittman, D.L., Blasco, M.A. and West, S.C. “Telomere maintenance requires the RAD51D recombination/repair protein” *Cell*, vol. 117, pp. 337-347, 2004

[42] Potts, P.R. and Yu, H. “ The SMC5/6 complex maintains telomere length in ALT cancer cells through SUMOylation of telomere-binding proteins” *Nat. Struct. Mol. Biol.*, vol. 14, pp. 581-590, 2007

[43] Gocha, A.R., Acharya, S. and Groden, J. “ WRN loss induces switching of telomerase independent mechanism of telomere elongation” *PLoS ONE*, vol. 9, e93991, 2014

[44] Stagno D’Alcontres, M., Mendez-Bermudez, A., Foxon, J.L., Royle, N.J., and Salomoni, P. “Lack of TRF2 in ALT cells causes pml dependent p53 activation and loss of telomeric DNA” *J. Cell Biol*, vol. 179, pp. 855-867, 2007

[45] Zeng, S., Xiang, T., Pandita, T.K., Gonzalez-Suarez, I., Gonzalo, S., Harris, C.C. and Yang, Q. “Telomere recombination requires the MUS81 endonuclease” *Nat. Cell Biol*, vol. 11, pp. 616-623 2009

[46] Li, B., Reddy, S. and Comai, L. “ Depletion of Ku70/80 reduces the levels of extrachromosomal telomeric circles and inhibits proliferation of ALT cells” *Aging*, vol. 3, pp.395-406, 2007

[47] Saharia, A. and Stewart, S.A. “FEN1 contributes to telomere stability in ALT-positive tumor cells” *Oncogene*, vol. 28, pp. 1162-1167, 2009

[48] Canudas, S., Houghtaling, B.R., Bhanot, M., Sasa, G., Savage, S.A., Bertuch, A.A. and Smith, S. “A role for heterochromatin protein 1gamma at human telomeres” *Genes Dev.*, vol. 25, no. 17, pp. 1807-1019, 2011

[49] Stavropoulos, D.J., Bradshaw, P.S., Li, X., Pasic, L., Truong, K., Ikura, M., Ungrin, M and Meyn, M.S. “The bloom syndrome helicase BLM interacts with TRF2 in ALT cells and promotes telomeric DNA synthesis” *Hum. Mol. Genet.*, vol. 402, pp. 555-560, 2002

[50] O'Sullivan, R.J., Arnoult, N., Lackner, D.H., Oganesian, L., Haggblom, C. Corpet, A., Almouzni, G. and Karlseder, J. "Rapid induction of alternative lengthening of telomeres by depletion of the histone chaperone ASF1" *Nat. Struct.Mol. Biol.*, vol. 21, pp. 167–174, 2014

[51] Poole, L.A., Zhao, R., Glick, G.G., Lovejoy, C.A., Eischen, C.M. and Cortez, D. "SMARCAL1 maintains telomere integrity during DNA replication" *Proc. Natl. Acad. Sci. USA.*, vol. 112, pp. 14864–14869, 2015

[52] Grudic, A., Jul-Larsen, A., Haring, S.J., Wold, M.S., Lonning, P.E., Bjerkvig, R. and Boe, S.O. "Replication protein a prevents accumulation of single-stranded telomeric DNA in cells that use alternative lengthening of telomeres" *Nucleic Acids Res.*, vol. 35, pp. 7267–7278, 2007

[53] Robertson, K. D. "DNA methylation and human disease" *Nature Reviews Genetics*, vol. 6, no. 8, pp. 597–610, 2005

[54] Goll, M.G., Kirpekar, F., Maggert, K.A., Yoder, J.A., Hsieh, C.L., Zhang, X., Golic, K.G., Jacobsen, S.E. and Bestor, T.H. "Methylation of tRNAAsp by the DNA methyltransferase homolog Dnmt2" *Science*, vol. 3, no. 5759 , pp. 395-398, 2006

[55] Jin, B., and Robertson, K. D. "DNA methyltransferases (DNMTs), DNA Damage Repair, and Cancer" *Adv Exp Med Biol*, vol. *754*, pp. 3–29, 2013

[56] Zhang, W. and Xu, J. "DNA methyltransferases and their roles in tumorigenesis" *Biomark Res.*, vol. 5, pp. 1-8, 2017

[57] Loughery, J. E. P., Dunne, P. D., O'Neill, K. M., Meehan, R. R., McDaid, J. R. and Walsh, C. P. "DNMT1 deficiency triggers mismatch repair defects in human cells through depletion of repair protein levels in a process involving

the DNA damage response" *Human Molecular Genetics*, vol. *20, no.* 16, pp. 3241–3255, 2011

[58] Subramaniam, D., Thombre, R., Dhar, A. and Anant, S. "DNA Methyltransferases: A Novel Target for Prevention and Therapy" *Frontiers in Oncology*, vol. 4, pp. 1-13, 2014

[59] Marion, R.M. Strati, K., Li, H., Tejera, A., Schoeftner, S, Ortega, S, Serrano, M. and Blasco, M.A. "Telomeres acquire embryonic stem cell characteristics in induced pluripotent stem cells" *Cell Stem Cell*, vol. 4, pp. 141-154, 2009

[60] Aguado, T., Guiterrez, F.J., Aix, E., Schneider, R.P., Giovinazzo, G, Blasco, M.A. and Flores, I. "Telomere length defines the cardiomyocyte differentiation potency of mouse induced pluripotent stem cells. *Stem Cells*, vol. 35, pp. 362-373, 2017

[61] Pucci, F., Gardano, L. and Harrington, L. "Short Telomeres in ESCS Lead to Unstable Differentiation" *Cell Stem Cell*, vol. 12, no. 4, pp. 479-486, 2013

[62] Arslan-Ergül, A., Erbaba, B., Karoğlu, E.T., Halim, D.O and Adams, M.M. "Short Term Dietary Restriction in Old Zebra Fish Changes Cell Senescence Mechanisms" *Neuroscience*, vol. 334, pp. 64-75, 2016

[63] Anchelin, M., Murcia, L., Alcaraz- Pérez, F., Martínez, C.M., Bernabé-García, M., Mulero, V. and Cayuela, M.L. "Behaviour of Telomere and Telomerase during Aging and Regeneration in Zebrafish" *PloS ONE*, vol. 62, no. 2, e16955, 2011

[64] Aubert, G., Hills, M. and Landsdorp, P.M. "Telomere Length Measurement-caveats and a critical assessment of the available technologies and tools" *Mutat Res.*, vol. 730, pp. 59-67, 2012

[65] Lindeman, L.C., Winata, C.L., Aanes, H., Mathavan, S.,Alestrom, P. and Collas, P. “Chromatin states od developmentally-regulated genes revealed by DNA and histone methylation patterns in zebrafish embryos” *Int J Dev Biol.*, vol. 545, no. 5, pp.303-813, 2010.

[66] Rajagopalan, D., Pandey, A.K., Xiuzhen, M.C., Lee, K.K., Hora, S., Zhang, Y., Chua, B.H., Kwok, H.S., Bhatia, S.S., Deng, L.W., Tenen, D.G., Kappei, D. and Jha, S. “TIP60 represses telomerase expression by inhibiting Sp1 binding to the TERT promoter” *PloS Pathog*, vol. 13, no. 10, e1006681, 2017

[67] Yang, J., Guo, R., Wang, H., Ye, X., Zhou, Z., Dan, J., Wang, H., Gong, P., Deng, W., Yin, Y., Mao, S., Wang, L., Ding, J., Li, J., Keefe, D.L., Dawlaty, M.M., Wang, J., Xu, G. and Liu L. “Tet Enzymes Regulate Telomere Maintenance and Chromosomal Stability of Mouse ESCs” *Cell Reports*, vol. 15, pp. 1809-1821, 2016

[68] Heng, J., Zhang, F., Guo, X., Tang, L., Peng, L., Luo, X, Xu, X., Wang, S., Dai, L. and Wang, J. “Integrated analysis of promoter methylation and expression of telomere related genes in breast cancer” *Oncotarget*, vol. 8, no. 15, pp.25442-25454, 2017

[69] Brosnan-Cashman, J.A., Yuan, M., Graham, M.K., Rizzo, A.J., Myers, K.M., Davis, C., Zhang, R., Esopi, D.M., Raabe, E.H., Eberhart, C.G., Heaphy, C.M. and Meeker, A.K. “ATRX loss induces multiple hallmarks of the alternative lengthening of telomeres (ALT) phenotype in human glioma cell lines in a cell line-specific manner” *PloS ONE*, vol. 13, no. 9, e0204159, 2018

APPENDIX

A.1 Plasmid Design and Site Directed Mutagenesis Targets

A.2 Sequences of Plasmids Used

A.3 Beta Galactosidase Images

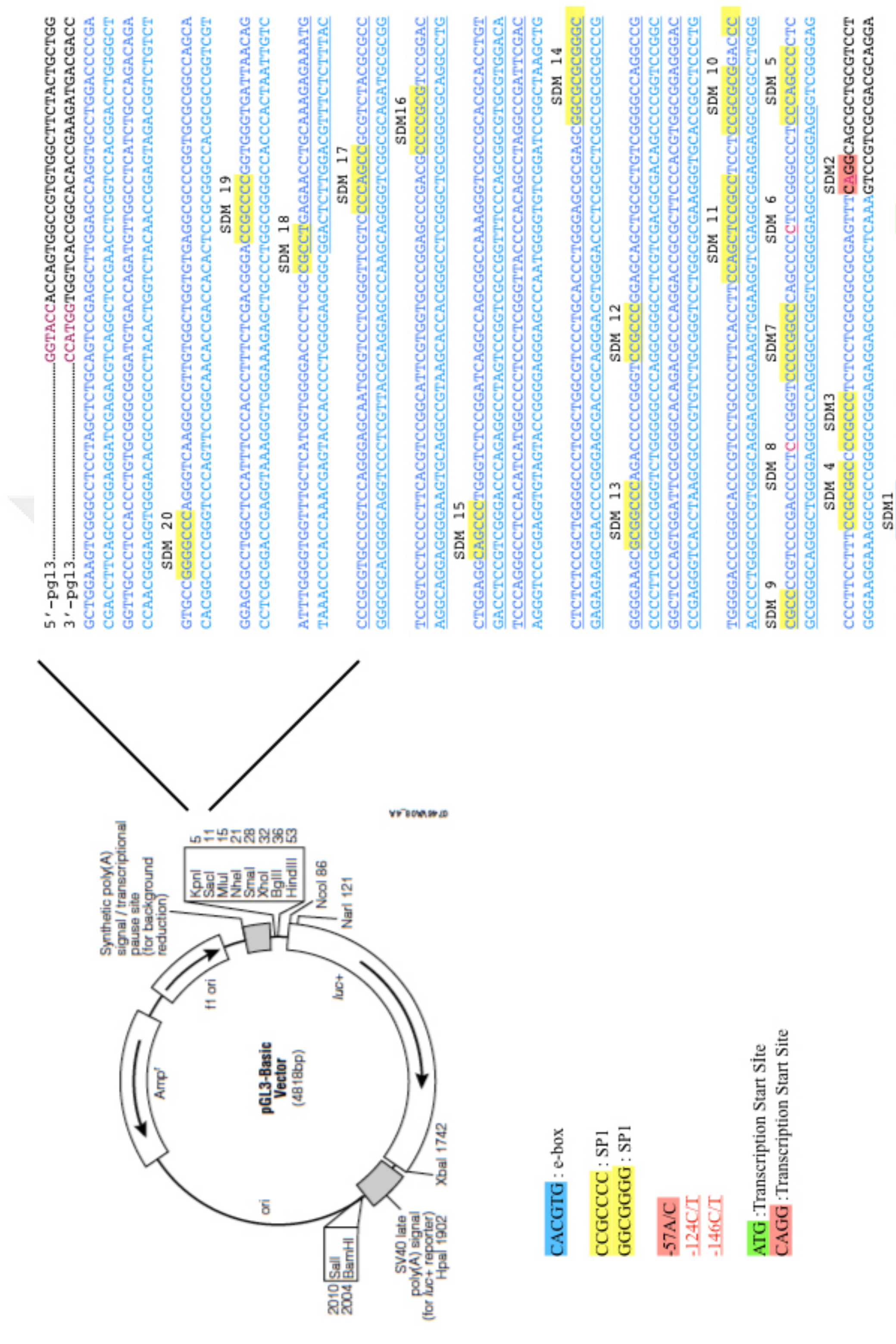

Figure A.1: Plasmid Construct with TERT promoter area.

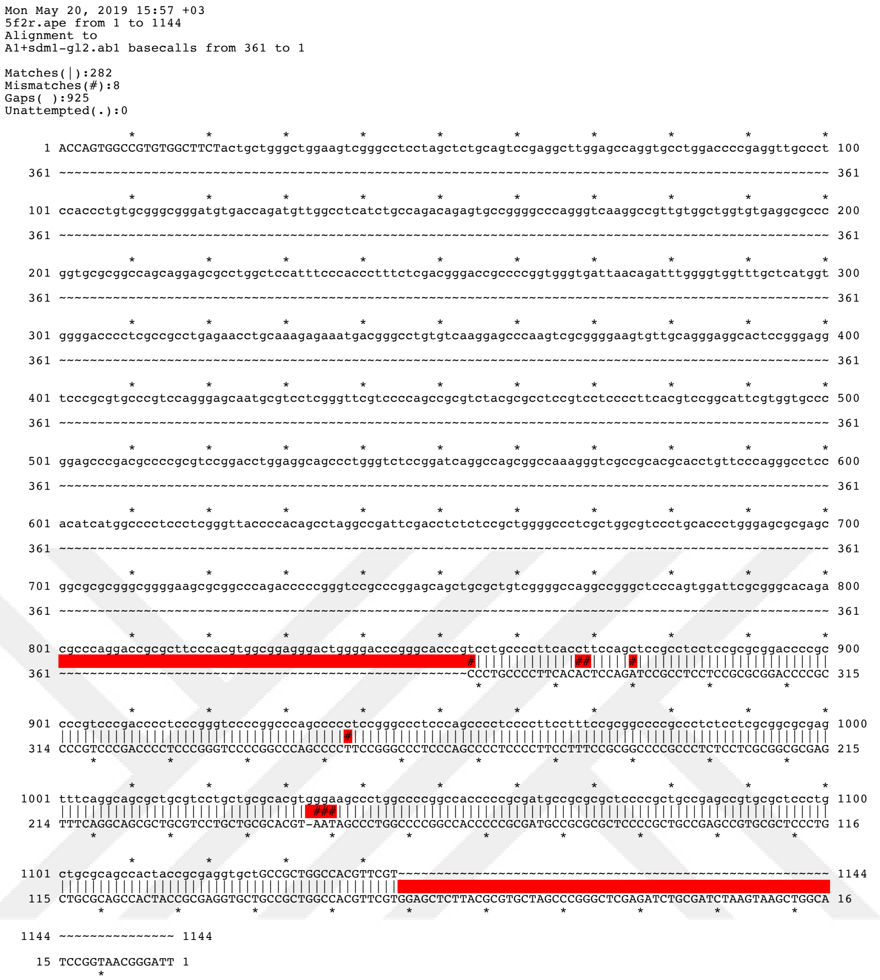

Figure A.2: Sequence of SDM 1. Promoter sequence is aligned to reference sequence (NC_000005.10, GRCh38.p7 1294771-1299989). Alignments are made with with Ape-A plasmid editor v2.0. Mismatches are highlighted with an #.

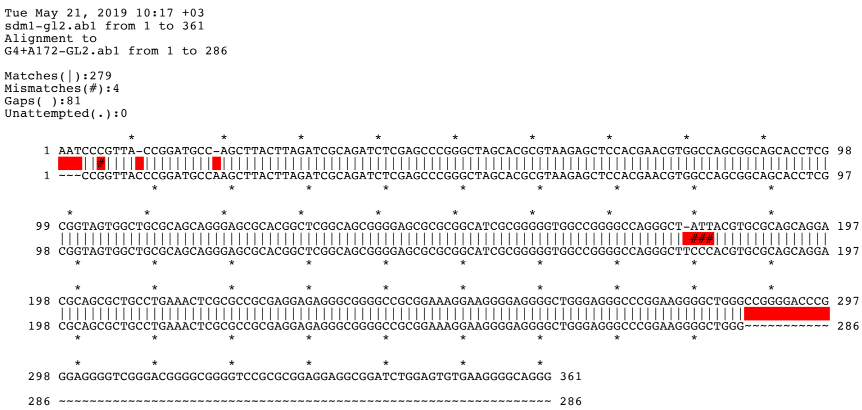

Figure A.3: Sequence of SDM 2. Promoter sequence is aligned to plasmid with no mutation. Alignments are made with with Ape-A plasmid editor v2.0. Mismatches are highlighted with an #.

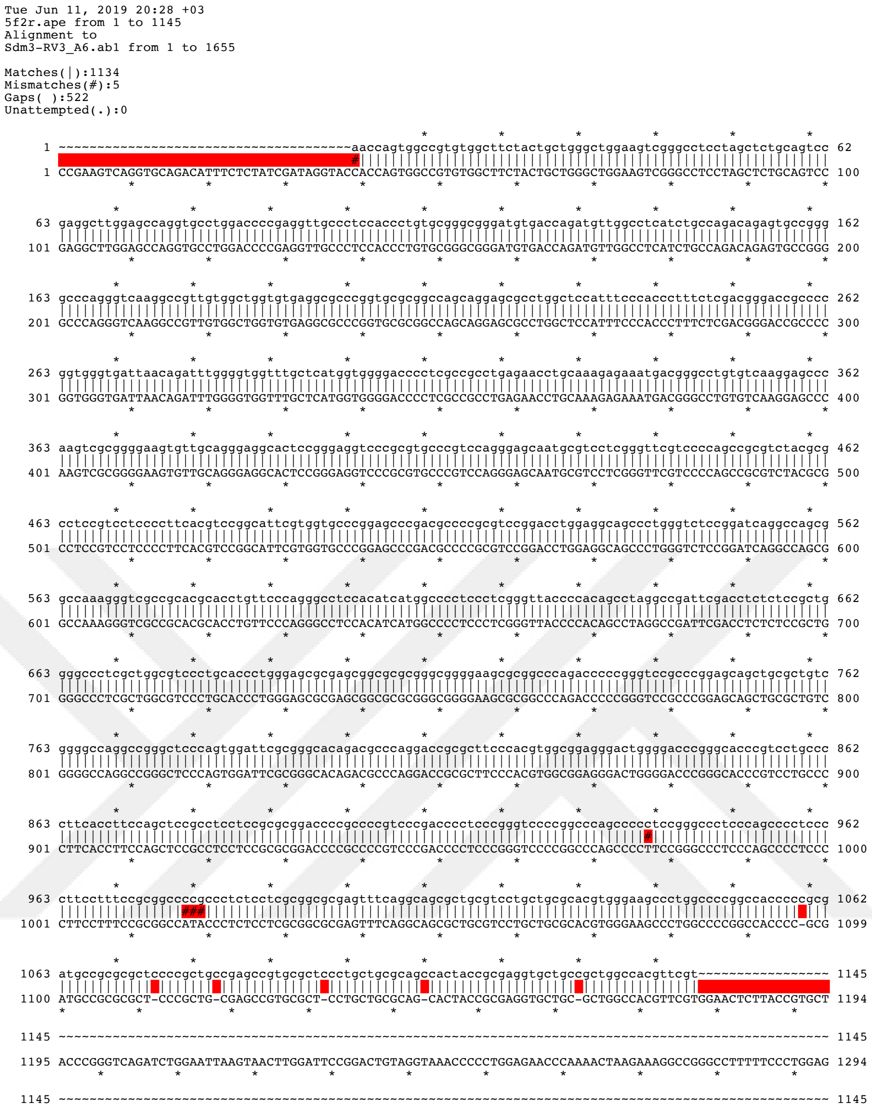

Figure A.4: Sequence of SDM 3. Promoter sequence is aligned to reference sequence (NC_000005.10, GRCh38.p7 1294771-1299989). Alignments are made with with Ape-A plasmid editor v2.0. Mismatches are highlighted with an #.

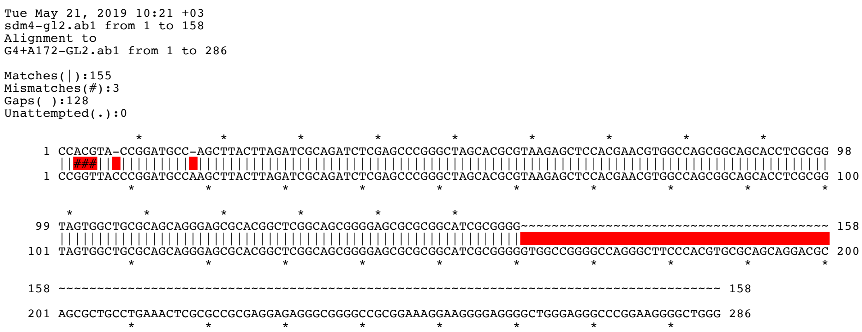

Figure A.5: Sequence of SDM 4. Promoter sequence is aligned to plasmid with no mutation. Alignments are made with with Ape-A plasmid editor v2.0. Mismatches are highlighted with an #.

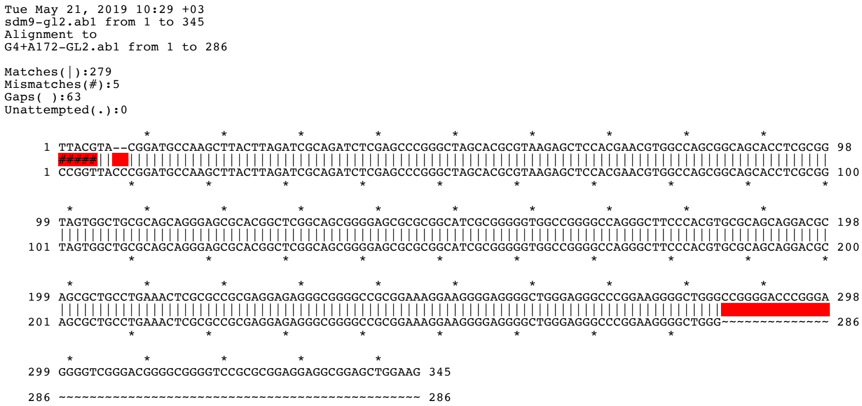

Figure A.6: Sequence of SDM 9. Promoter sequence is aligned to plasmid with no mutation. Alignments are made with with Ape-A plasmid editor v2.0. Mismatches are highlighted with an #.

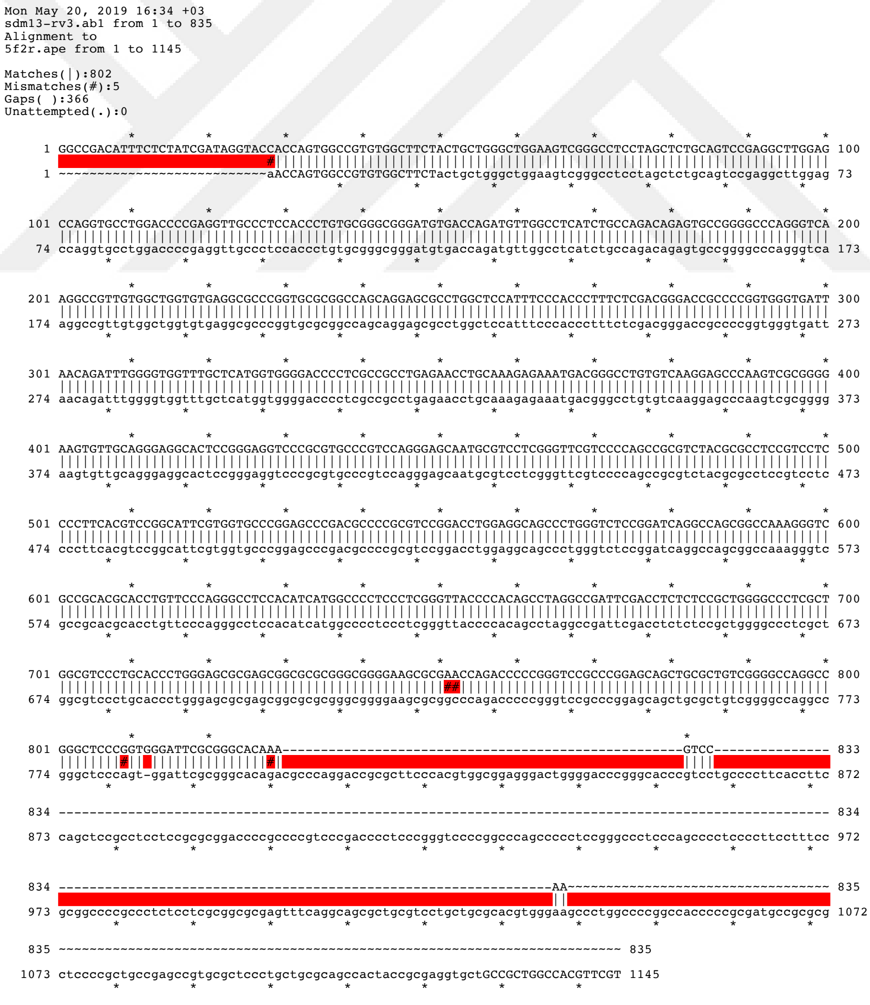

Figure A.7: Sequence of SDM 13. Promoter sequence is aligned to reference sequence (NC_000005.10, GRCh38.p7 1294771-1299989). Alignments are made with with Ape-A plasmid editor v2.0. Mismatches are highlighted with an #.

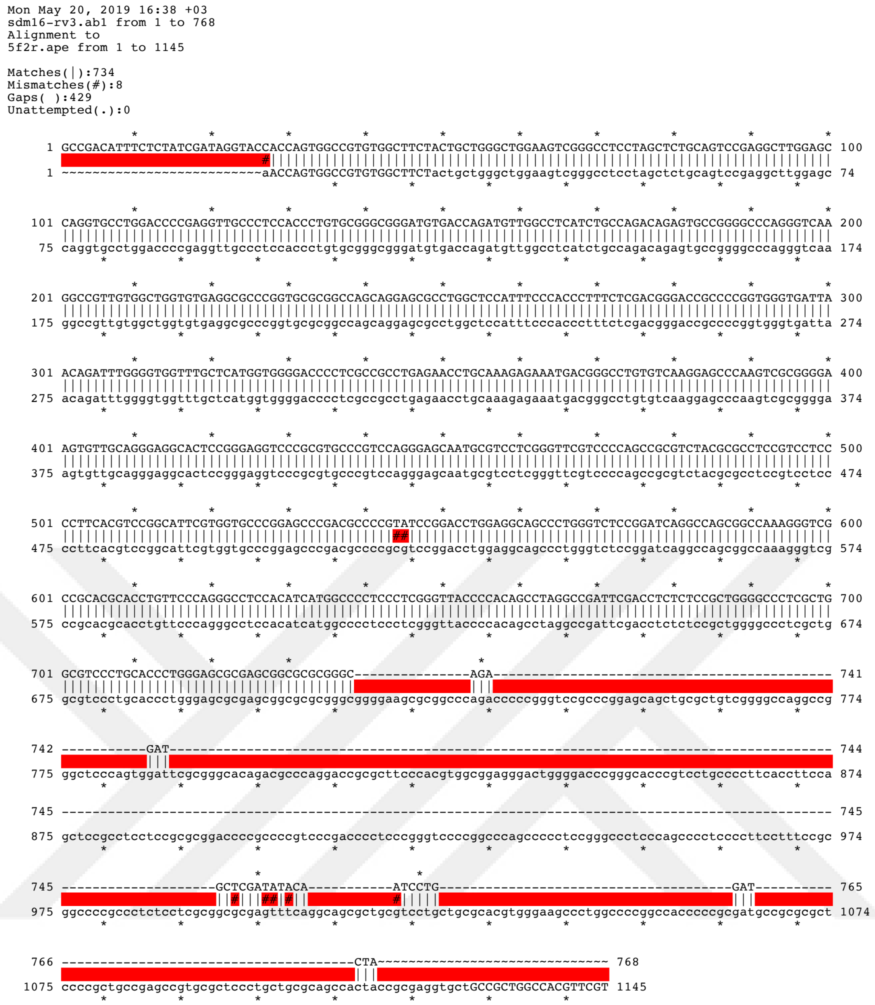

Figure A.8: Sequence of SDM 16. Promoter sequence is aligned to reference sequence (NC_000005.10, GRCh38.p7 1294771-1299989). Alignments are made with with Ape-A plasmid editor v2.0. Mismatches are highlighted with an #.

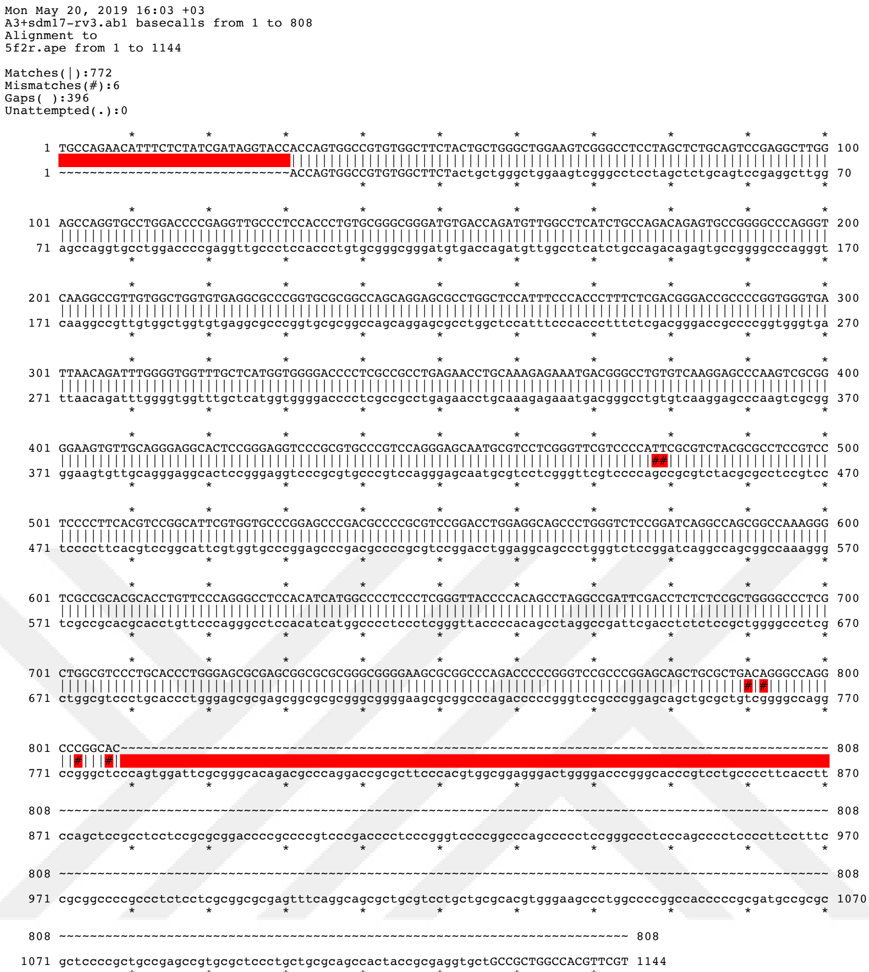

Figure A.9: Sequence of SDM 17. Promoter sequence is aligned to reference sequence (NC_000005.10, GRCh38.p7 1294771-1299989). Alignments are made with with Ape-A plasmid editor v2.0. Mismatches are highlighted with an #.

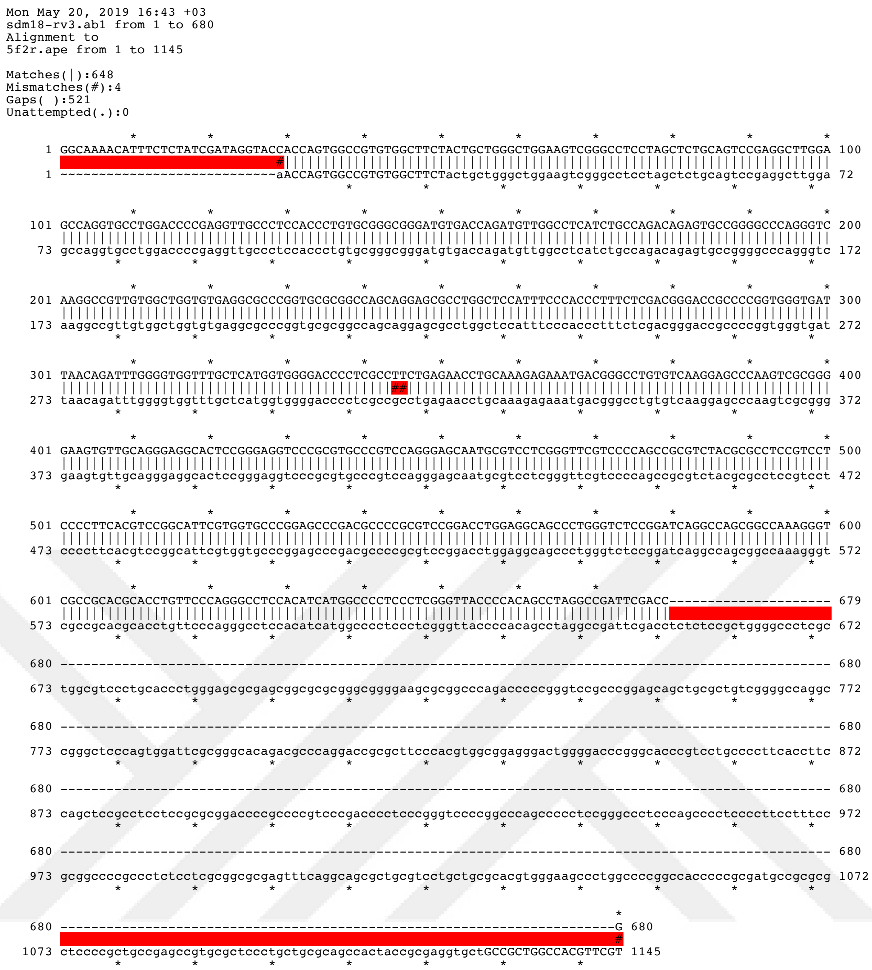

Figure A.10: Sequence of SDM 18. Promoter sequence is aligned to reference sequence (NC_000005.10, GRCh38.p7 1294771-1299989). Alignments are made with with Ape-A plasmid editor v2.0. Mismatches are highlighted with an #.

```
Fri Jul 05, 2019 14:05 +03
G3+A172-RV3.ab1 basecalls from 1 to 850
Alignment to
F5+A172SDM19-RV3.ab1 from 1 to 711

Matches(|):706
Mismatches(#):5
Gaps( ):139
Unattempted(.):0

  1 GGGGGCCGAAATTTCTCTATCGATAGGTACCACCAGTGGCCGTGTGGCTTCTACTGCTGGGCTGGAAGTCGGGCCTCCTAGCTCTGCAGTCCGAGGCTTG 100
  1 GGG--CCGACATTTCTCTATCGATAGGTACCACCAGTGGCCGTGTGGCTTCTACTGCTGGGCTGGAAGTCGGGCCTCCTAGCTCTGCAGTCCGAGGCTTG 98

101 GAGCCAGGTGCCTGGACCCCGAGGTTGCCCTCCACCCTGTGCGGGCGGATGTGACCAGATGTTGGCCTCATCTGCCAGACAGAGTGCCGGGGCCCAGGG 200
 99 GAGCCAGGTGCCTGGACCCCGAGGTTGCCCTCCACCCTGTGCGGGCGGATGTGACCAGATGTTGGCCTCATCTGCCAGACAGAGTGCCGGGGCCCAGGG 198

201 TCAAGGCCGTTGTGGCTGGTGTGAGGCGCCCGGTGCGCGGCCAGCAGGAGCGCCTGGCTCCATTTCCCACCCTTTCTCGACGGGACCGCCCCGGTGGGTG 300
199 TCAAGGCCGTTGTGGCTGGTGTGAGGCGCCCGGTGCGCGGCCAGCAGGAGCGCCTGGCTCCATTTCCCACCCTTTCTCGACGGGACCTATCCGGTGGGTG 298

301 ATTAACAGATTTGGGGTGGTTTGCTCATGGTGGGGACCCCTCGCCGCCTGAGAACCTGCAAAGAGAAATGACGGGCCTGTGTCAAGGAGCCCAAGTCGCG 400
299 ATTAACAGATTTGGGGTGGTTTGCTCATGGTGGGGACCCCTCGCCGCCTGAGAACCTGCAAAGAGAAATGACGGGCCTGTGTCAAGGAGCCCAAGTCGCG 398

401 GGGAAGTGTTGCAGGGAGGCACTCCGGGAGGTCCCGCGTGCCCGTCCAGGGAGCAATGCGTCCTCGGGTTCGTCCCCAGCCGCGTCTACGCGCCTCCGTC 500
399 GGGAAGTGTTGCAGGGAGGCACTCCGGGAGGTCCCGCGTGCCCGTCCAGGGAGCAATGCGTCCTCGGGTTCGTCCCCAGCCGCGTCTACGCGCCTCCGTC 498

501 CTCCCCTTCACGTCCGGCATTCGTGGTGCCCGGAGCCCGACGCCCCGCGTCCGGACCTGGAGGCAGCCCTGGGTCTCCGGATCAGGCCAGCGGCCAAAGG 600
499 CTCCCCTTCACGTCCGGCATTCGTGGTGCCCGGAGCCCGACGCCCCGCGTCCGGACCTGGAGGCAGCCCTGGGTCTCCGGATCAGGCCAGCGGCCAAAGG 598

601 GTCGCCGCACGCACCTGTTCCCAGGGCCTCCACATCATGGCCCCTCCCTCGGGTTACCCCACAGCCTAGGCCGATTCGACCTCTCTCCGCTGGGGCCCTC 700
599 GTCGCCGCACGCACCTGTTCCCAGGGCCTCCACATCATGGCCCCTCCCTCGGGTTACCCCACAGCCTAGGCCGATTCGACCTCTCTCCGCTGGGGCCCTC 698

701 GCTGGCGTCCCTGCACCCTGGGAGCGCGAGCGGCGCGCGGGCGGGGAAGCGCGGCCCAGACCCCCGGGTCCGCCCGGAGCAGCTGCGCTGTCGGGGCCAG 800
699 GCTGGCGTCCCT---------------------------------------------------------------------------------------- 710

801 GCCGGGCTCCCAGTGGATTCGCGGGCACAGACGCCCAGGACCGCGCTTCT 850
711 -------------------------------------------------C 711
```

Figure A.11: Sequence of SDM 19. Promoter sequence is aligned to reference sequence (NC_000005.10, GRCh38.p7 1294771-1299989). Alignments are made with with Ape-A plasmid editor v2.0. Mismatches are highlighted with an #.

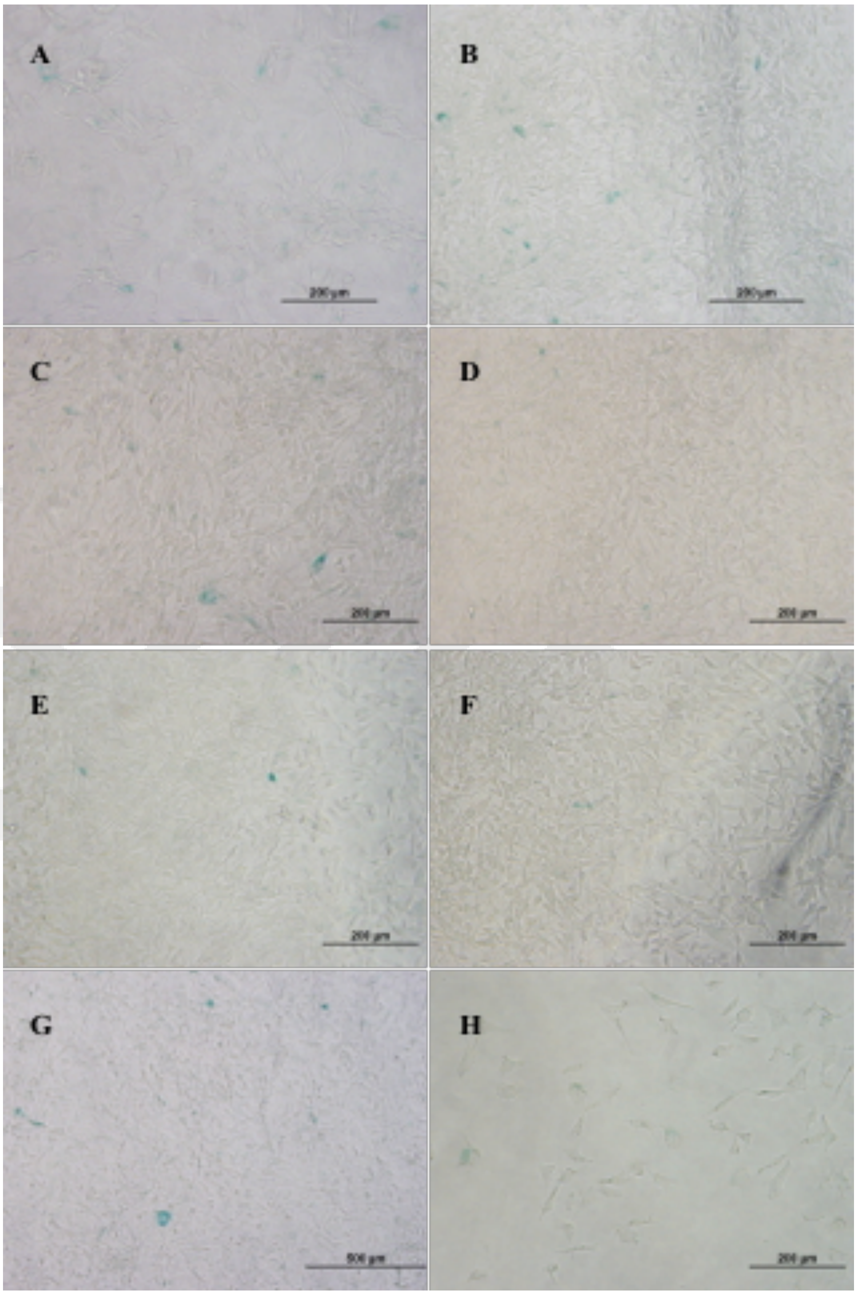

Figure A.12: Beta-Galactosidase Staining of A172 cell line. A)10 nM Adriamycin siRNA, B) 25 nM DNMT1 siRNA, C) 25 nM DNMT3B siRNA, D) 25 nM GAPDH siRNA, E) 25 nM Scrambled siRNA, F) No treatment, G) 10 nM Azacytidine, H) 20 uM Azacytidine. Images are taken with Olympus DP71 CKX41, 96 hours post treatment. 10x lens is used for imaging.

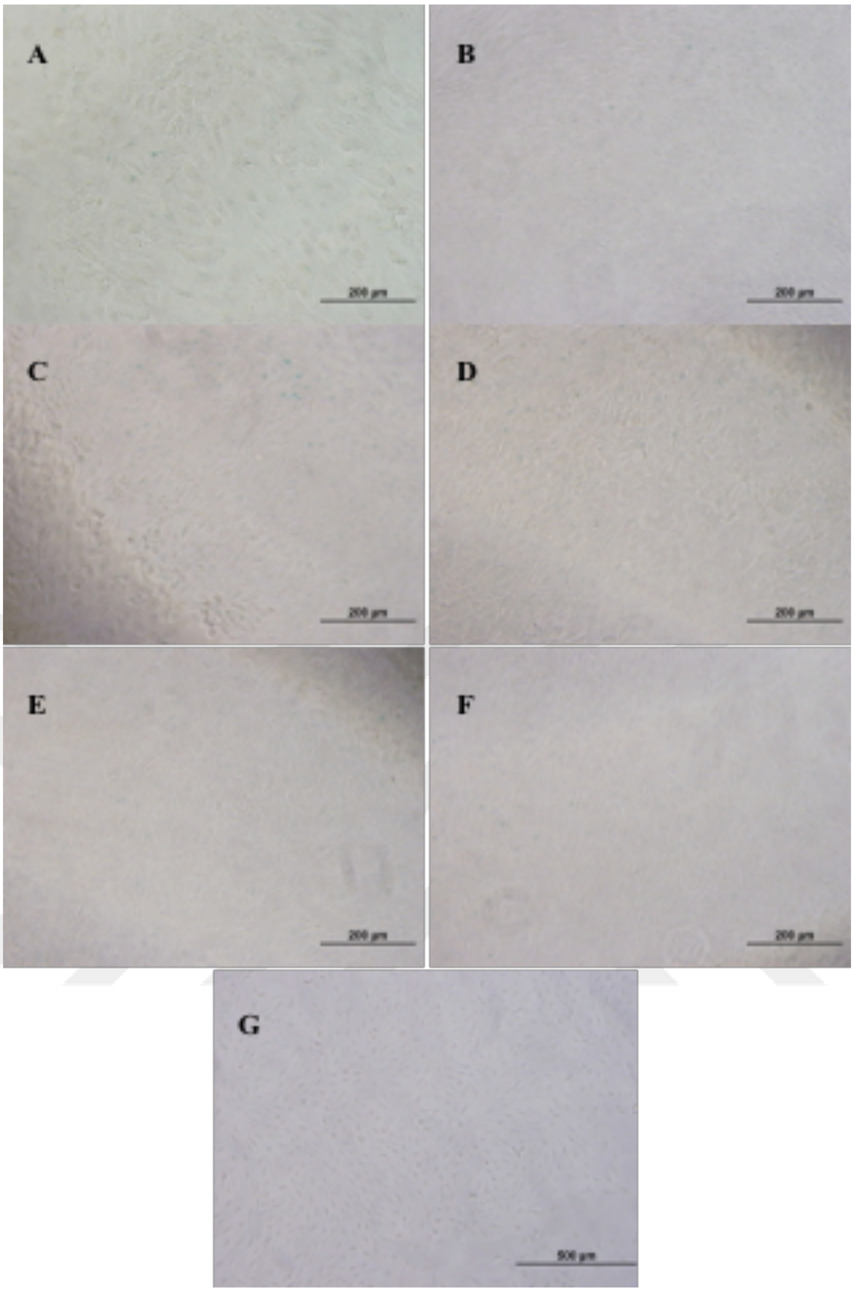

Figure A.13: Beta-Galactosidase Staining of A172 cell line. A)10 nM Adriamycin siRNA, B) 25 nM DNMT1 siRNA, C) 25 nM DNMT3B siRNA, D) 25 nM GAPDH siRNA, E) 25 nM Scrambled siRNA, F) No treatment, G) 10 nM Azacytidine. Images are taken with Olympus DP71 CKX41, 96 hours post treatment. 10x lens is used for imaging.

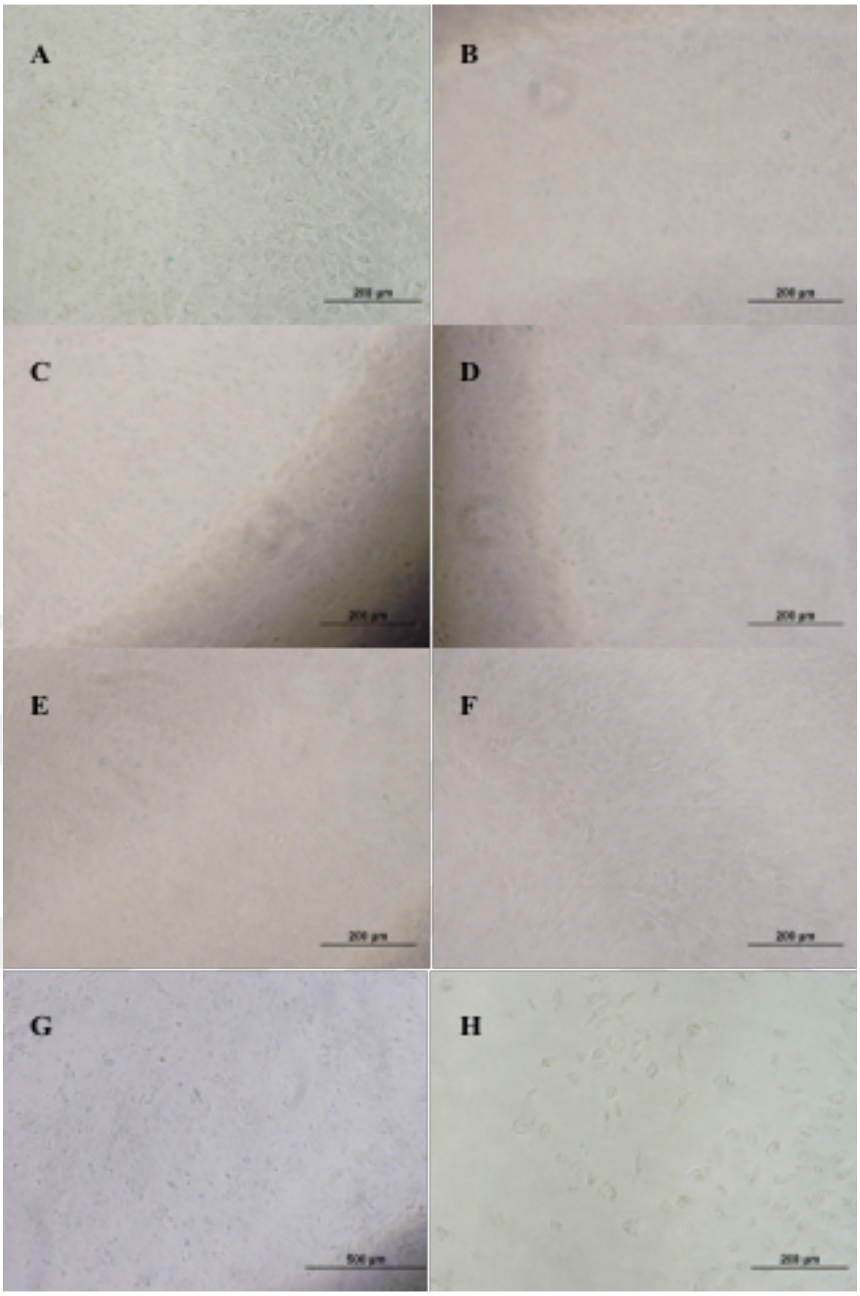

Figure A.14: Beta-Galactosidase Staining of SW1088 cell line. A)10 nM Adriamycin siRNA, B) 25 nM DNMT1 siRNA, C) 25 nM DNMT3B siRNA, D) 25 nM GAPDH siRNA, E) 25 nM Scrambled siRNA, F) No treatment, G) 10 nM Azacytidine, H) 20 uM Azacytidine. Images are taken with Olympus DP71 CKX41, 96 hours post treatment. 10x lens is used for imaging.